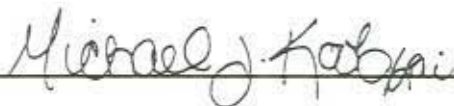


FITNESS FOR PURPOSE EVALUATION OF THE
COUNTERWEIGHT SHEAVE/TRUNNION ASSEMBLY
FOR
OREGON DEPARTMENT OF TRANSPORTATION

WJE NO. 1997.3010

June 2000

Prepared by:



Michael J. Koob, S.E.



Jonathan C. McGormley, S.E.



Robert D. Gessel, ASNT Level III

WISS, JANNEY, ELSTNER ASSOCIATES, INC.
330 Pfingsten Road
Northbrook, Illinois 60062-2095
(847) 272-7400



TABLE OF CONTENTS

	Page
1.0 – BACKGROUND	1
1.1 – Project Overview	2
1.1.1 - Phase 1 - Review of previous work	2
1.1.2 - Phase 2 - Develop and execute disassembly and testing plan	2
1.1.3 - Phase 3 - Develop a fitness for purpose evaluation of the existing assemblies	3
1.2 – Sheave/Trunnion Description	3
2.0 – DISASSEMBLY	6
2.1 – Preparation	6
2.2 – Trunnion Removal	6
3.0 – NONDESTRUCTIVE EVALUATION AND SAMPLING PROGRAM	10
3.1 – Sheave Examination and Sample Removal	10
3.2 – Trunnion Examination and Sample Removal	11
4.0 – DEFECT EVALUATION AND MATERIAL TESTING	20
4.1 – Trunnion Defect Evaluation	20
4.1.1 – Oilway weld repair defects	20
4.1.2 – Internal trunnion defects	21
4.1.3 – Keyway retainer fillet weld cracks	21
4.2 – Sheave Defect Evaluation	21
4.3 – Sheave/Trunnion Assembly Material Properties	22
4.3.1 – Chemical composition and weldability	22
4.3.2 – Tensile properties	22
4.3.3 – Fracture toughness and fatigue crack growth rate	23
5.0 – UT PROCEDURES AND TESTING OF SOUTH TOWER TRUNNIONS	29
5.1 – Inspection Procedures	29
5.2 – Ultrasonic Scans of Trunnions	30
5.3 – Discussion of Ultrasonic Indications	31
6.0 - FIELD TESTING AND ANALYSIS OF SHEAVE WHEEL	36
6.1 - Instrumented Areas	36
6.2 – Measured Stresses	36
6.3 – Comparison of Measured and Analytical Stresses	36
7.0 - SERVICE LIFE ESTIMATE	41
7.1 – Load History	41
7.1.1 – Other lift span bridge fatigue histories	41
7.1.2 – I-5 Bridge loading history	42
7.2 – Sheave Fatigue Life Estimate	42
7.3 – Trunnion Fatigue Life Estimate	43
8.0 – CONCLUSIONS AND RECOMMENDATIONS	47
8.1 - Conclusions	47
8.2 – Recommendations	48
9.0 – REFERENCES	50

FITNESS FOR PURPOSE EVALUATION OF THE
COUNTERWEIGHT SHEAVE/TRUNNION ASSEMBLY
FOR
OREGON DEPARTMENT OF TRANSPORTATION
WJE NO. 1997.3010
June 2000

1.0 – BACKGROUND

The I-5 Columbia River Bridge consists of twin, three lane structures carrying traffic in the northbound and southbound directions between Portland, Oregon and Vancouver, Washington. The east bridge was completed in 1917 and retrofitted in 1960, following completion of the companion west bridge. Both the east and west bridges include a vertical lift span to accommodate ship traffic as shown in Fig. 1.1.

The sheave/trunnion assemblies are part of the moveable span lifting mechanisms. Modifications to the east bridge sheave/trunnion assemblies were performed during the 1960 retrofits and most recently in 1997. The first modifications included installation of tapered roller bearings to replace the original lubricated bushing system. The trunnions were shortened and ground with a taper at each end to accommodate the roller bearing installation. Lubrication grooves or oilways in the original trunnion bearing surface were filled with weld metal prior to machining the trunnion ends. New sheaves were fabricated and installed on the shortened trunnions. In 1997, the north sheave/trunnion assemblies of the east bridge were replaced after questionable indications in the northeast trunnion were detected using nondestructive evaluation methods.

Ultrasonic inspection performed by the Oregon Department of Transportation (ODOT) in 1987 and 1993 identified flaws approximately 14 in. from the east end of the northeast trunnion near the second weld-filled oilway. Additional follow-up inspections by ODOT found the same indications, with no

Wiss, Janney, Elstner Associates, Inc.

apparent change. Acoustic emission (AE) tests were conducted in 1994 on all four trunnions of the east bridge by the BIRL Industrial Research Laboratory of Northwestern University. AE tests were repeated in 1996 for the trunnion that exhibited questionable indications. AE signals received from the trunnion were reported to be in close correlation with, and were generated from, the same general vicinity from which the ultrasonic indications were reported.

In July 1997, Wiss, Janney, Elstner Associates, Inc. (WJE) was asked by ODOT to develop a test procedure and conduct a more rigorous UT inspection of the suspect region of the east shaft as shown in Fig. 1.2¹. Special calibration standards and transducers were prepared to evaluate the trunnion. After careful examination, no crack-like discontinuities were detected within the suspect area of the trunnion. However, the UT examination procedure found indications believed to be small nonmetallic inclusions in the forged steel trunnion.

The north two sheave/trunnion assemblies on the north tower of the east bridge were subsequently removed from service in September 1997. The northeast sheave/trunnion was retained for further testing and assessment.

1.1 – Project Overview

In September 1997, the northeast sheave/trunnion assembly of the I-5 Columbia River Bridge in Portland, Oregon was removed and replaced. The sheave/trunnion assembly that was removed was closely examined and evaluated to facilitate development of an accurate fitness for purpose and fatigue life estimate for two remaining in-service sheave/trunnion assemblies at the south end of the east bridge. The project was divided into three phases, as described below.

1.1.1 – Phase 1 - Review of previous work – A review of previous stress analysis work on the sheave/trunnion assemblies was performed. The previous stress analysis work included computer modeling and instrumentation performed by DGES Inc.² and ODOT³.

1.1.2 – Phase 2 - Develop and execute disassembly and testing plan – The northeast sheave/trunnion assembly was shipped from storage at an ODOT facility in Portland, Oregon to Northbrook, Illinois for dismantlement. The sheave to trunnion keys were fillet welded to the trunnion during installation. These welds exhibited cracking and were carefully examined prior to disassembly.

Wiss, Janney, Elstner Associates, Inc.

The sheave was sandblasted to remove the lead-based paint. All removed paint was disposed according to applicable regulations. The paint removal permitted a complete and thorough nondestructive evaluation (NDE) of the sheave to identify possible fabrication defects, or cracks. The NDE work included visual inspection, magnetic particle, dye penetrant and ultrasonic testing. Identified defects were removed for further examination, in addition to samples being obtained for material testing. All sheave samples were sent to Dr. John W. Fisher, Director of the Engineering Research Center for Advanced Technology for Large Structural Systems (ATLSS) at Lehigh University.

The trunnion was shipped to ATLSS where all nondestructive evaluation, material testing, fractographic, and metallographic work was performed. Fracture toughness, tensile properties, microstructure and weldability were determined for the cast steel sheave and the forged steel trunnion.

1.1.3 – Phase 3 - Develop a fitness for purpose evaluation of the existing assemblies – Based on the analysis and testing information, a fatigue life estimate for the two remaining in-service sheave/trunnion assemblies was calculated. The crack growth threshold and crack growth rate (da/dN) of the trunnion and sheave materials were also quantified.

Using the information gained from the NDE and material testing, an evaluation program was developed and implemented for the remaining two in-service sheave/trunnion assemblies.

1.2 – Sheave/Trunnion Description

The 12 ft-2 in. diameter cast steel sheave consists of eight stiffened spokes spanning between the 3 ft wide rim and the center tapered hub. Sixteen wire rope cables connecting the counterweight to the lift span portion of the bridge pass over the sheave. Figure 1.3 shows portions of the counterweight sheave drawings from the 1960 retrofit. Material specifications for the 1960 replacement sheave fabricated by American Bridge called for ASTM A-27-56T Grade 65-35 fully annealed.

The modified trunnion consists of forged steel measuring 5 ft-6 ¼ in. long that includes several shoulders or steps in the outside diameter and a 5 ⅞ in. diameter center bore penetrating the shaft. A drawing of the shaft is shown in Fig. 1.4. The trunnions are oriented on the bridge in the east/west direction. Three keyways are located in the trunnion as shown in Fig. 1.4. The east keyways were identified as 1A, 2A, and 3A while the west keyways were labeled 1B, 2B, and 3B.

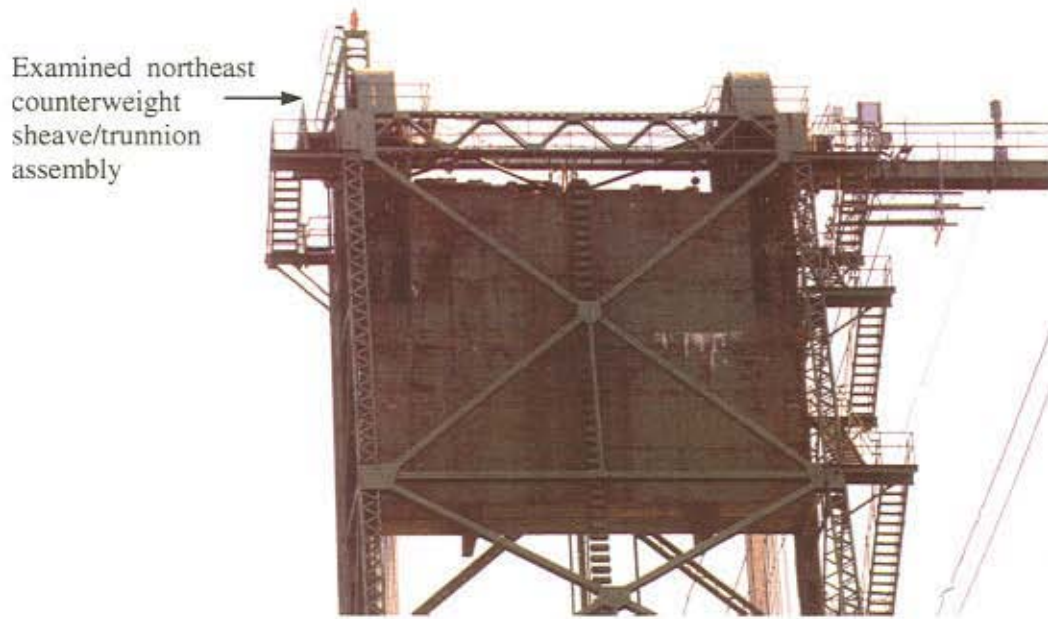


Fig. 1.1 – North tower of 1917 lift span structure showing counterweight sheave/trunnion assemblies

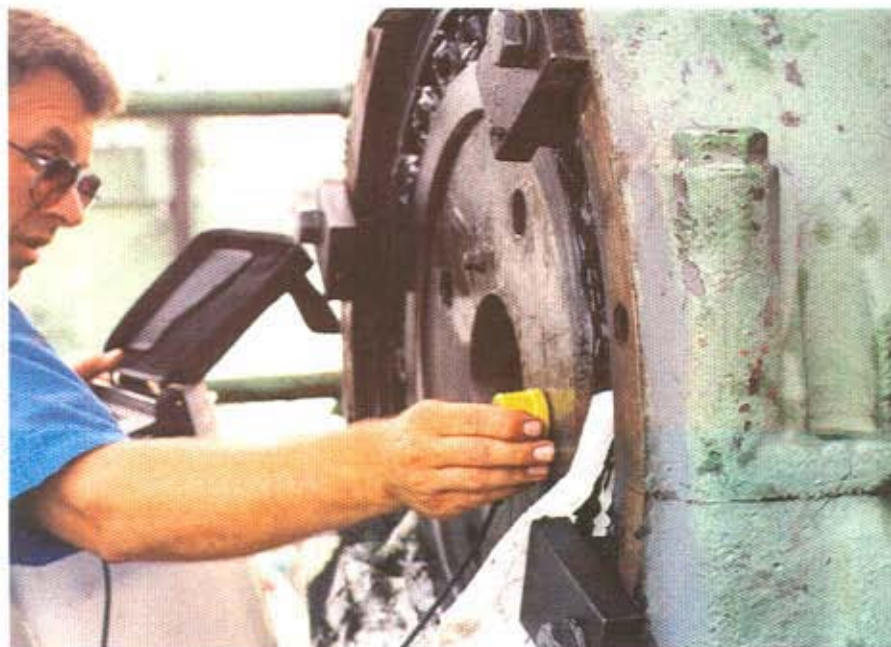


Fig 1.2 – 1997 UT examination of northeast trunnion (east face)

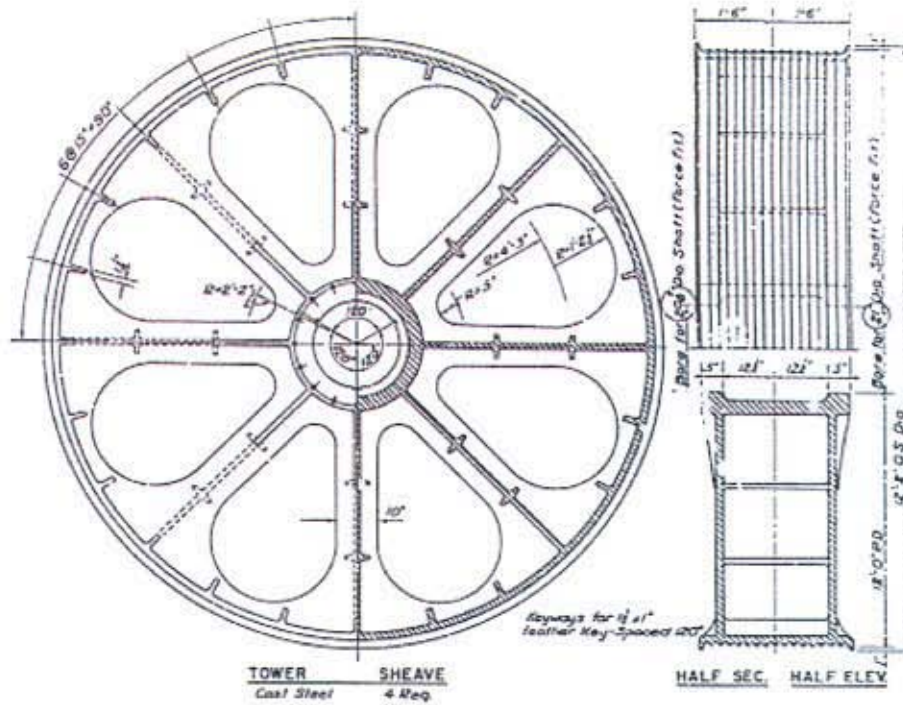


Fig. 1.3 – Sheave details from 1960 retrofit drawings

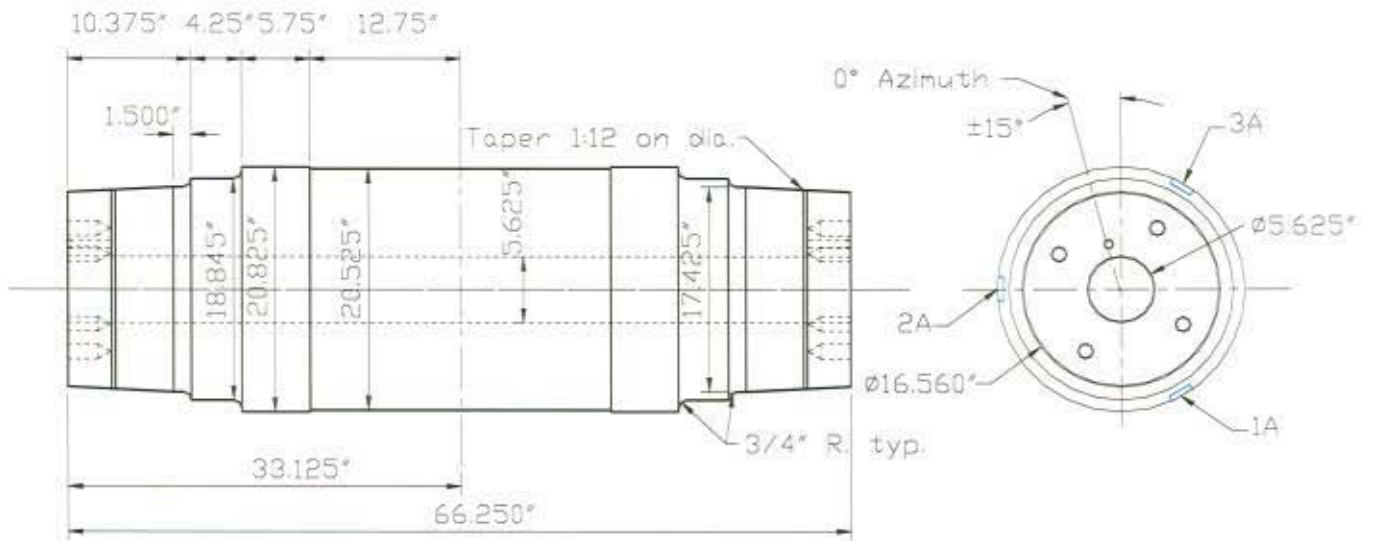


Fig. 1.4 – Trunnion dimensions after the 1960 modifications

2.0 – DISASSEMBLY

Removal of the trunnion from the sheave was necessary to fully evaluate possible defects in the trunnion. Because of our in-house laboratory facilities, the complete counterweight sheave/trunnion assembly was transported by special permit truck from an ODOT storage facility in Portland, Oregon to WJE's Northbrook, Illinois laboratory for disassembly. Figure 2.1 shows the sheave/trunnion assembly as it was shipped from Oregon.

2.1 – Preparation

Grease was cleaned from the assembly upon its arrival in Northbrook. A containment enclosure was erected around the assembly to capture lead-based paint during sandblasting operations. The sheave was subsequently sandblasted to white metal as shown in Fig. 2.2. The trunnion and sheave key fillet welds were protected during the sandblasting. The sandblast waste was disposed in a licensed special waste landfill.

Before attempting to remove the trunnion from the sheave, the six sheave keyway retainer welds (three on each end) were closely examined. Because of the stainless steel weld metal used, dye penetrant was employed to highlight the fillet weld cracks. Weld cracks were observed along the weld tie or through the throat of all six fillet welds. Figure 2.3 shows a cracked key retainer weld at east keyway 1B.

2.2 – Trunnion Removal

During lift span mechanical rehabilitation projects, trunnions are occasionally removed from the sheave by hydraulic jacking or a jacking press. However, if high jacking forces in excess of 600 kips do not result in displacement, trunnions are typically removed by destructive methods. Because the trunnion in this project was to be removed intact, a removal plan was implemented which involved pushing the tapered trunnion from the sheave wheel without damaging it. After several unsuccessful attempts to push the trunnion from the sheave using jacking forces up to 600 kips, a high capacity jacking system was designed, fabricated and subsequently used to move the trunnion. The jacking system is shown in Fig. 2.4. Jacking forces in excess of 1,000 kips were applied to finally initiate movement.

Wiss, Janney, Elstner Associates, Inc.

As the trunnion was pushed from the sheave, the large trunnion shoulder became wedged within the sheave wheel. Slots were cut in the sheave wheel at the center hub and rim so that jacks could be inserted into the rim slots to pry open the hub. Using several jacking operations, the undamaged trunnion was pushed all the way through the sheave wheel and removed.



Fig. 2.1 – Counterweight sheave/trunnion assembly in Northbrook, Illinois



Fig. 2.2 – Sheave/trunnion assembly after sandblasting



Fig. 2.3 – Cracked key retainer weld at keyway 1B



Fig. 2.4 – Jacking system used to remove trunnion intact

3.0 – NONDESTRUCTIVE EVALUATION AND SAMPLING PROGRAM

A sampling program was implemented in order to classify the sheave/trunnion material properties and to better characterize, through fractographic and metallographic methods, the origin of any possible defects and evidence of extension by fatigue. Initially, both the sheave and trunnion were closely examined using nondestructive evaluation test methods to locate questionable indications. These indications were subsequently removed and later subjected to fractographic examination, metallographic cross sectioning, and material testing.

3.1 – Sheave Examination and Sample Removal

The sheave wheel was carefully inspected following sandblasting using visual and MT procedures to find cracks and casting defects. Mr. Robert Gessel, a WJE ASNT Level III MT technician, performed the work. Virtually all surfaces of the sheave were inspected, excluding only the outside rim and the machined hub surfaces. The visual and MT inspections were correlated with the stress information obtained from the DGES, Inc. analytical and ODOT field testing studies. None of the indications that were detected with magnetic particle examination appeared to be related to loading or operation of the sheave but rather were related to the casting process.

The sheave was inspected using both direct and indirect methods of magnetization. An alternating current yoke was used where access would permit or where necessary to achieve the appropriate magnetic field. Alternating current prods with a magnetizing current maintained at 75 to 100 amps per inch were utilized in portions of the sheave where the sheave geometry impeded application of the appropriate magnetic field when using the yoke. Application of the prods is shown in Fig. 3.1. Magnetic particle test areas were overlapped to assure sufficient inspection coverage and to mitigate possible masking of discontinuities due to over-saturation of the magnetic field.

Considerable welding during fabrication was observed on the sheave to correct casting defects and attach stiffeners. Many shrinkage cracks and nonmetallic inclusions related to the weld repairs and casting, respectively were observed. Most indications could easily be removed by grinding. Minor shrinkage cracks were frequently observed in small radiuses and at section thickness changes of the sheave. Typically, indications that occurred in association with casting inclusions were randomly located and

Wiss, Janney, Elstner Associates, Inc.

oriented. Two of the deeper cracks located in high stress regions were removed by coring for fractographic examination. Figure 3.2 shows one of these cracks shown highlighted by magnetized particles in the sheave spoke. In addition, two large steel samples were cut from the sheave wheel for material and chemical testing. Figure 3.3 identifies the sheave sample locations.

3.2 – Trunnion Examination and Sample Removal

After removal of the trunnion from the sheave, Mr. Robert Gessel conducted the NDE testing on the trunnion at Lehigh University. Mr. Gessel marked and discussed the exact locations of concern with Dr. Eric Kaufmann and Dr. John Fisher. A cutting plan for the fractographic and metallographic evaluation work was developed and executed.

Prior to UT inspection, the trunnion was prepared for testing by smoothing the end and center bore surfaces. The end surfaces were smoothed with a course grit emery cloth while a beaded hone was used to smooth the center bore surface. The removed trunnion prepared for UT and MT examination is shown in Fig. 3.4. Procedures for ultrasonic examination utilized all available surfaces of the trunnion including outside surfaces previously inaccessible.

A point of reference was established using a permanent feature of the shaft. The threaded oilway port visible at the end of the shaft was defined as 0° azimuth, with clockwise reference as viewed from the east end of the shaft in the operating configuration. Figure 1.4 from Chapter 1 illustrates this reference position. Indications detected and recorded were referenced by azimuth, radial distance from the bore surface, and distance from the shaft end (east).

Transducers used for the inspection were appropriately contoured and angled for each surface being inspected. Axial scans with longitudinal waves at zero degrees (straight beam) and 12 degrees were introduced from each end surface. Scans from the center bore utilized a zero degree longitudinal wave and a 45 degree shear wave having axial orientation. A shear wave transducer with an incident angle of 45 degrees was used to scan from the outside radius of the trunnion. Calibration of the ultrasonic flaw detector and the various transducer assemblies was performed using several test standards including a Type 2 IIW calibration block, a trunnion calibration standard fabricated from mild steel with

Wiss, Janney, Elstner Associates, Inc.

known defects, and mild steel test blocks for correction and verification of contoured transducer distance calibrations.

Areas of the trunnion where ultrasonic indications were previously identified were carefully scrutinized using axial scans to locate apparent discontinuities. Other transducer angles, center bore, or outside radius scans were then used for defect verification and characterization. Using the straight beam radial scan from inside the trunnion center bore, the weld-filled oilway grooves were detected indicating that the fusion of filler weld metal with the trunnion base metal was of very poor quality.

Inspection of the exterior surfaces at the trunnion ends detected cracks that apparently originated in the oilway groove weld filler metal. The cracks were not detected with axial or center bore ultrasonic scans, however some could be detected using shallow surface scans with a shear wave probe. Most of these cracks required magnetic particle examination for detection as shown in Figs. 3.5a and 3.5b. Indications often appeared to follow weld metal fusion lines, were frequently oriented transverse to the axis of the trunnion, and sometimes extended into adjacent base metal. The cracks detected at weld metal filled oilways were not associated with previously detected ultrasonic indications identified during previous UT work. However, the axial location appears to be approximately one inch from the 13 in. axial location indicated in many of the acoustic emission tests. The inability to detect the oilway cracks with scans from the trunnion center bore or end surfaces may be primarily attributed to the poor fusion of the weld filler metal, which establishes an acoustic interface that impedes or reflects the propagation of the interrogating wave.

Two types of defect indications were identified in the trunnion as a result of the in-depth NDE work. The first defect type was either a surface crack-like discontinuity or sub-surface discontinuity at a welded oilway. The second defect was an internal discontinuity in the vicinity of the inner bore. Both types of defects were selected for additional examination. A summary of the defect indications is provided in Table 3.1. Ultrasonic data sheets locating these defects are found in Appendix A.

All of the surface or sub-surface discontinuities detected both by MT and UT methods were located near keyways where modifications to fill oilways with weld metal had been performed during the 1960 retrofit work. Surface defects were identified by MT at keyways 1A, 3A, and 1B. Sub-surface crack-

Wiss, Janney, Elstner Associates, Inc.

like indications were detected by UT at keyways 3A and 2A along the length of the weld. The crack-like indications were contained within the weld metal material in all cases except keyway 1B where it appeared that the indication extended beyond the weld fusion line into the trunnion shaft base metal.

Seven internal defects were detected within the trunnion by UT axial and/or center bore scanning methods. These defects were grouped at the east end of the trunnion close to the center bore suggesting they were similar in origin.

As noted earlier, the fillet welds at all six keyway retainer welds were cracked. These welds were small and of poor quality possibly developing after welding due to improper preheat and weld shrinkage. A nonmagnetized stainless filler metal of unknown grade was used for these retainer welds. Nondestructive tests using a visible dye liquid penetrant were performed to enhance the inspection and to locate cracks that may not be visually observed. NDE of the welds found no indications of cracking from the weld root or weld toe into the trunnion base metal. A keyway retainer weld crack was selected for additional fractographic evaluation to verify the NDE results.

Data collected from examination of the removed trunnion was used in the selection and removal of specimens for fractographic and metallographic analysis. Figure 3.6 shows the layout for saw-cutting to remove defects from the trunnion. A section of the trunnion end that appeared to be free of significant discontinuities was marked for removal as an ultrasonic standard for use in future inspections of the south tower trunnions.

Table 3.1 – SUMMARY OF DETECTED INDICATIONS WITHIN REMOVED NORTH TOWER TRUNNION

Trunnion End	Approx. Radial Orientation	Approx. Axial Orientation from Near End	Inspection Method			Notes
			Visual	Magnetic Particle	Ultrasonic	
East	135° - Keyway 1	13 in. - 14 in.	None	2 small indications 0.44 transverse 0.31 diagonal	N.F. at root filled groove. 0° bore scan	MT indications masked * from bore & axial Appendix. B Sht. 1
	255° - Keyway 2	12 in. - 14 in.	None	1 small transverse indication 0.08 length	N.F. at root filled groove. 0° bore scan	MT indications masked * from bore & axial scan Appendix B Sht. 2
	15° - Keyway 3	13 in - 14 in.	None	2 small indications 0.25 transverse 0.25 diagonal	N.F. at root filled groove. 0° bore scan	MT indications masked * from bore & axial scan Appendix B Sht. 3
	15°	9 in. - 15 1/2 in.	N/A	N/A	45° bore scan 0° radial 0° axial	Embedded NM inclusions Appendix B Sht. 7
	60°	8 1/2 in.	N/A	N/A	45° bore scan 0° radial 0° axial	Embedded NM inclusions Appendix B Sht. 8
	80°	14 1/2 in.	N/A	N/A	45° bore scan 0° radial 0° axial	Embedded NM inclusions Appendix B Sht. 9
	150°	13 in. to 15 in.	N/A	N/A	45° bore scan 0° radial 0° axial	Embedded NM inclusions Appendix B Sht. 10
	165°	15.2 in.	N/A	N/A	45° bore scan 0° radial 0° axial	Embedded NM inclusions Appendix B Sht. 11
	260°	9 in. - 14 in.	N/A	N/A	45° bore scan 0° radial 0° axial	Embedded NM inclusions Appendix B Sht. 12
West	135° - Keyway 1	10 1/2 in. - 12 1/2 in. 14 in.	None	2 small transverse indications 0.60 & 0.01	N.F. at root filled groove. 0° bore scan	MT indications masked * from bore scan Appendix B Sht. 4
	255° - Keyway 2	11 in. - 13 in.	None	None	N.F. @ root filled groove	MT indications masked * from bore & axial Appendix B Sht. 5
	15° - Keyway 3	11 in. - 14 1/2 in.	None	None	N.F. @ root filled groove	MT indications masked * from bore & axial Appendix B Sht. 6

N.M. = Non-Metallic

N.F. = Non Fusion

* N.F. in groove prevents detection

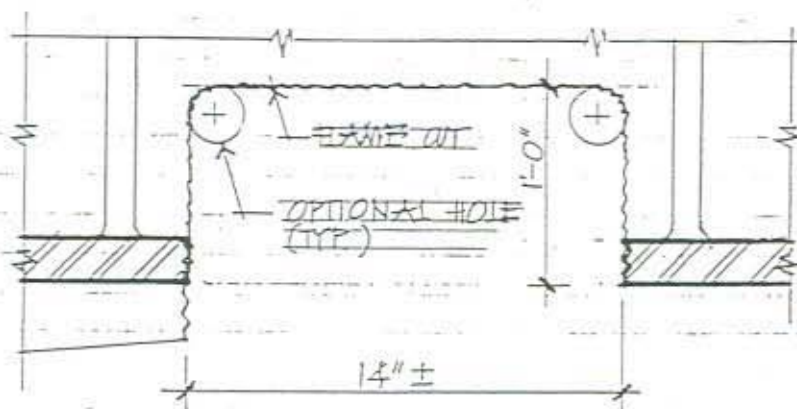
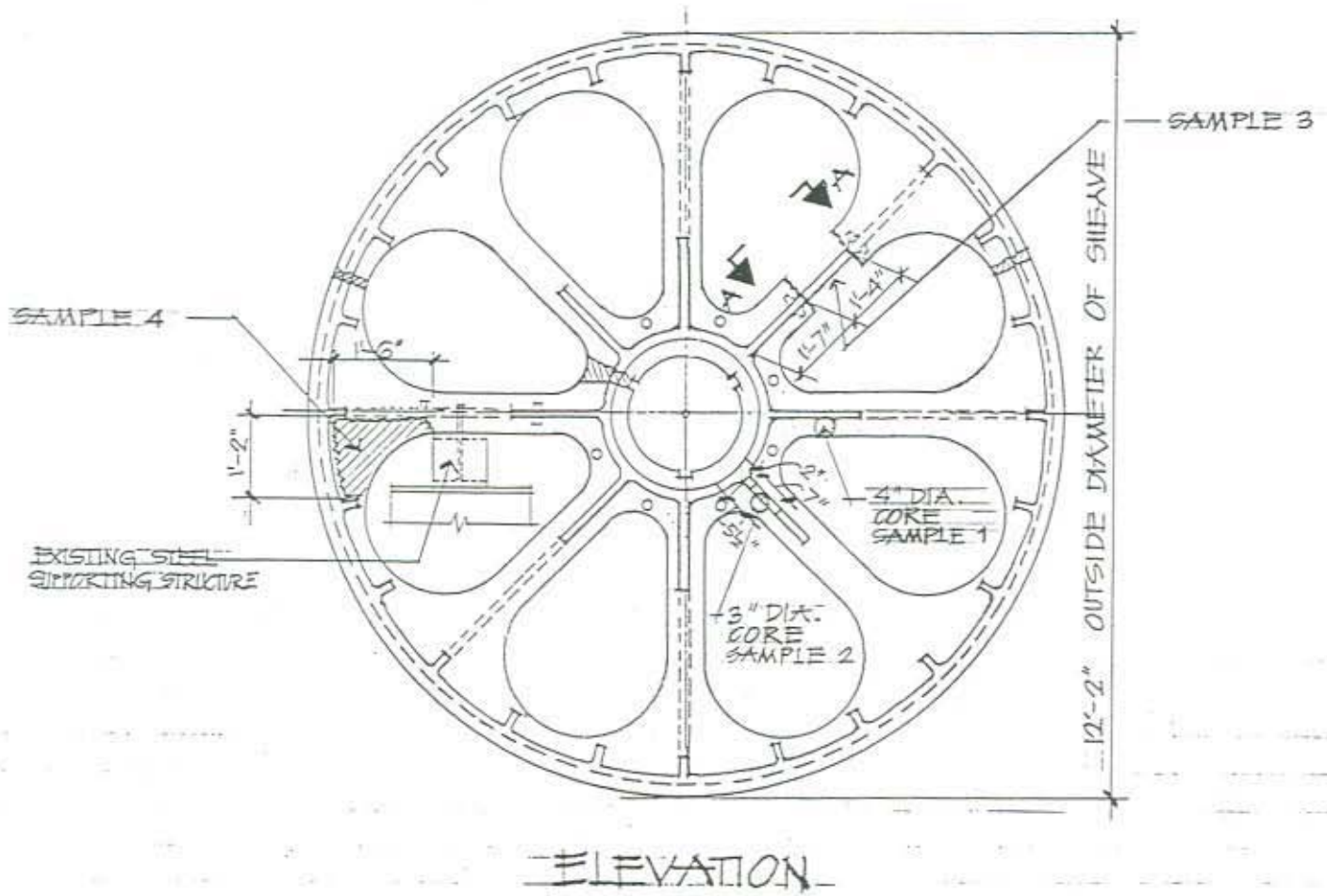


Fig. 3.1 – Magnetic particle testing of sheave spokes using prods



Fig. 3.2 – Apparent shrinkage crack detected in sheave by MT

WJE Wiss, Janney, Elstner Associates, Inc. 330 Pfingsten Rd., Northbrook, Illinois 60062	MADE BY BSB	SHEET NUMBER 1
	CHECKED BY MJK	PROJ. NUMBER 973010
WHEEL SAMPLES FOR MATERIAL TESTING AND SAMPLES CONTAINING CRACKS		DATE 01/04/99

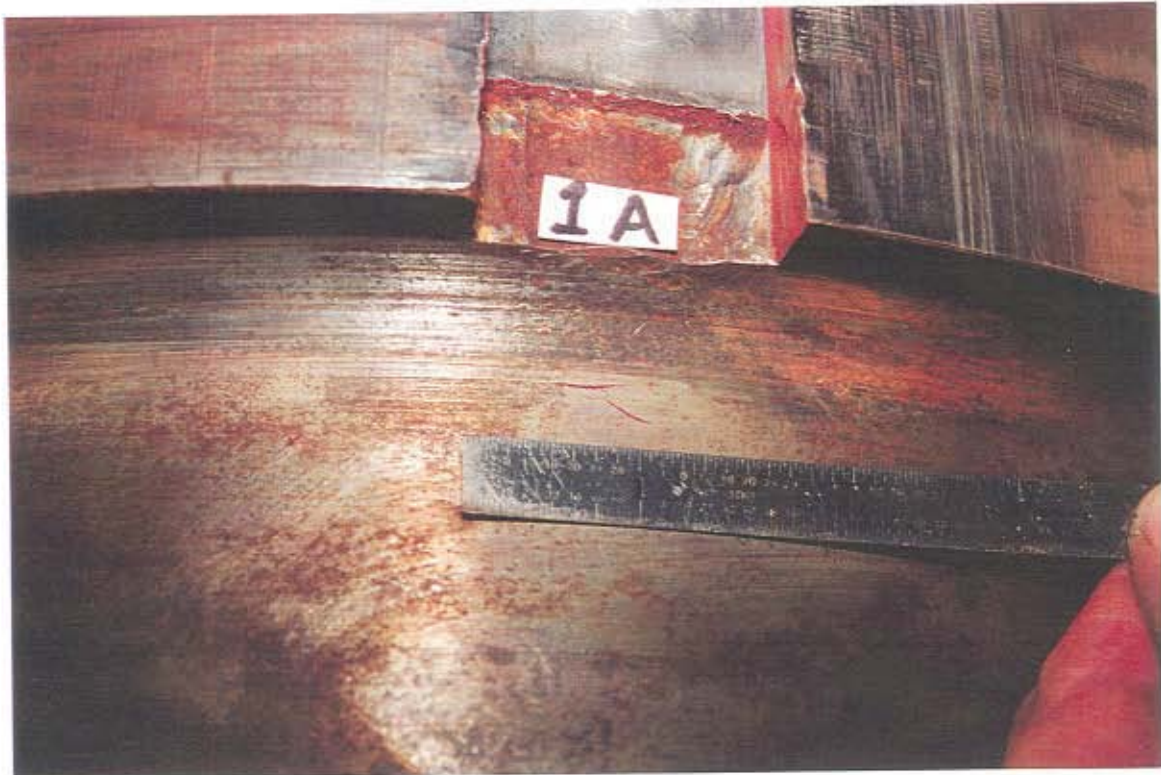


<u>SAMPLE NO.</u>	<u>DESCRIPTION</u>
1	4" DIA. CORE CONTAINING CRACK
2	3" DIA. CORE WITH GROUND CRACK
3	SPOKE & WEB PLATE SAMPLE FOR MATERIAL TESTING
4	SPOKE / RIM SAMPLE FOR MATERIAL TESTING

Fig. 3.3 – Sheave sample locations



Fig. 3.4 – Trunnion after removal from sheave and prepared for NDE



a) Defect 1A. Note random orientation of defects.



b) Defect 1B. Note dissimilar metals defining the weld filled oilway

Fig. 3.5 – Defects at keyways detected by MT examination

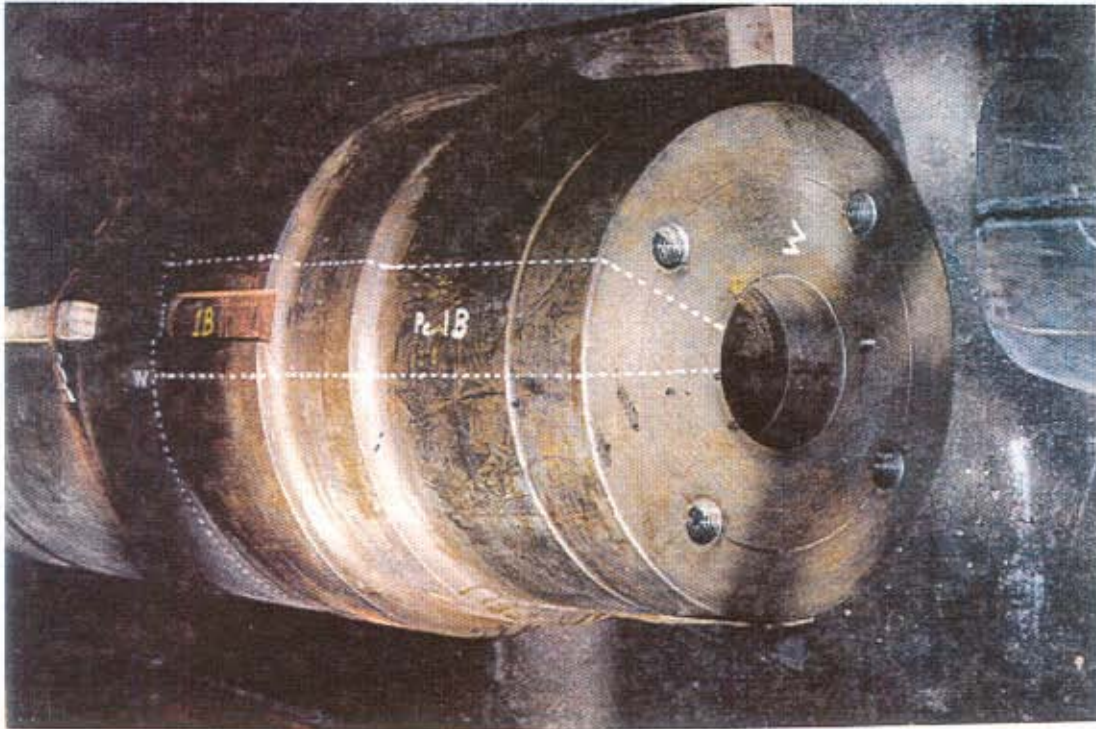


Fig. 3.6 – Trunnion prepared for sample removal

4.0 – DEFECT EVALUATION AND MATERIAL TESTING

Selected defects identified during the NDE work and removed under the sampling program were subjected to additional testing at ATLSS. This testing included both fractographic evaluation and metallographic cross sectioning. Material testing of the samples included chemical analyses to characterize the composition and assess weldability, tensile tests to determine yield and tensile strengths, Charpy-V notch and compact tension tests to quantify material toughness, and fatigue crack growth rate tests to aid in fatigue life estimates. A report prepared by Dr. Kaufmann and Dr. Fisher detailing the defect evaluation and material testing is included in Appendix B⁴.

4.1 – Trunnion Defect Evaluation

Seven defects were selected for additional fractographic or metallographic evaluation based upon the NDE work.

4.1.1 – Oilway weld defects – Surface defects aligned with keyway 1A and 1B using MT methods were subjected to fractographic examination. These defects were identified as 1A and 1B. Defect 1A measured $\frac{3}{4}$ in. wide and had a maximum depth of $\frac{1}{2}$ in. Similarly, defect 1B was $\frac{3}{8}$ in wide with a maximum depth of $\frac{3}{8}$ in. The dark discoloration exhibited on the crack surface is likely due to exposure to lubricants and air. Clear evidence of fatigue crack extension is seen on both crack surfaces after ultrasonic cleaning as shown in Figs. 4.1 and 4.2.

Viewing the crack surface of 1B with the scanning electron microscope (SEM) revealed a smooth, semi-elliptical crack growth region and an initial defect as shown in Fig. 4.3. Increased magnification of the semi-elliptical region verified the presence of fatigue striations while further magnification of the initial defect suggested its origin to be weld metal hydrogen cracking. Less conclusive fatigue crack extension was observed in 1A where several weld metal slag inclusions were identified. When viewed under higher magnification, semi-elliptical regions appeared fatigue-like although no fatigue striations could be seen.

The defect at keyway 3A was selected for metallographic cross-sectioning to characterize the subsurface defects identified by UT. The sample was cross-sectioned longitudinally along the weld

Wiss, Janney, Elstner Associates, Inc.

centerline. Numerous weld defects were found along the multi-pass weld, which included incomplete fusion defects and slag inclusions as shown in Fig. 4.4

4.1.2 – Internal trunnion defects – Four of the internal defects, UT1, UT2x, UT2z, and UT4, identified during UT examination were investigated. All four indications were internal near the center bore of the trunnion. A saw cut was made in two orthogonal directions at each of the positions determined by UT. With the exception of UT1, no defects were observed. The defect at UT1 was determined to be a shrinkage cavity measuring $\frac{3}{32}$ in. in diameter which occurred during original production of the trunnion. The defect at UT1 is shown in Fig. 4.5. No crack extension was observed microscopically. Due to the small size of UT1, the other defects could have been removed or missed during cutting.

4.1.3 – Keyway retainer fillet weld cracks – The retainer weld from keyway 1B was examined metallographically. The sample was cross-sectioned as shown in Fig. 4.6 where the weld crack is visible. No crack extension into the trunnion base metal was found. The weld metal was identified as austenitic stainless steel.

4.2 – Sheave Defect Evaluation

The two cores removed from the sheave were cross-sectioned and examined metallographically. Sample #1 showed multiple surface cracks between $\frac{3}{16}$ in. to $\frac{1}{4}$ in. deep surrounding a large internal shrinkage cavity measuring 1 in. long. The shrinkage cracks were most likely a result of hot tearing during cooling and shrinkage of the sheave casting in the vicinity of the void as seen in Fig. 4.7. No fatigue crack extension of the crack tip regions was observed under microscopic examination. The cracks found in Sample #1 should have experienced fatigue crack propagation due to the expected low threshold stress range for cracks of these depths. This strongly suggests that the stress ranges at this location in the sheave were low.

The crack surfaces in Sample #2 were removed by grinding during the MT work before the sample was removed; therefore, no comment could be made as to the origin or growth of the crack. A sub-surface cavity similar to the one found in Sample #1 was identified. This is the most likely source of the MT indications.

4.3 – Sheave/Trunnion Assembly Material Properties

The material evaluation included a chemical composition and weldability study, microstructure examination, tensile property tests, Charpy V-notch tests, compact tension tests, and fatigue growth rate tests.

Two trunnion and sheave locations were selected for material evaluation. For the trunnion, one sample was selected from the outside surface while another was selected near the center bore to account for the gradient in properties expected in a large forging. For the sheave, Sample #3 was removed from a spoke area while Sample #4 was taken from the rim/spoke intersection. The two sheave samples were extracted from material that had measured thickness of 1 ³/₈ in. and 1 ¹/₂ in., respectively.

4.3.1 – Chemical composition and weldability – Chemical composition analyses for the trunnion and sheave samples were performed by a commercial testing laboratory by standard optical emission spectroscopy. The overall composition of the trunnion is similar to a modern day 1040 carbon steel used in forgings.

The weldability of the trunnion would not be considered very good. The relatively high carbon content (0.39 wt% at outside sample) and carbon equivalent (0.44 at outside sample) would make welds susceptible to hydrogen cracking. In addition, a low manganese to sulfur ratio (Mn/S =15) in combination with the high carbon levels have been shown to cause increased susceptibility to heat affected zone (HAZ) hot cracking. To avoid HAZ cracking, careful control of hydrogen and high preheat temperatures for welding would be required. The cracking observed at the weld-filled oilways is consistent with the hot cracking observed fractographically.

The sheave chemical composition was found to correspond to a modern day 1030 carbon steel composition used in castings. Proper welding of the casting should not be difficult.

4.3.2 – Tensile properties – Standard tensile specimens were fabricated from the four material samples. The trunnion specimens were oriented parallel to the trunnion axis. The tensile information is provided in Table 4.1. Tensile elongation exceeded an average of 20 percent for all specimens except sheave Sample #3 which contained a small casting defect.

Table 4.1 - TENSILE PROPERTIES

Specimen	Avg. Yield Point (ksi)	Avg. Tensile Strength (ksi)
Trunnion	36	75
Sheave	37	72

4.3.3 – Fracture toughness and fatigue crack growth rate – At the same four sample locations, standard Charpy V-notch (CVN) test specimens were fabricated and tested. Eighteen specimens were fabricated at each location to permit the tests to be performed over a range of test temperatures, which included the transition temperature range. Room temperature CVN energy for both the trunnion and sheave samples averaged about 7 ft-lbs with an upper shelf average energy value of 57 ft-lbs and 42 ft-lbs at 275 degrees F for the trunnion and sheave, respectively.

The static fracture toughness of the trunnion material at a minimum service temperature of -10 degrees F is represented by a dynamic toughness at 150 degrees F. Using the Barsom-Rolfe CVN- K_{IC} temperature shift correlation, the average static fracture toughness of the trunnion at the minimum service temperature would be $K_{IC}=64 \text{ ksi-in}^{1/2}$. Similarly, an average $K_{IC}=55 \text{ ksi-in}^{1/2}$ was calculated for the sheave.

To obtain a more direct measure of the static fracture toughness, standard compact tension tests were fabricated and tested for one trunnion and sheave sample. Four test specimens from each of the two samples were fabricated with one duplicate pair being tested at the minimum service temperature of -10 degrees F and the other pair at room temperature. Specimens P1 through P4 were machined from trunnion material while specimens S1 through S4 were machined from sheave material.

The behavior of the sheave and trunnion samples was very similar despite one being forged and the other cast. All of the specimens failed brittlely with only a small amount of crack tip plasticity when tested at the minimum service temperature. Similar failures, with slightly more plasticity, were observed at tests performed at room temperature. Figure 4.8 compares the crack tip plasticity regions for two trunnion samples at -10 degrees F and 68 degrees F, respectively.

The J_{IC} fracture toughness was computed as $J = J_{elastic} + J_{plastic}$ and subsequently converted to an approximate K_c . At the minimum service temperature, $K_c=58 \text{ ksi-in}^{1/2}$ and $K_c=50 \text{ ksi-in}^{1/2}$ for the trunnion

Wiss, Janney, Elstner Associates, Inc.

and sheave, respectively. These results indicate good agreement with the K_{IC} values calculated from the CVN test data. Reference Dr. Kaufmann's and Dr. Fisher's report in Appendix B for a more complete discussion of the compact tension tests.

Standard fatigue crack growth rate tests were also performed on both materials using automated PC controlled testing software. Using duplicate specimens for each sample, the crack growth rate behavior (da/dN vs. ΔK) was established. To generate growth rate test data similar to full reversal conditions, specimens were tested at a low stress ratio ($R=0.1$). Using the da/dN vs. ΔK plots and regression analysis indicated a $\Delta K_{th} \cong 10 - 11 \text{ ksi-in}^{3/2}$. However, because crack closure effects influenced data at the lower growth rates, the actual thresholds are likely lower. Reference Section III.5, Page 9 in Appendix B for a more complete discussion and test data.

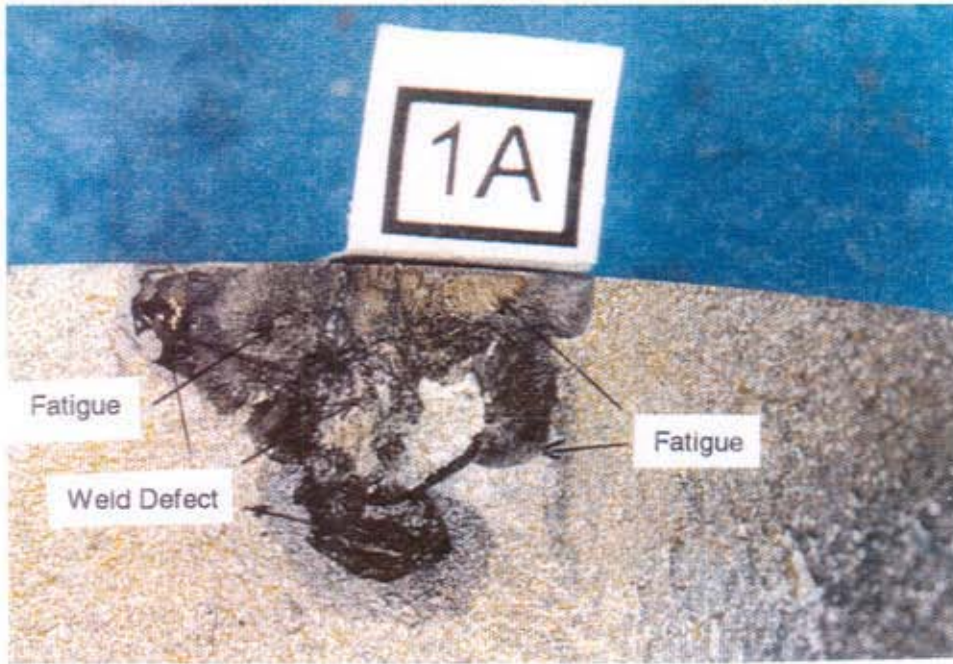


Fig. 4.1 - Initial defects at keyway 1A with fatigue crack extension after ultrasonic cleaning. (ATLSS)

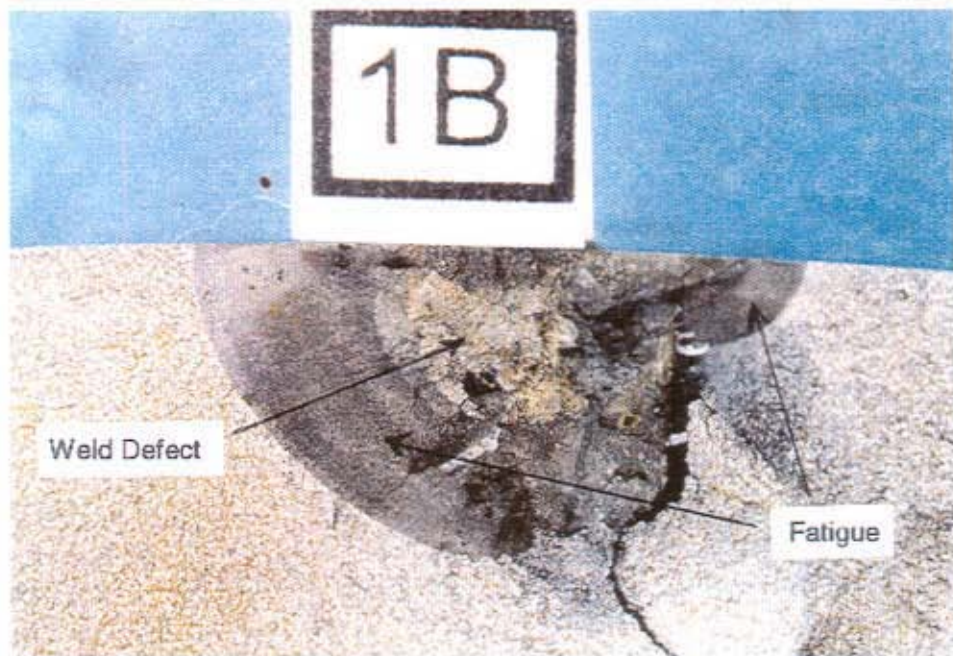


Fig. 4.2 - Initial defect at keyway 1B with fatigue crack extension after ultrasonic cleaning. (ATLSS)

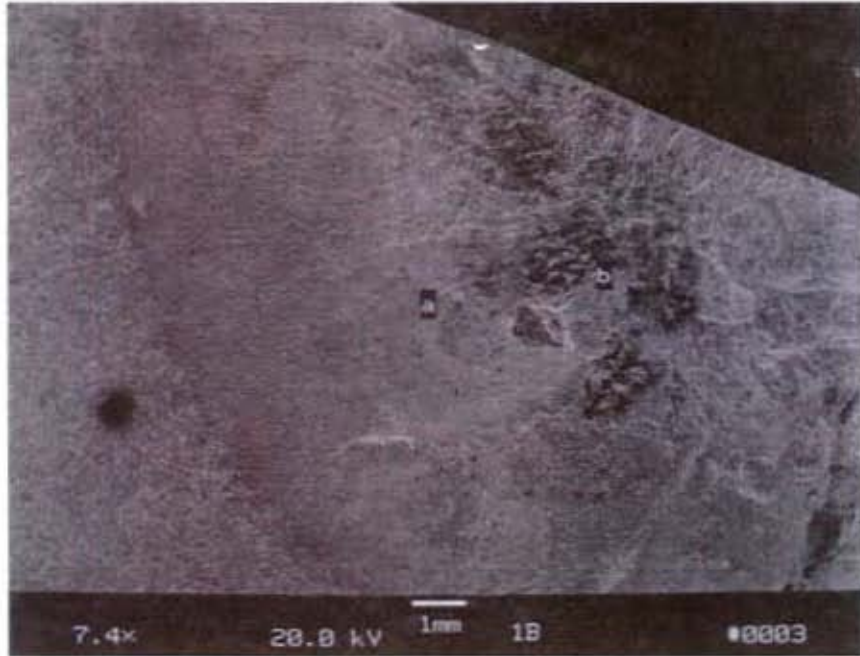


Fig. 4.3 – Semi-elliptical crack growth region shown under SEM Mag. 7.4x. (ATLSS)

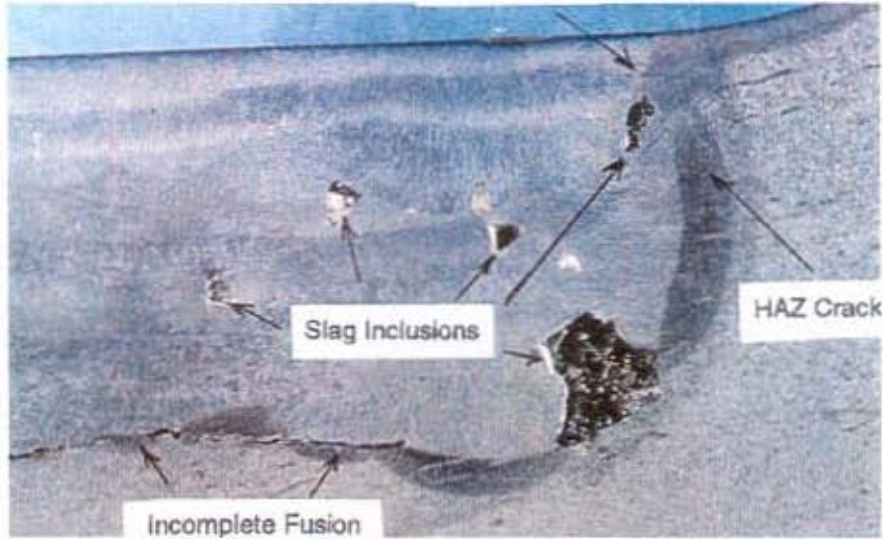


Fig. 4.4 – Numerous weld defects at keyway 3A after metallographic cross-sectioning. (ATLSS)

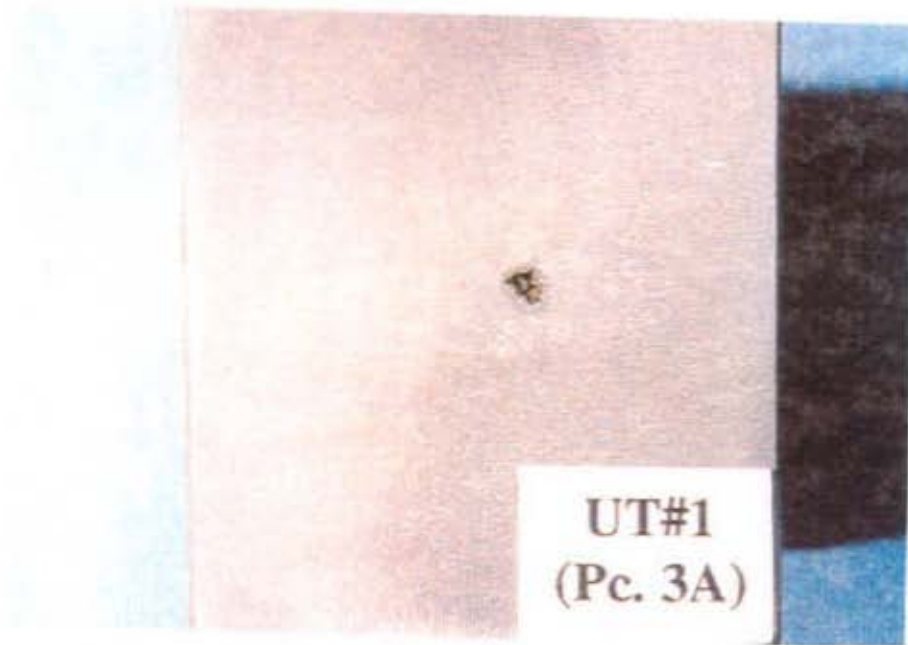


Fig. 4.5 – Internal shrinkage cavity within trunnion. (ATLSS)

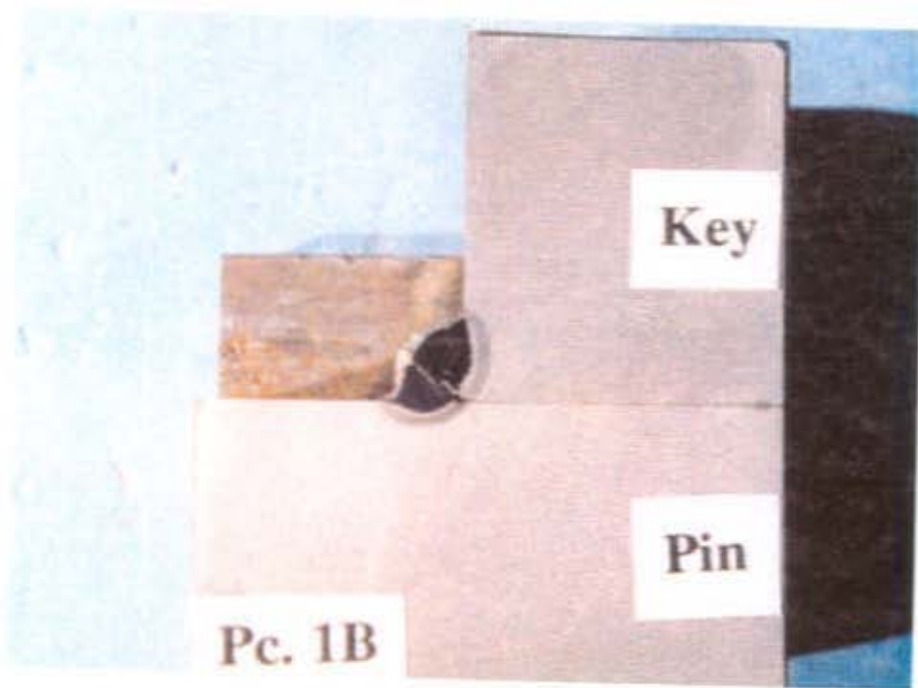


Fig. 4.6 – Cracked retainer weld at Keyway 1B. (ATLSS)

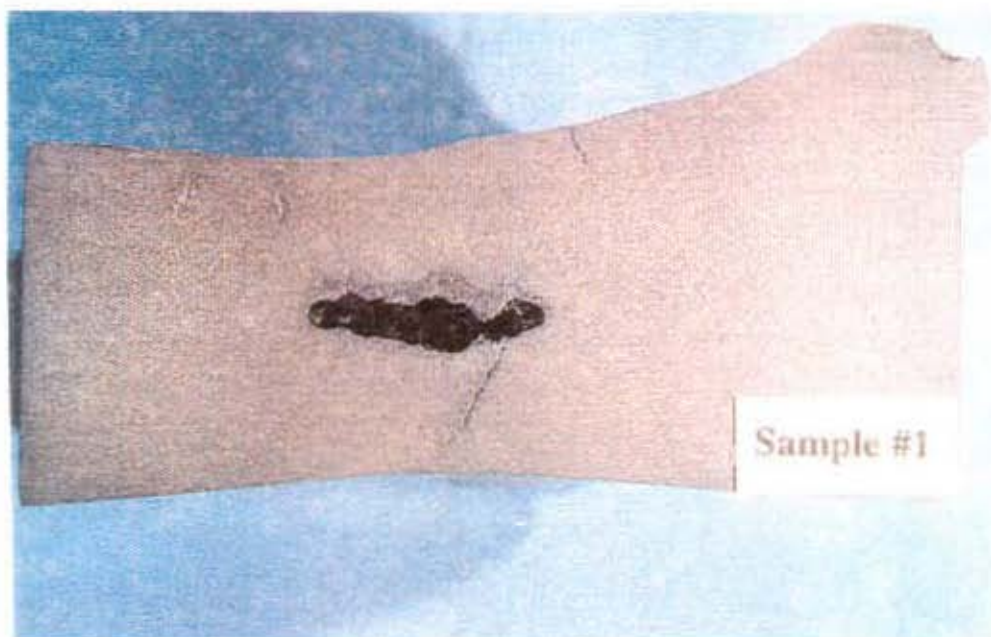
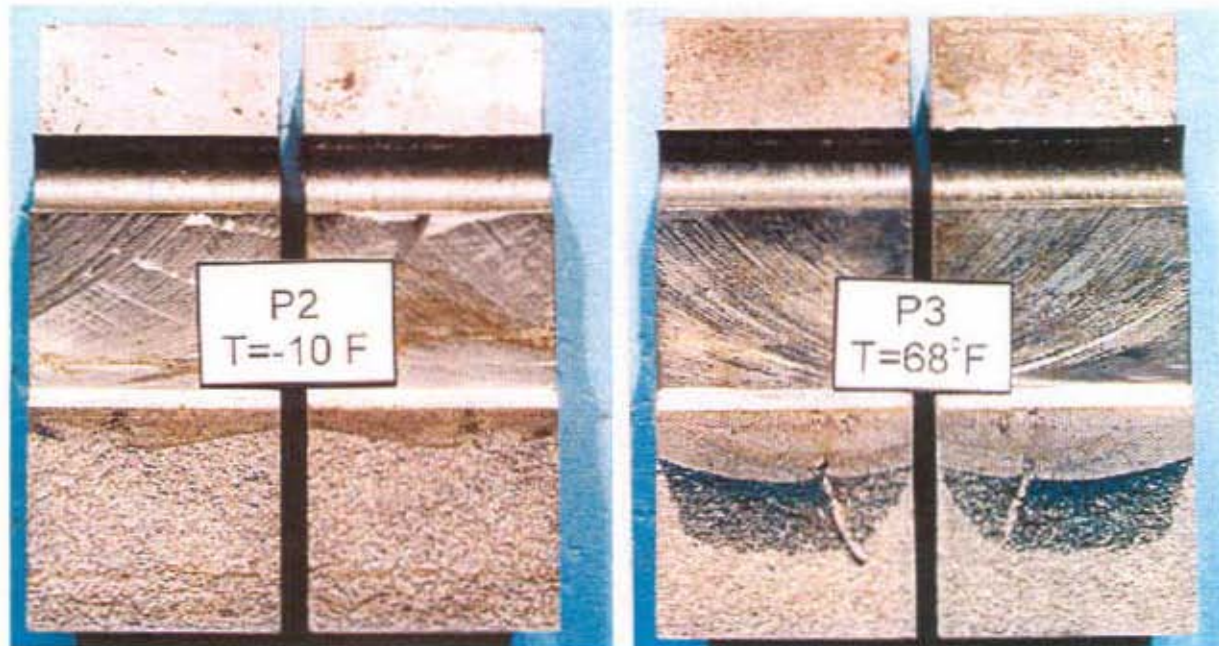


Fig. 4.7 – Internal shrinkage cavity in sheave Sample #1. Note shrinkage cracks initiating from defect. No indications of fatigue crack extension were observed. (ATLSS)



a) Sample P2 tested at -10 degrees F

b) Sample P3 tested at 68 degrees F

Fig. 4.8 – Compact tension specimens from trunnion comparing fracture surfaces

5.0 – UT PROCEDURES AND TESTING OF SOUTH TOWER TRUNNIONS

Inspection of the two remaining, in-service trunnions located in the south tower of the I-5 Columbia River Bridge was performed in July 1999. Ultrasonic techniques and procedures were specifically developed for the inspection. A trunnion calibration standard fabricated with material cut from the previously removed northeast trunnion aided the interpretation and characterization of the ultrasonic indications. Several ultrasonic indications were detected near critical locations in both trunnions; however, no cracks could be positively identified.

5.1 – Inspection Procedures

The south tower sheave/trunnion assemblies are identical to the removed assemblies from the north tower. The configuration and dimensions of the south trunnions, including keyways, threaded bolts holes, and oilways are as shown in Chapter 1, Fig. 1.4. Access for inspection was limited to the center bore and the end surfaces.

Procedures for field inspection of the south trunnions were similar to the procedures performed on the removed trunnion. A Krautkramer-Branson ultrasonic flaw detector was used for all inspections. Initial inspections with longitudinal axial scans from the end surfaces were used to determine length and to detect major discontinuities. An additional scan from the end surfaces was conducted using a longitudinal transducer with an incident angle of 12 degrees oriented towards the outside radius of the trunnion. The 12 degree scan is designed to detect cracks originating at the trunnion surface that are oriented transverse to the axis and to offer an alternate orientation of the sound beam for better characterization of detected indications.

Prior to inspection, the accessible trunnion surfaces were cleaned and prepared for ultrasonic scanning as shown in Fig. 5.1. ODOT personnel removed covers and bearing retainers from the trunnion ends and cleaned lubricant from the center bore and end surface. The end surfaces were smoothed using course grit emery cloth while a beaded hone was used to prepare the center bore surface for scanning. Some scale within the bore had to be removed by chipping before scanning. Calibration of the ultrasonic flaw detector and the various transducer assemblies was performed using several test standards including a Type 2 IIW calibration block, a trunnion calibration standard fabricated with material from the north

Wiss, Janney, Elstner Associates, Inc.

trunnion, and mild steel test blocks for correction and verification of contoured transducer distance calibrations. The trunnion calibration standard is illustrated in Fig. 5.2.

The inspection procedures established for the south trunnions entitled *Ultrasonic Examination Procedure for South Tower Trunnions for the I-5 Columbia River Bridge* are presented in Appendix C. All aspects of the ultrasonic examination including surface preparation, instrument and transducer calibration, scanning techniques and procedures, documentation of signal trace deflections, evaluation of indications, as well as instrument and personnel requirements and qualification are contained within the procedures.

5.2 – Ultrasonic Scans of Trunnions

Five different ultrasonic test scans were used in the examination of the trunnions. Initial axial scans were performed using a straight beam transducer with the instrument calibrated at a range of 100 in. Overall trunnion length was established based on the back reflection from the distant end of the trunnion. A second straight beam scan was employed with the instrument calibrated at a sound path range of 20 in. This provided a broader signal trace spread for better definition of near end indications. A third straight beam scan from within the center bore provided evaluation of sound transmission quality, distance to the outside radius and location of trunnion keyways as well as partial evaluation of the oilway welded filler metal fusion quality. Keyway locations were identified for purposes of orientation. Three punch marks were made at the trunnion end face to identify each keyway location. The nominal 45 degree scan from within the center bore in conjunction with the nominal 12 degree axial scan from the trunnion end were the primary scans used to interrogate critical areas of the trunnions.

Several conditions of interest were identified during the UT examination that may affect the inspection and evaluation of trace indications. Perhaps of greatest significance is the poor fusion quality observed in association with weld metal filled oilways. This condition may be the source of some of the indications or it may be masking other discontinuities from detection. In addition, the alignment of the center bore was observed to drift off of center alignment along its length, which resulted in some variance in sound path lengths during center bore scans.

Wiss, Janney, Elstner Associates, Inc.

Indications of significance were identified only in the vicinity of the keyways and former oilways. Several discontinuities were characterized as cracks originating in filler metal of the oilways and cracked retainer welds at keys. A summary of significant indications is presented in Table 5.1.

5.3 –Discussion of Ultrasonic Indications

Ultrasonic signal trace deflections require careful analysis for characterization and evaluation. Location and orientation, signal strength, trace profile, and data from alternate scanning angles were all components of the evaluation process. A variety of conditions may affect the collected data, such as couplant and surface condition (particularly within the center bore), measurement to the entry point of the transducer, and transducer and flaw detector calibrations. Geometric features of the trunnion, embedded inclusions, and poor weld fusion quality within weld-filled oilways are the source of most spurious indications. Even under the most favorable scanning conditions, some small indications may still be difficult to characterize.

Indications detected from straight beam axial scans were typically characterized as nonmetallic inclusions. Such discontinuities have been present in the trunnion since its original forging. Detected inclusions were randomly distributed and relatively small (less than $3/16$ in. diameter). Embedded discontinuities did not affect the inspection with respect to detection of cracks in critical areas of the trunnion.

A reduced sound path distance observed when using the straight beam transducer within the center bore identified lack of fusion between the weld-filled oilways and the trunnion base metal or between the individual passes of the weld filler metal within the oilway. Although frequently detected in both trunnions, non-fusion was intermittent and randomly located along the filled oilways.

Axial scans using a 10 to 12 degree longitudinal angle beam transducer with the beam oriented towards the outside radius are capable of detecting most significant discontinuities. The slight beam angle may prohibit detection of many of the embedded discontinuities. Also, the low incident angle with respect to the poorly fused oilway welds may result in a reflection of the beam away from the critical inspection areas. Cracks however, that have propagated beyond the oilways into the trunnion base metal will generate a discernable reflection.

Wiss, Janney, Elstner Associates, Inc.

The nominal 45 degree transducer used within the bore is theoretically capable of detecting early cracking and or significant discontinuities. Interpretation of the scan requires a precise understanding of the axial and radial position of the transducer as well as an accurate determination of the transducer incident angle. The actual transducer angle used in the 1999 inspection measured 42 degrees as calibrated on the trunnion standard.

The initial results of the UT work identified several indications of concern. Follow-up study of recorded data, transducer position, beam characteristics, and incident angle suggested that most of these indications were not where they initially were thought to have occurred. From the study, it was determined that sound path distances beyond the "first leg" were not reliable for characteristic evaluation. In addition, the signal trace amplitudes were found to be sensitive to transducer contact and couplant distribution. Considering these findings, many of the indications most likely originated in the keyway fillet welds or from the weld fill metal discontinuities.

All indications identified as possible cracks occurred in the vicinity of the oilways. The maximum estimated depth for suspected cracks was approximately $\frac{1}{2}$ in., the design depth of the oilway. Therefore, no crack extension into the trunnion base metal was detected. Crack extension into the outer surface of the trunnion was not identified due to the shielding effects of the poorly fused weld-filled oilways.

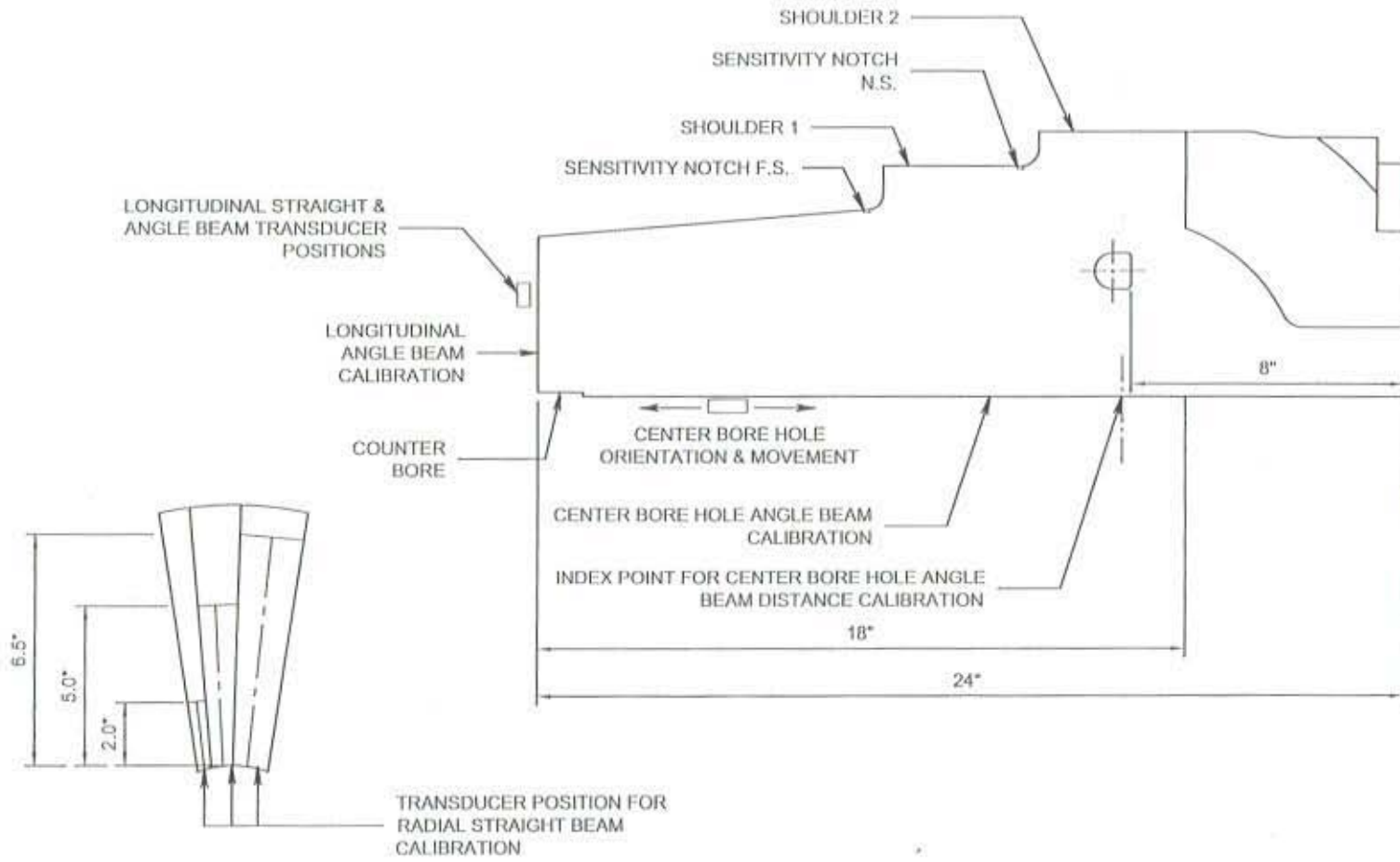
Detection of crack growth in critical areas of the trunnion is highly probable with careful use of the WJE UT procedure. In most cases cracks below the critical size should be detected with use of an axial angle beam scan. Implementation of the nominal 45 degree bore scan virtually assure early detection of discontinuities outside the weld filled oilways while providing an alternate orientation for defect evaluation and characterization.

Table 5.1 – SUMMARY OF 1999 ULTRASONIC EXAMINATION OF SOUTH TOWER TRUNNIONS

Trunnion	End	Scan	Azimuth	Distance from End	Notes
South East	East	45°(S) Bore	200°	8.8	Possible embedded inclusion. Low signal response amplitude.
	West	45°(S) Bore	Full	9.44	Near outer surface - possible machine groove. Moderate signal response amplitude.
		45°(S) Bore	Full	13.48	Near outer surface - possible machine groove. Moderate signal response amplitude.
		45°(S) Bore	80°	14.1	Near outer surface - possible crack or weld discontinuity. Moderate signal response amplitude.
	West	45°(S) Bore	Full	8.7	Near outer surface - possible machine groove. Moderate signal response amplitude.
		45°(S) Bore	Full	12.61	Possible machine groove. Moderate signal response amplitude.
		45°(S) Bore	180°	14.35	Near outer surface and transition to 2nd shoulder. Low signal response amplitude - possible crack or fill weld discontinuity
12°(L) Axial		175°	15.4	Approx. at keyway - possible feather key track weld. Moderate signal response amplitude.	
South West	East	45°(S) Bore	180°	14.0 - 14.5	Possible crack or discontinuity in fill weld. Moderate signal response amplitude.
		12°(L) Axial	175°	14.0 - 14.5	Possible crack or discontinuity in fill weld. Moderate signal response amplitude.
	West	0°(L) Axial	90°	8.5 & 8.8	Non-Metallic (N.M.) Inclusion 1.0 - 1.5 from bore surface. Moderate signal response amplitude.
		12°(L) Axial	175°	8.5 & 8.8	Non-Metallic (N.M.) Inclusion 1.0 - 1.5 from bore surface. Moderate signal response amplitude.
		0°(L) Axial	178 - 185°	8.5 & 8.8	N.M. Inclusion 4.5 from bore surface. Low signal response amplitude.
		45°(S) Bore	180°	8.78	Minor discontinuity. Low signal response amplitude.
		0°(L) Axial	270°	9.25	N.M. Inclusion 2.75 from bore hole
		45°(S) Bore	45°	11.15	0.6+/- from outer surface - possible crack or discontinuity in fill weld. Low amplitude.



Fig. 5.1 – Preparation of south tower trunnion for ultrasonic examination



* ACTUAL SOUND PATH IS APPROXIMATELY 0.05 LESS THAN INDICATED. REFER TO PROCEDURES FOR RADIAL STRAIGHT BEAM CALIBRATION

Fig. 5.2 – Ultrasonic Calibration Standard

6.0 – FIELD TESTING AND ANALYSIS OF SHEAVE WHEEL

A field testing program was carried out by ODOT³ on the counterweight sheave wheel of the I-5 Columbia River Bridge in 1996 to provide information about live load stress levels in the sheave wheel during bridge lift operations. The measured stress range data was also used to verify the finite element analysis performed by DGES Inc.³

6.1 – Instrumented Areas

Two uniaxial weldable strain gages were attached to the sheave wheel at locations determined by the finite element analysis to exhibit high stresses. Gage 1 was welded on the under side surface of the transverse rim stiffener. Gage 2 was installed on the spoke flange tip at the tangency point of the spoke and large radius near the rim of the wheel. Figure 6.1 shows the layout and numbering of the two strain gages. Photographs of the instrumented sheave wheel are provided in Fig. 6.2.

6.2 – Measured Stresses

Figure 6.3 shows the change in stress at Gages 1 and 2 computed from measured strain during the lifting and lowering operation of the span. Both gages were zeroed at the fully seated or closed position. The lift span was raised to the maximum height of 135 ft resulting in $4 \frac{2}{3}$ rotations of the sheave wheel. The lift span was held at the maximum height for about 90 seconds and then lowered to the seating position. Strain data was converted to stress using the equation $S = \epsilon E$ where ϵ is strain recorded from the response and E is the Modulus of Elasticity for steel 29×10^6 psi.

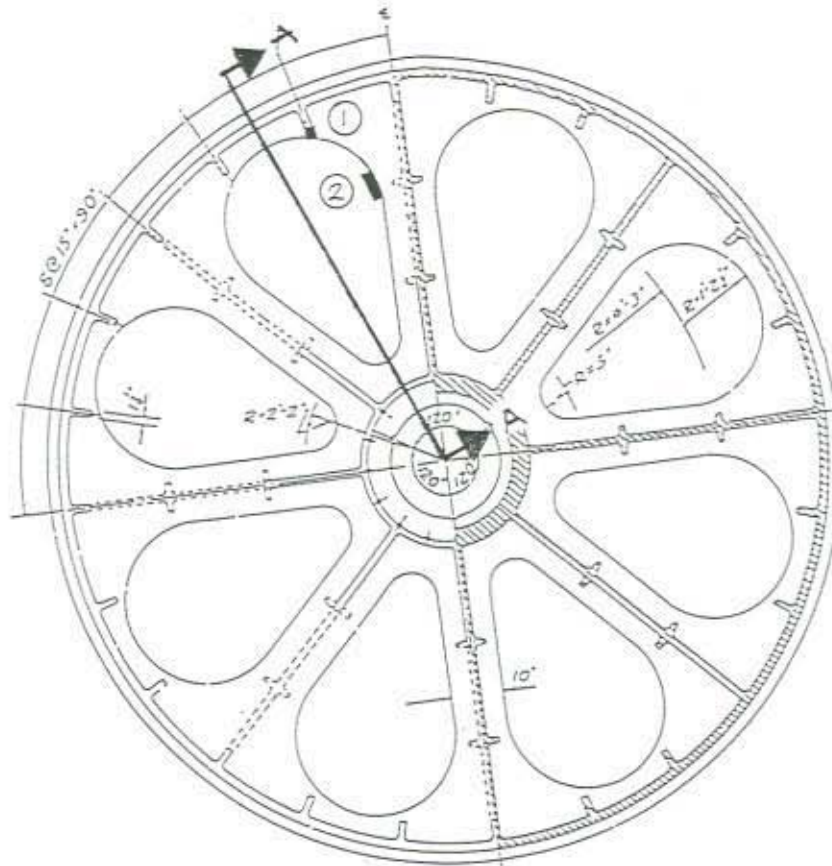
Gage 1 located on the rim stiffener reveals a stress range of approximately 19.0 ksi. Note that since Gage 1 was zeroed when the stiffener was subjected to maximum tensile stress, the response remains totally in the compressive range. Gage 2 located on the flange tip of the spoke exhibits a stress range of approximately 31.0 ksi.

6.3 – Comparison of Measured and Analytical Stresses

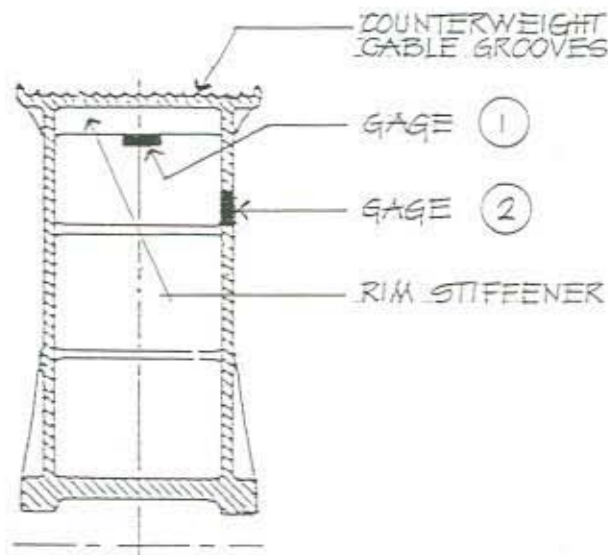
DGES Inc. was retained by ODOT to conduct a counterweight sheave analysis and design for the two new replacement sheaves. A major portion of their work was the analysis of the existing sheave wheel that included both simplified analysis and finite element analysis (FEA). For the Gage 1 location, rim stiffener, the FEA calculated a stress range of 17.2 ksi for the total wire rope force of 613 kips.

Wiss, Janney, Elstner Associates, Inc.

Assuming the DGES model to be correct, the ratio of measured to calculated is $19.0/17.2 = 1.10$ or within 10 percent. This suggests excellent agreement between actual and predicted stresses. For the Gage 2 location, spoke flange tip, the FEA calculated a stress range of 28.5 ksi for a total wire rope load of 613 kips. Comparing the DGES model values to the field test measurement results in a ratio of $31.0/28.5 = 1.09$ or within 9 percent. Again this indicates excellent agreement between the FEA model and field testing results. Note that the total wire rope load was measured by WJE during the north tower trunnion replacement and was found to be approximately 720 kips. This results in values within 6 and 8 percent.

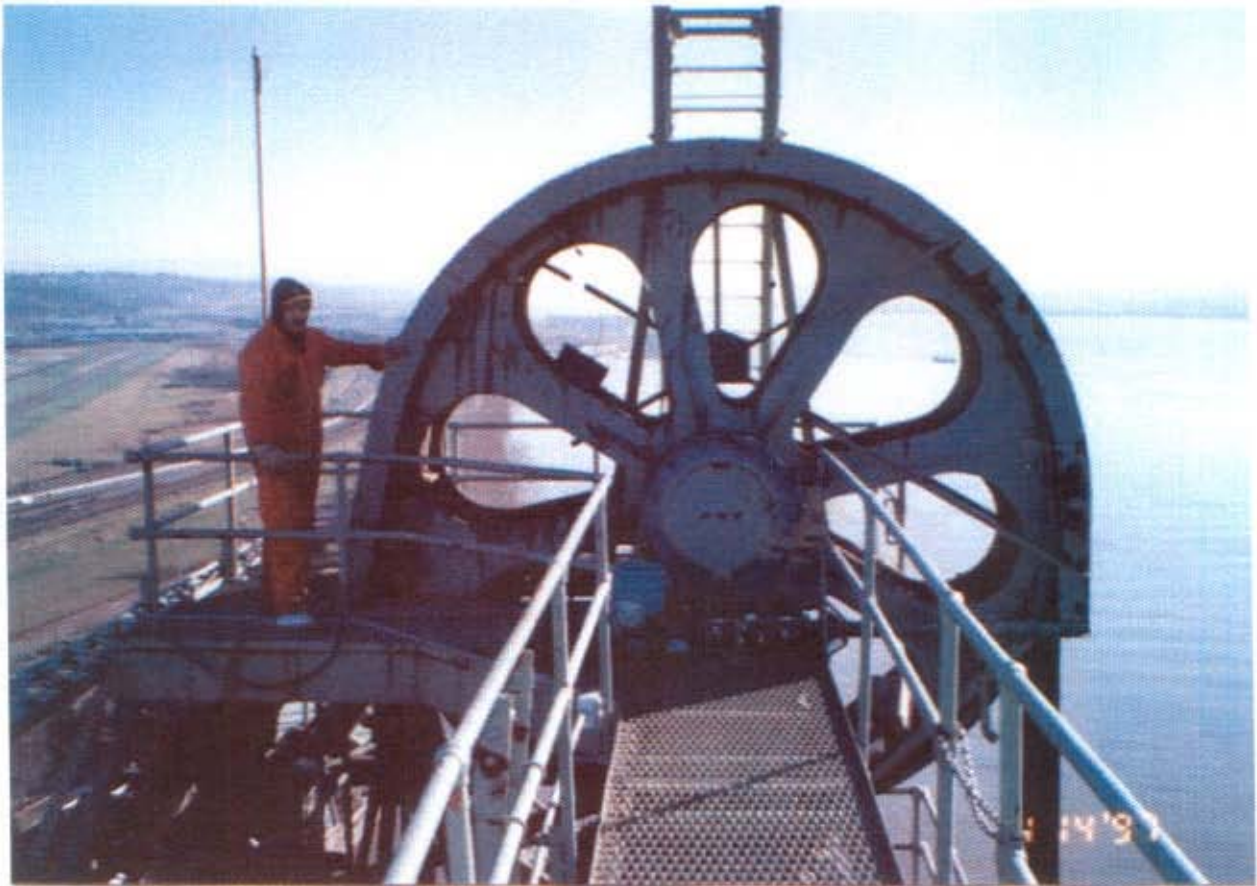


SHEAVE WHEEL ELEVATION SHOWN IN APPROXIMATE ORIENTATION WITH LIFT SPAN SEATED

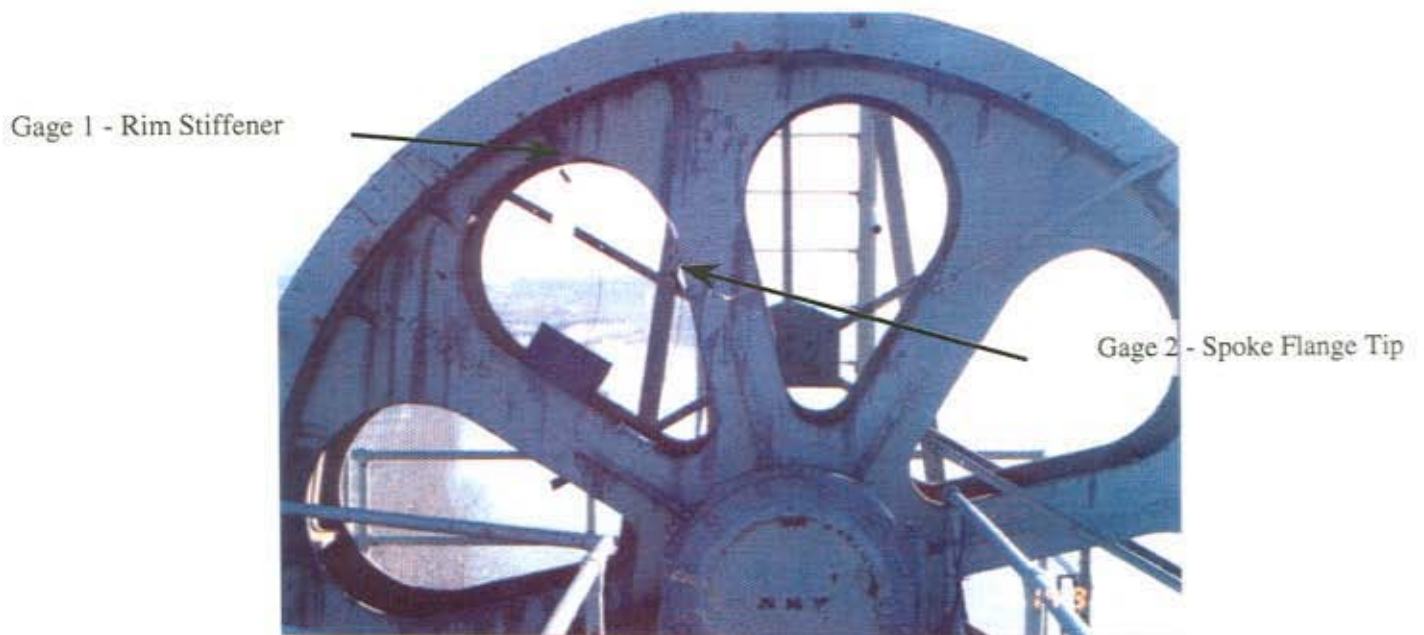


SECTION A-A (HALF SECTION THROUGH WHEEL)

Fig. 6.1 – Location of sheave wheel strain gages

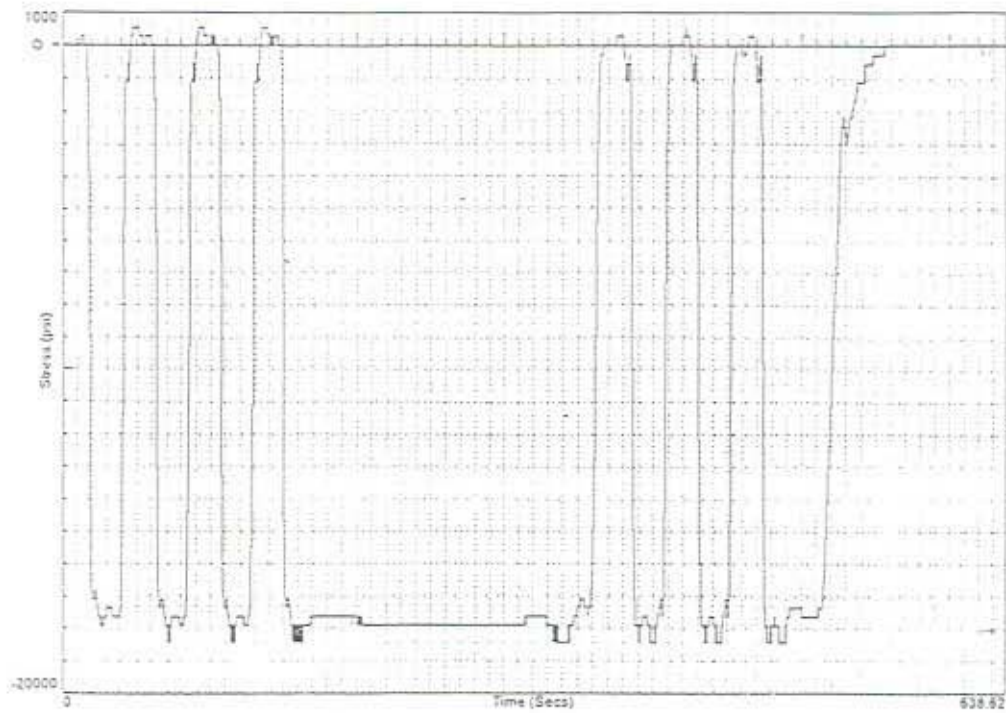


a) Overall view of Northeast sheave

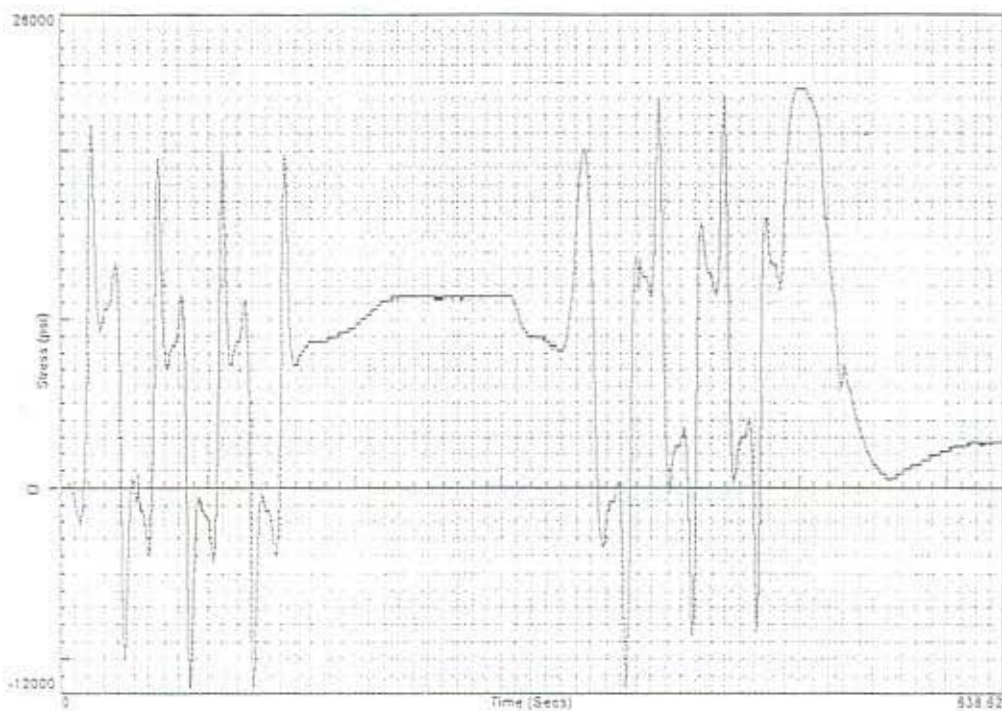


b) Close-up view showing instrumented web opening

Fig. 6.2 – Instrumented sheave wheel



a) Gage 1, rim stiffener



b) Gage 2, spoke flange tip

Fig. 6.3 – Dynamic stress response measured during lifting and closing of bridge

7.0 - SERVICE LIFE ESTIMATE

As discussed in Chapter 4, the oilway weld defects were the only defects in both the trunnion and sheave, which exhibited indications of fatigue crack extension. The locations of these defects were consistent with maximum outer fiber bending stresses in the trunnion and their close proximity to the machined radius and keyway stress concentration effects. Because no evidence of crack extension was observed from the internal defects, the service life analysis focused on the weld-filled oilway with defect IB for which crack extension due to fatigue was observed and for which striation spacing could be measured.

7.1 - Load History

7.1.1 - Other lift span bridge fatigue histories: - In recent years, a number of shafts and trunnions used in lift bridges that were designed or built prior to the 1960's have developed fatigue cracks; some of which have occasionally fractured the shaft. Cracks have developed at keyways and at changes in the shaft diameter when the trunnions experienced several reversal stress cycles during each lift and lowering of the structure. Rotations of more than 180 degrees result in a complete reversal in the stress cycle.

Specifications used to design movable bridges evolved from the ASEA Specifications. The allowable bending stresses for trunnions up to 1983 were taken as 15 ksi for ASTM A608 Class C steel when the rotation was more than 180 degrees. In the structures that experienced cracking, the tension design stress was between 9.8 ksi and 17 ksi.

Table 7.1 provides a summary of stresses and rotations experienced by structures that developed cracks in the trunnions at the radius. Note that two of the sheaves had the trunnion welded to the shaft. Those welds occurred on the major diameter of the shafts.

It can be seen that the I-5 trunnion crack is consistent with the general behavior observed in other structures. Fatigue cracking has developed at a weld repair and exceeds Category C for the Columbia River Bridge. However, based on the experience with these other structures, significant residual life should exist as the stress range will rapidly decrease as the crack extends out of the high stress concentration region.

Wiss, Janney, Elstner Associates, Inc.

Finally, it should be noted that only two of these structures experienced complete failure of the trunnion shaft. One was the Valleyfield structure and the second was St. Lambert over the St. Lawrence Seaway⁴. Note that both of these bridges experienced in excess of 700,000 stress cycles.

7.1.2 – I-5 Bridge loading history – Based upon the bridge service log, the bridge typically lifts between 500 and 700 times per year since its retrofitting in 1960. Each standard 90 ft lift requires a total of approximately six revolutions of the sheave/trunnion assembly to raise and lower the bridge resulting in between 3000 and 4200 cycles per year. Therefore, the removed sheave/trunnion assembly has experienced between 111,000 to 155,400 cycles since it was retrofitted and subsequently removed in 1997.

As described in Chapter 6, the stress range in the sheave was measured at two locations to verify analytical work performed by DGES, Inc. The field measurements found the stress range at the rim stiffener and spoke flange tip to be 19.0 ksi and 31.0 ksi, respectively. No fatigue cracking was observed at defects extracted from these regions.

Stresses for the trunnion calculated by ODOT indicate a stress range of 19.6 ksi for the full lift cycle ($2 \times \sigma_{\max} = 9.8$ ksi). Stress calculations by WJE suggest the maximum trunnion stress range is approximately 15 ksi. The difference in stress range between ODOT and WJE is a result of assuming different points of bearing. In either case, the full stress range is applicable considering the high residual stresses, which exist in the weld-filled oilways. The machined radius at the shoulder would increase this by the stress concentration factor $K_t \cong 2.2$.

The stress intensity range, ΔK , at defect 1B was estimated using the measured striation spacing observed under the microscope and the crack growth relationship for steel ($da/dN = 3.6 \times 10^{-10} \Delta K^3$). The striations measured 1.18×10^{-5} in. resulting in a stress intensity range, $\Delta K = 32$ ksi-in^{1/2}.

7.2 – Sheave Fatigue Life Estimate

A substantial amount of research has been directed toward the evaluation of steel bridges, structures and weldments to fatigue and fracture⁵. The east steel sheave wheel contains numerous built-in defects due to fabrication. These include shrinkage cavities, casting voids, attachment welds, and

Wiss, Janney, Elstner Associates, Inc.

weld repairs carried out during fabrication. As discussed in Chapter 5, several samples containing cracks and defects were extracted for evaluation. The sheave wheel defects examined were found to have originated during the manufacturing process of casting. Although some of these defects contained crack-like discontinuities no indications of crack extension by fatigue were found.

A large body of test data on the fatigue strength of various details in steel bridge construction has been developed. This data is usually presented in the S-N form shown in Fig. 7.1 where the lines of the various detail categories are 95 percent confidence limits for 95 percent survival. Using the measured stress ranges for the high stressed areas of the sheave wheel of 19.0 ksi and 31.0 ksi and considering the sheave wheel casting material with inherent fabrication defects to perform between Category B and Category C, the number of cycles required to reach fatigue life can be predicted. For Gage 1, rim stiffener, $S_r=19.0$ ksi relates to a fatigue life of 1,000,000 cycles and Gage 2, spoke flange tip, $S_r=31.0$ ksi predicts a fatigue life equal to 225,000 cycles as shown in Fig. 7.1.

Considering an estimated 111,000 to 155,400 cycles have already been applied to the sheave wheel and a measured spoke flange tip stress range of 31.0 ksi, a total fatigue life equal to 225,000 cycles is predicted using the fatigue performance of the material between Categories B and C. This would provide at least 25 years of additional service at the average 3,600 cycles/year frequency. Using the measure stress range recorded at the rim stiffener (19.0 ksi) and the Category B-C fatigue limit results in life projection of 1,000,000 cycles. This suggests a remaining fatigue life in excess of 100 years. Although, it must be pointed out that the 25 year remaining life prediction is related to a small high stress region of the spoke and the nominal stress range in the sheave wheel spokes is significantly reduced away from this area resulting in a much longer fatigue life. Therefore, fatigue cracks may develop in the spoke at these small high stress regions possibly requiring modification to extend the fatigue life. With minor modification or retrofitting it is anticipated that the fatigue life of the sheave wheel can be conservatively extended to provide a remaining life in excess of 50 years.

7.3 – Trunnion Fatigue Life Estimate

Based on the fractographic analysis for defect 1B in the trunnion, the initial edge crack measured $\frac{1}{4}$ in. deep by $\frac{5}{16}$ in. long. Fatigue extension increased the crack depth and length to $\frac{3}{8}$ in. by $\frac{4}{8}$ in.,

Wiss, Janney, Elstner Associates, Inc.

respectively. Therefore, a semi-elliptical edge crack model appeared appropriate for the observed crack extension.

For the semi-elliptical edge crack model, the stress intensity range was calculated using the relationship $\Delta K = F_2 F_g S_r \sqrt{\pi a}$. Substituting the ODOT stress range ($S_r = 19.6$ ksi), crack depth at the measured striation spacing ($a = 3/16$ in.), and estimated stress intensity range using the striation spacing ($\Delta K = 32$ ksi-in^{1/2}) into the relationship provided an estimate of the stress concentration factor, $F_2 F_g = 1.64$. This value is similar to the stress concentration, $K_t \cong 2.2$, at the trunnion shoulder.

Integrating the crack growth relationship using $F_2 F_g = 1.64$ and $F_e F_g = 1.0$ (no stress gradient) resulted in a fatigue life, $N = 11,000$ cycles and $N=49,000$ cycles, respectively. When the predicted fatigue life is compared to the estimated 111,000 to 155,400 cycles already experienced by the trunnion, this suggests that the stress gradient decays rapidly as the crack extends and that the initial weld defect likely required cycles to initiate fatigue cracking.

Using a factor of safety of three against crack instability and the fracture toughness, $K_{IC}=61$ ksi-in^{3/2} from the CVN and static fracture toughness (J_{IC}) tests, a comparable value of 57.5 ksi-in^{3/2} at the lowest anticipated service temperature, produces a crack depth of approximately 1 in. when substituting the maximum ODOT calculated service stress $\sigma_{max} = 9.8$ ksi into the edge crack equation.

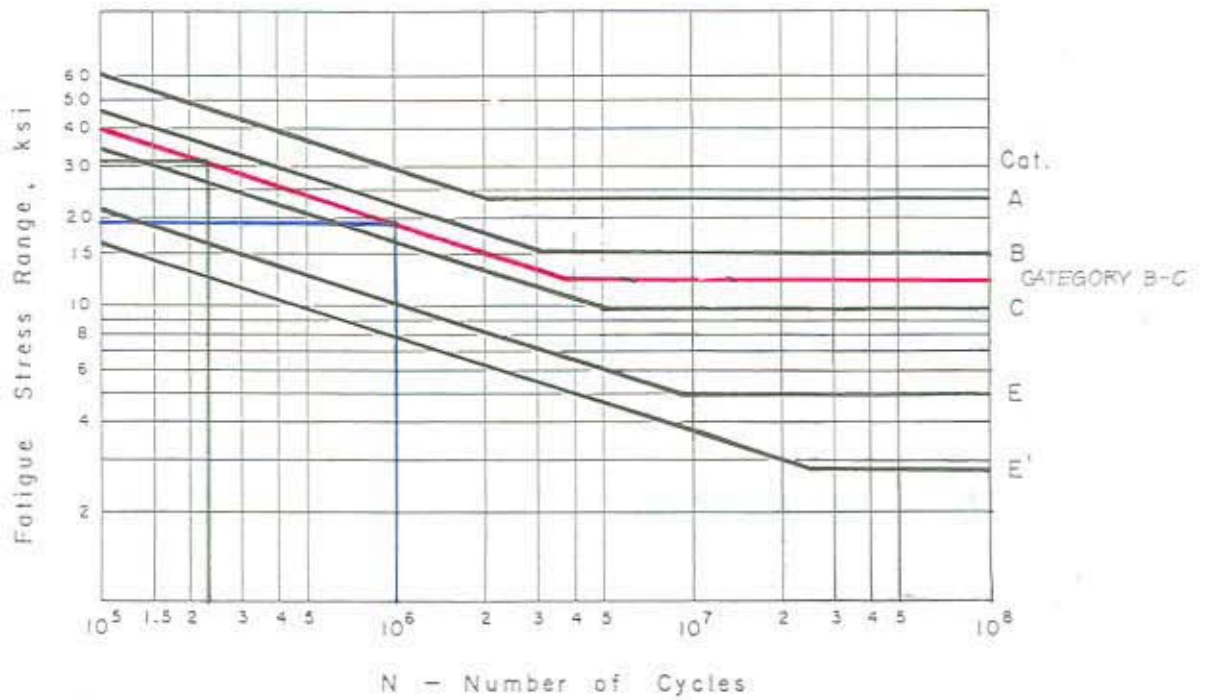
As the crack grows, the stress gradient decays until the correction factors $F_e F_g = 1.12$, which is the known edge crack relationship. Substituting this into the crack growth relationship using an initial crack depth of $3/8$ in. and a maximum crack depth of 1 in. results in a fatigue life, $N = 62,720$ cycles. This would correspond to 18 years of additional service at the current operating rate. Therefore, there is no immediate concern for the performance of the remaining south trunnions since no defects were identified more than $1/2$ in. in depth. Note that using the WJE calculated stress range of 15 ksi would increase the remaining service life to 40 years.

Table 7.1 – SUMMARY OF TRUNNIONS WITH FATIGUE CRACKS

Bridge	Design Stress, ksi	Stress Concentration K_t	Stress Range, ksi = $k_t S_r$	Life Cycles
1. Valleyfield East St. Louis, IL	13.5	1.70	47.0	900,000
2. Caughmawaga St. Lawrence Seaway	10.3	1.72	35.4	600,000
3. St. Lambert St. Lawrence Seaway	13.0	1.75	45.5	700,000
4. Shippings Port New Jersey	16.0	1.75	56.0	600,000
5. Carleton Maine	17.0	2.18	74.0	450,000
6. Hackensack River Br. New Jersey	9.7	2.15	41.7	1,170,000
7. Newark Bay Bridge New Jersey	9.7	2.15	41.7	1,170,000
8. Duluth Minnesota	12.8	2.05	52.5	1,000,000
9. I-5 Columbia River	9.8 or (7.5)	2.20	43.0 (33.0)	155,000

FLANGE TIP OF SPOKE
 GAGE ② $S_r = 31$ ksi
 $N \approx 225,000$ cycles

RIM STIFFENER
 GAGE ① $S_r = 19$ ksi
 $N \approx 1,000,000$ cycles



NOTE: SHEAVE WHEEL CASTING PERFORMANCE BETWEEN CATEGORY B AND C.

Fig. 7.1 – Fatigue resistance curves for various details with the Category B-C added for assessment of the sheave wheel material.

8.0 – CONCLUSIONS AND RECOMMENDATIONS

An in-depth investigation was performed to accurately assess the condition of one of the counterweight sheave/trunnion assemblies removed from the north tower of the I-5 Columbia River Bridge. The trunnion examined was reported to have contained crack-like indications. The purpose of the investigation was to determine a service life estimate for the two remaining counterweight sheave/trunnion assemblies in the south tower using information obtained from the removed assembly.

As part of this work, the removed sheave and trunnion were thoroughly examined using NDE techniques. Based on the NDE findings, fractographic and metallographic examinations were used to document and characterize the observed defects for fatigue. Material properties were also determined to aid in an accurate assessment of the sheave and trunnion fatigue life. The south tower trunnions were then inspected to assess their current condition using UT procedures developed from the investigation. From the south tower examination, in-depth investigation, and previous analytical and field testing data performed by others, a remaining service life was estimated for the south tower sheave/trunnion assemblies in addition to several other conclusions regarding the in-depth investigation.

8.1 – Conclusions

1. The estimated service life of the two south tower trunnions without risk of fracture is projected to provide an additional 25 years of service considering the current annual operating rate and the observed defect sizes and extension by fatigue of the examined trunnion.
2. The estimated remaining sheave service life exceeds 25 years based on the measured stress range (31.0 ksi) and the lack of fatigue crack extension from defects in high stress regions of the sheave. It must be pointed out that the area that governs the 25-year remaining service life is a small high stress region of the spoke. Nominal stresses in the spoke reduce significantly away from this area. Therefore, with minor modifications or retrofitting to cracks in this area, it is anticipated that the fatigue life of the sheave can be extended to over 50 years.
3. The only defects with fatigue extension detected by NDE were located in the trunnion. These defects are related to the modification of the oilway grooves where weld metal was used to fill the grooves prior to machining the trunnion for the new roller bearings. Other defects observed in the

Wiss, Janney, Elstner Associates, Inc.

trunnion or sheave such as inclusions, hot tears, and shrinkage cracks showed no evidence of extension by fatigue.

4. Welding of the oilways would have been extremely difficult due to the poor weldability of the trunnion material and lubricant contamination of the groove. As noted, lubricant contamination or residue was still visible during the fractographic examination of the defects.
5. Discontinuities within the weld-filled oilways shield UT examination of the grooves from within the center bore or from the end face as is required for in-service inspection. However, using the WJE UT procedures, cracks extending outside the grooves can be detected. In addition, it was found that the UT signal trace amplitudes and indication locations were susceptible to transducer contact and couplant distribution making replicable results more difficult.
6. The mechanical properties of the trunnion and sheave were found to be consistent with properties expected of forged and cast components of this size and of this period of manufacture.

8.2 – Recommendations

From the results of this in-depth investigation, WJE finds no reason to recommend repair or replacement of the existing south tower counterweight sheave/trunnion assemblies. Our investigation has shown that these assemblies are currently adequate to perform bridge lifting operations for an additional 25 years.

Furthermore, the study has indicated that crack growth in the trunnion and sheave will be slow and crack extension in the trunnion will significantly reduce the stress intensity factor. Assuming regular in-depth inspections are carried out, ODOT may be assured that at least 25 years of additional service will be provided by the assemblies.

WJE recommends in-depth multi-year inspections of the trunnion at a similar level as to what was performed in 1999 in order to determine whether crack growth is occurring. This inspection will use non-destructive ultrasonic test methods in accordance with the WJE developed procedure included in this report. These inspections will focus on critical areas to identify crack-like defects and monitor crack growth. A qualified ASNT Level III UT inspector shall perform or closely direct the inspections. WJE

Wiss, Janney, Elstner Associates, Inc.

recommends that the next in-depth inspection be performed in 2001. Unless conditions of concern or noticeable crack growth are noted, additional in-depth inspections should follow in five-year intervals.

9.0 – REFERENCES

1. Scroggins, G, P.E., *Interstate 5 Lift Span Rehab for Oregon D.O.T., Counterweight Sheave Analysis and Design*, DGES, Inc., January 9, 1997
2. Lovejoy, S, P.E., *Field Test of the Lift Span / Counterweight Sheave on the Interstate 5 (Columbia River) Bridge, Bridge #1377*, Oregon Department of Transportation, Bridge Engineering Section., Salem, OR, January 16, 1997
3. McGormley, J.C., S.E. and Koob, M.J., S.E., *I-5 Columbia River Lift Span Bridge. Special Testing Services*, WJE No. 971016, Wiss, Janney, Elstner Associates, Inc., Northbrook, IL, September 3, 1997
4. Kaufmann, E.J., PhD and Fisher, J.W., PhD, *Final Report, Evaluation of Material Properties, Defects, and Service Life Estimate of the Counterweight Sheave/Trunnion Assembly of the I-5 Columbia River Bridge*, ATLSS Engineering Research Center, Lehigh University, Bethlehem, PA, June 2000
5. Fisher, J.W., PhD, *Bridge Fatigue Guide, Design and Details*, American Institute of Steel Construction, New York, NY, 1977

APPENDIX A -ULTRASONIC INSPECTION DATA FROM REMOVED TRUNNION

WJE	Wiss, Janney, Elstner Associates, Inc. 83 South King Street, Suite 820, Seattle, Washington 98104	MADE BY	RDG	SHEET NUMBER	C-1
		CHECKED BY		PROJ. NUMBER	973010
Client: Oregon State D.O.T.		DATE	Oct 1998		
Project: I-5 Counterweight Sheave Trunion Study					

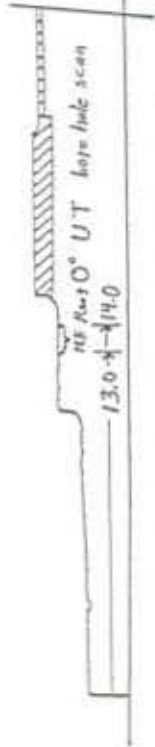
Table of Contents

<u>Sheet No.</u>	<u>Description</u>
1	1A Keyway area - MT Indications / UT Indications
2	2A Keyway area - MT Indication / UT Indications
3	3A Keyway area - MT Indications / UT Indications
4	1B Keyway area - MT Indications / UT Indications
5	2B Keyway area - UT Indications
6	3B Keyway area - UT Indications
7	15° Azimuth vicinity UT Axial & Borehole scan indications UT 1 X & Z
8	60° Azimuth vicinity UT Axial & Borehole scan indications UT 2 X & Z / UT 4
9	80° Azimuth vicinity UT Axial & Borehole scan indications UT 3
10	150° Azimuth vicinity UT Axial & Borehole scan indications UT 5
11	165° Azimuth vicinity U.T. Axial scan indications UT 6
12	260° Azimuth vicinity UT Axial scan indications UT 7 X & Z
13	Section Cut for Ultrasonic Test Standard
14	General Configuration & Orientation

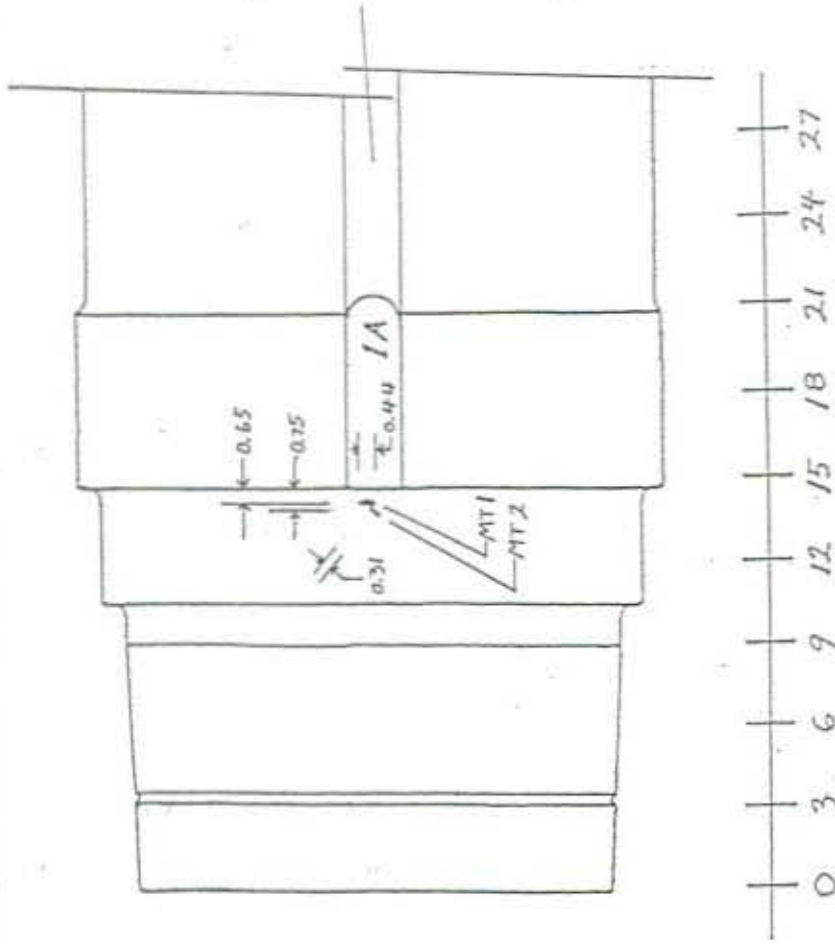
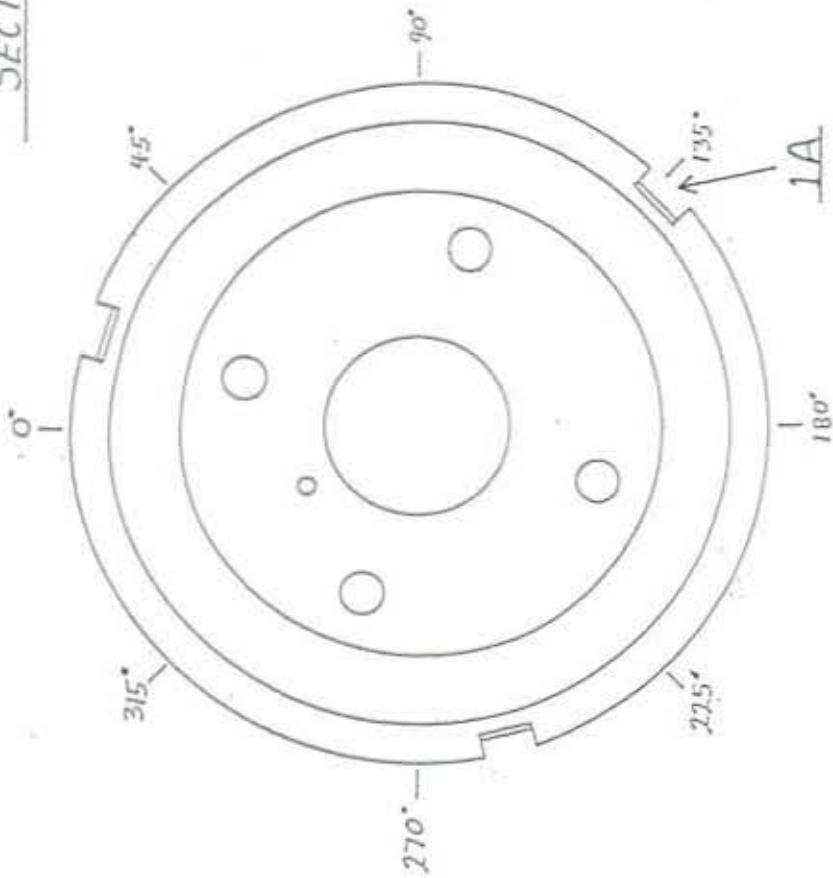
WJE	Wiss, Janney, Elstner Associates, Inc. 83 South King Street, Suite 820, Seattle, Washington 98104	MADE BY	RDG	SHEET NUMBER	C-2
		CHECKED BY		PROJ. NUMBER	983010
Client: Oregon State D.O.T.		DATE	OCT 19 98		
Project: I-5 Counterweight Sheave Trunion Study					

Table of Contents - cont.

<u>Sheet No.</u>	<u>Description</u>
15	General Sectioning Guide for Fractographics
16	Items #1&2 for analysis - located near keyway 1A
17	Items #3&4 for analysis - located near keyway 1B
18	Item #5 for analysis - located in keyway 3A area
19	Item #6 for analysis - located @ 15° azimuth-East end
20	Items #7&8 for analysis - located @ 60° azimuth-East end



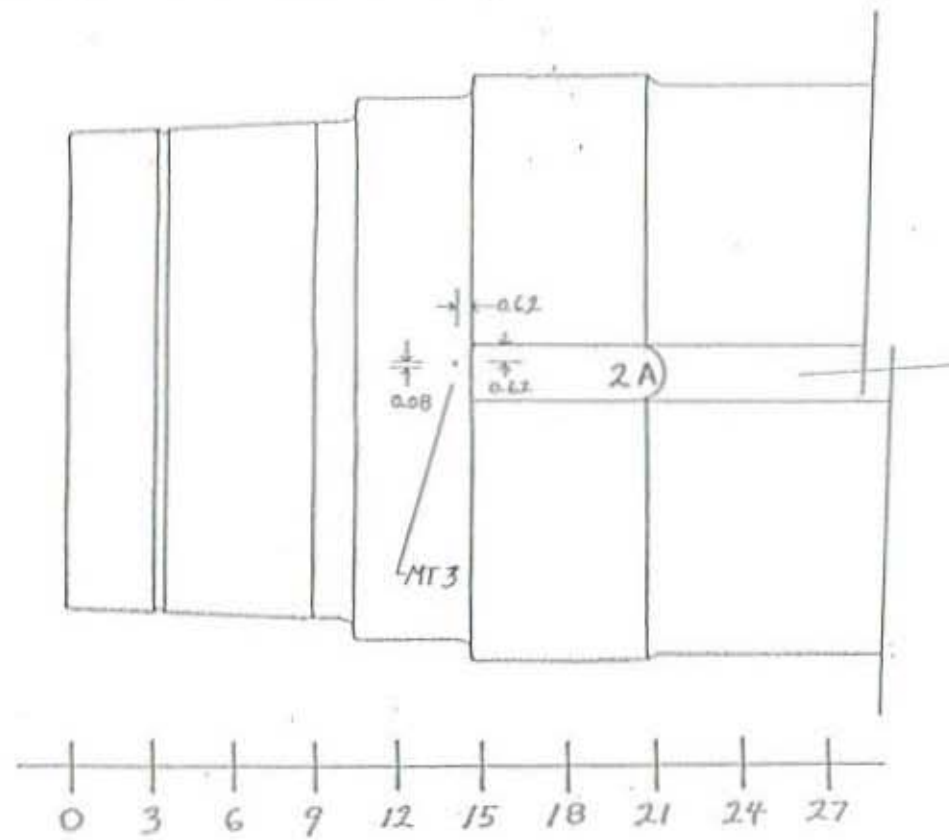
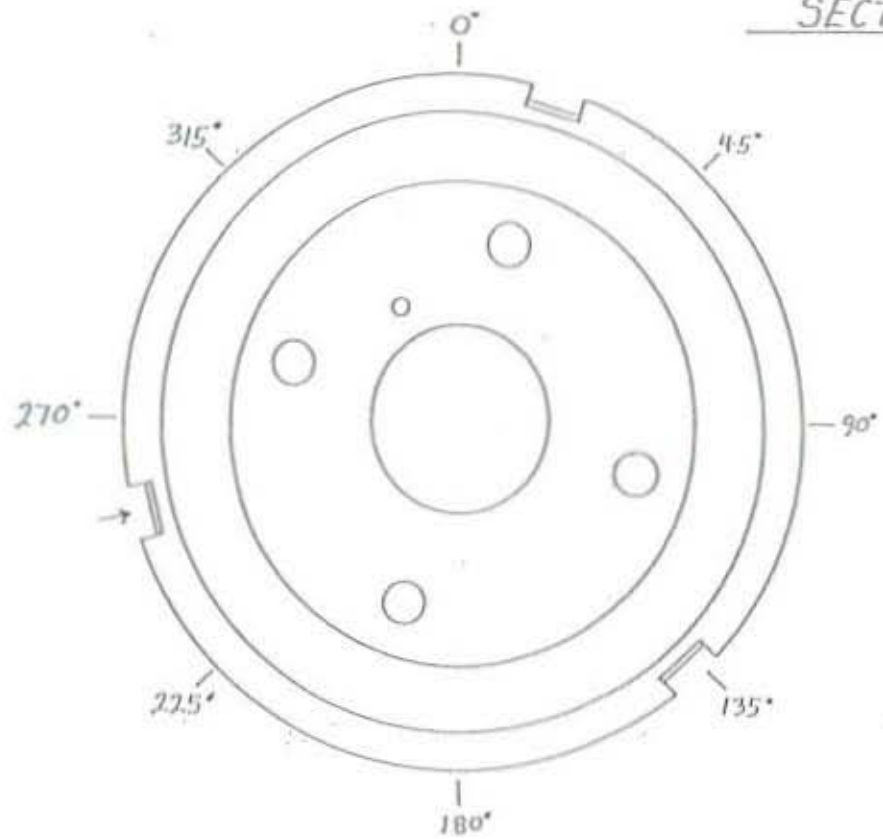
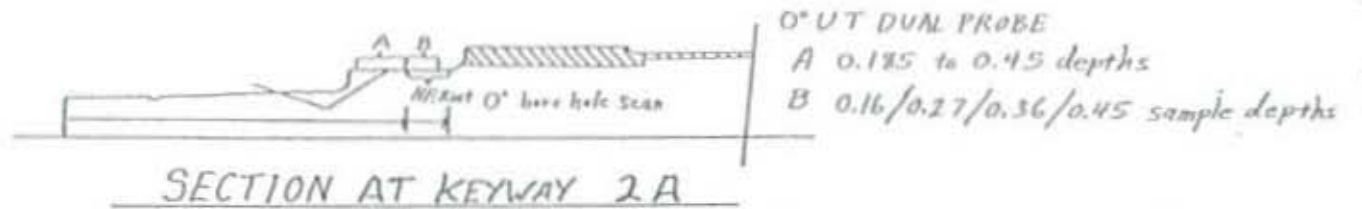
SECTION AT KEYWAY 1A



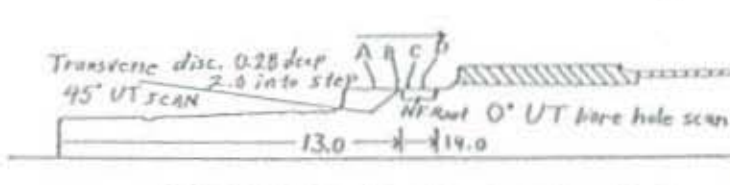
EAST END

SURFACE AT KEYWAY 1A (EAST END)

COUNTERWEIGHT SHEAVE TRUNNION

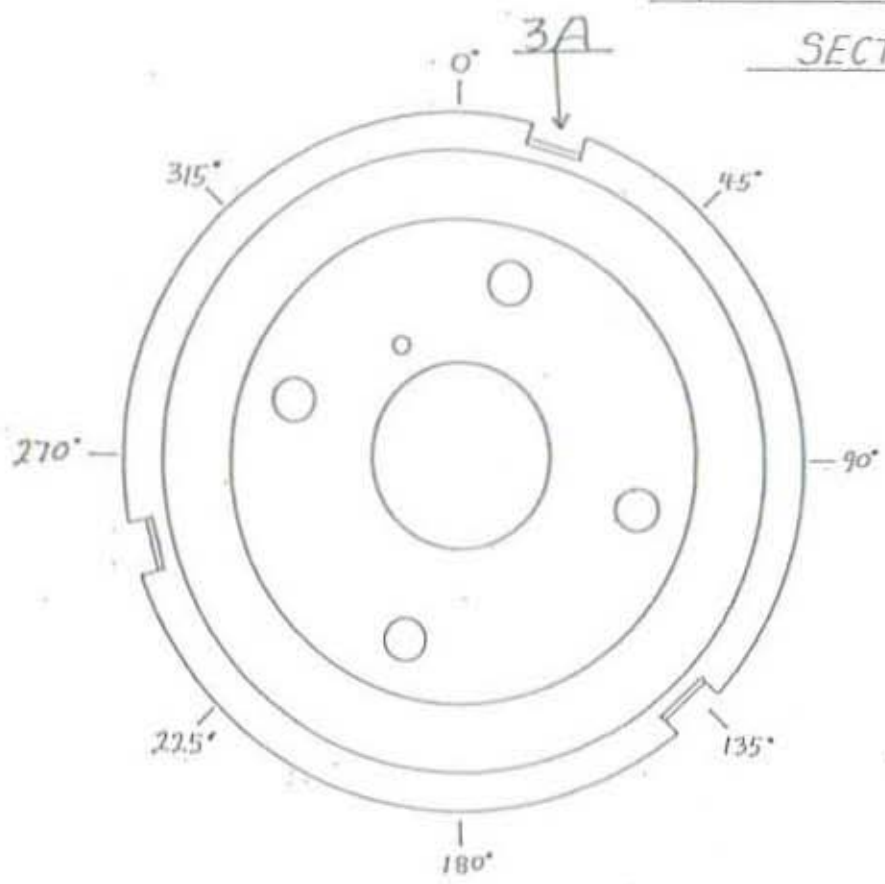


COUNTERWEIGHT SHEAVE TRUNNION

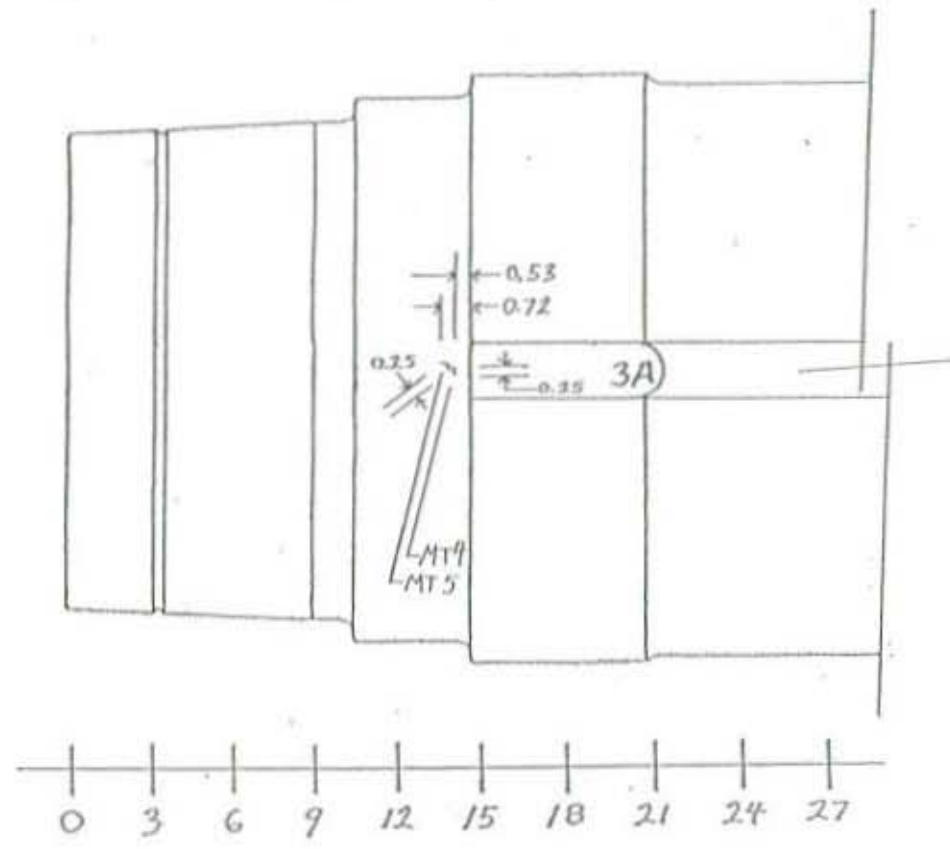


0° UT DUAL PROBE			
A	0.53 deep	0.125 length	
B	0.42 deep	0.25 length	
C	0.31 deep	0.25 length	
D	0.45 deep	0.50 length	

SECTION AT KEYWAY 3A

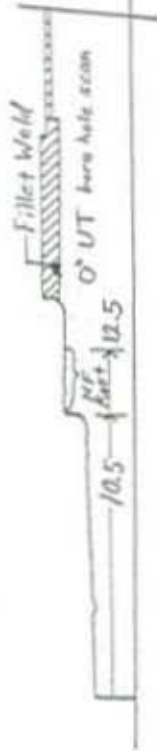


EAST END

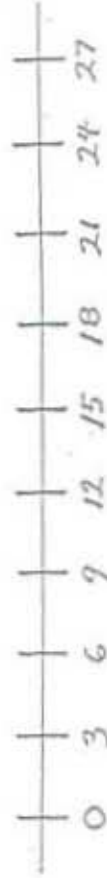
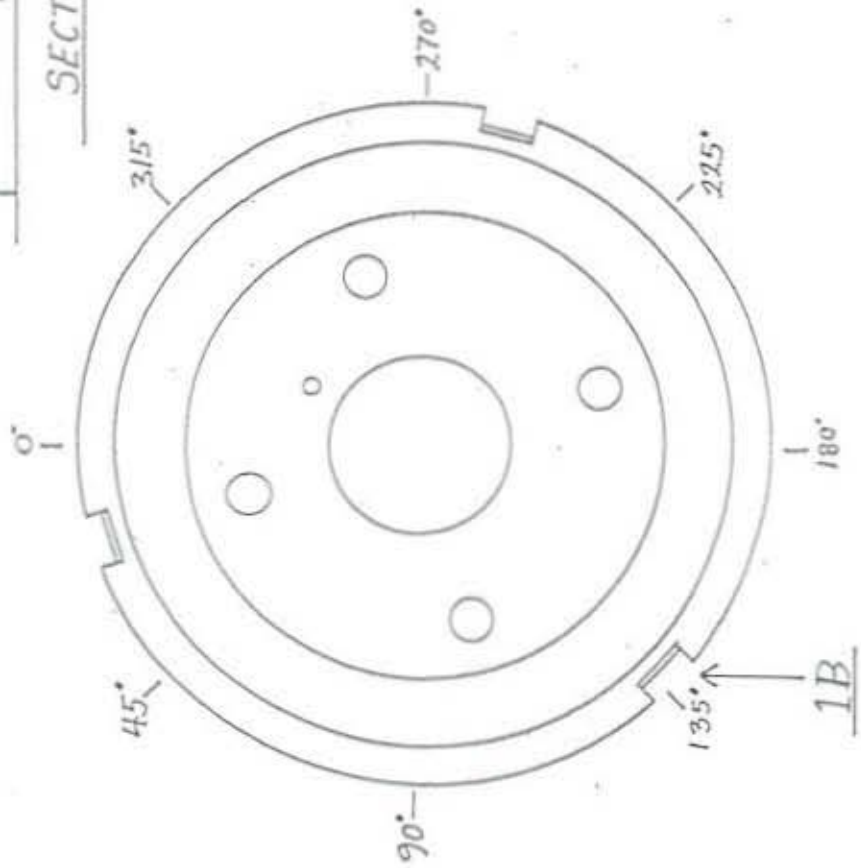


SURFACE AT KEYWAY 3A (EAST END)

COUNTERWEIGHT SHEAVE TRUNNION



SECTION AT KEYWAY 1B

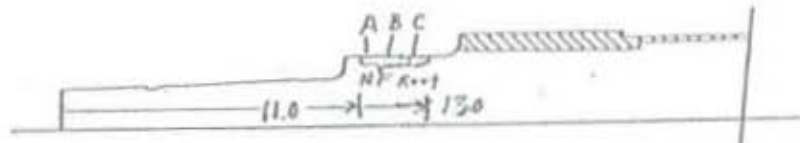


WEST END

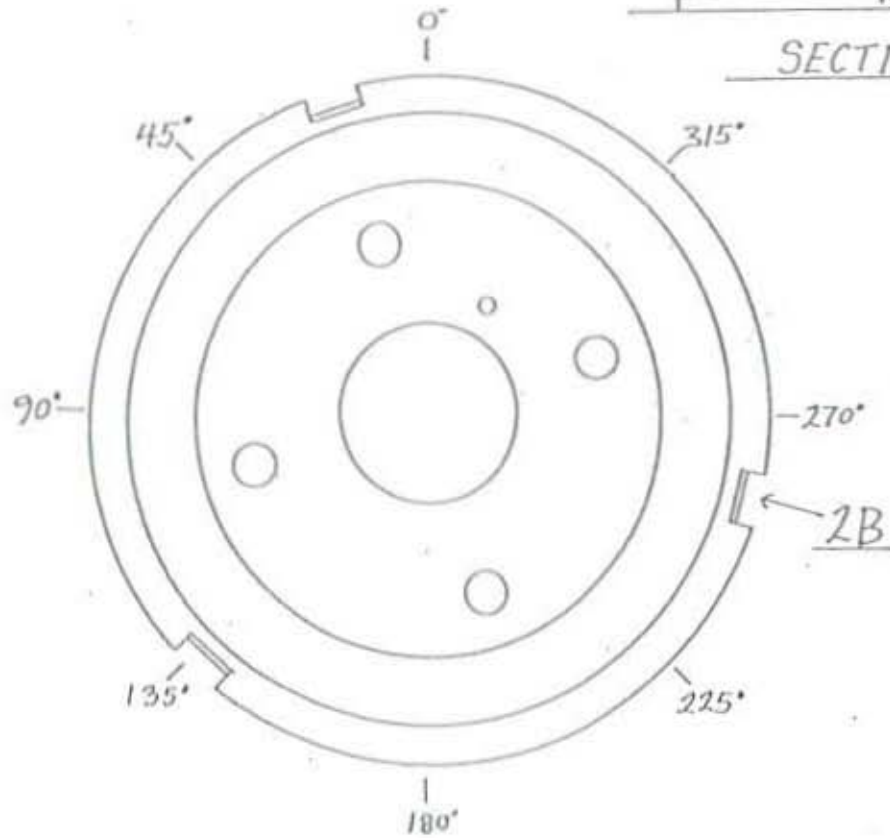
SURFACE AT KEYWAY 1B (WEST END)

COUNTERWEIGHT SHEAVE TRUNNION

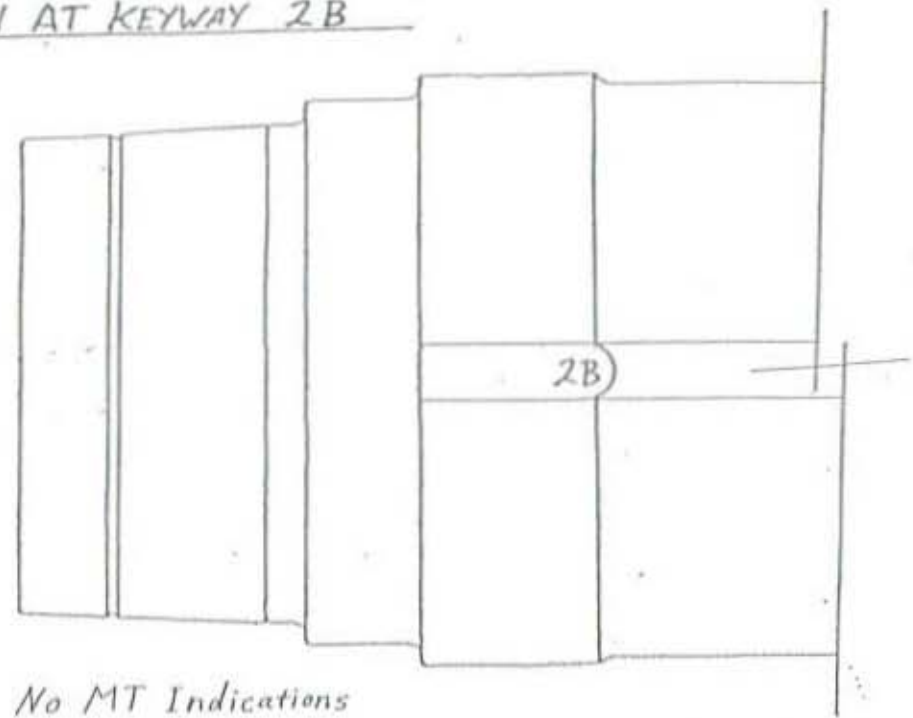
0° UT DUAL PROBE
 A 0.236 depth
 B 0.143 depth
 C 0.12-0.40 depth



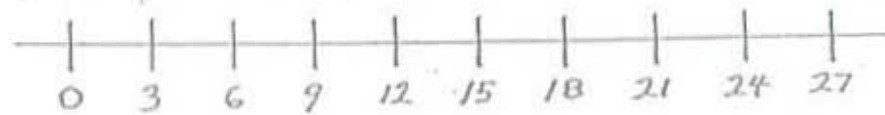
SECTION AT KEYWAY 2B



WEST END



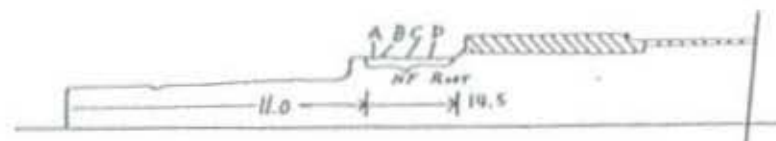
No MT Indications



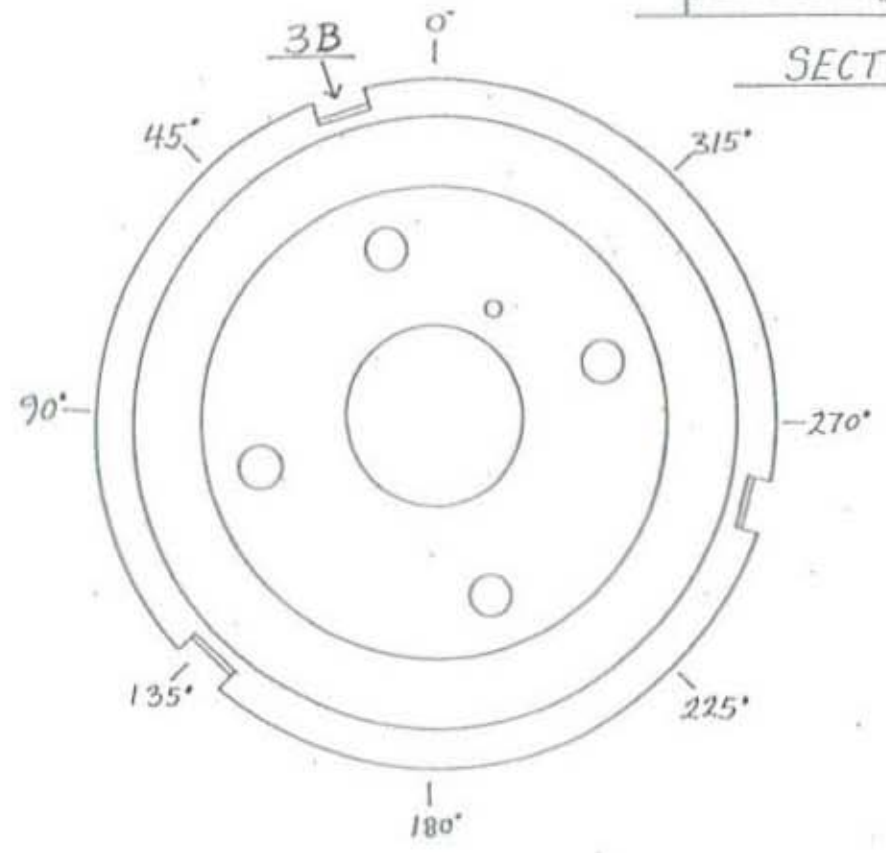
SURFACE AT KEYWAY 2B (WEST END)

COUNTERWEIGHT SHEAVE TRUNNION

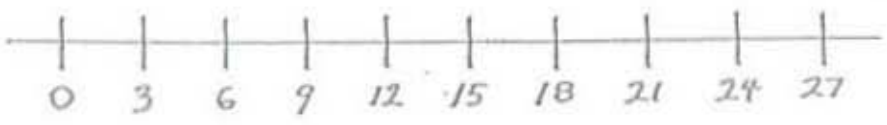
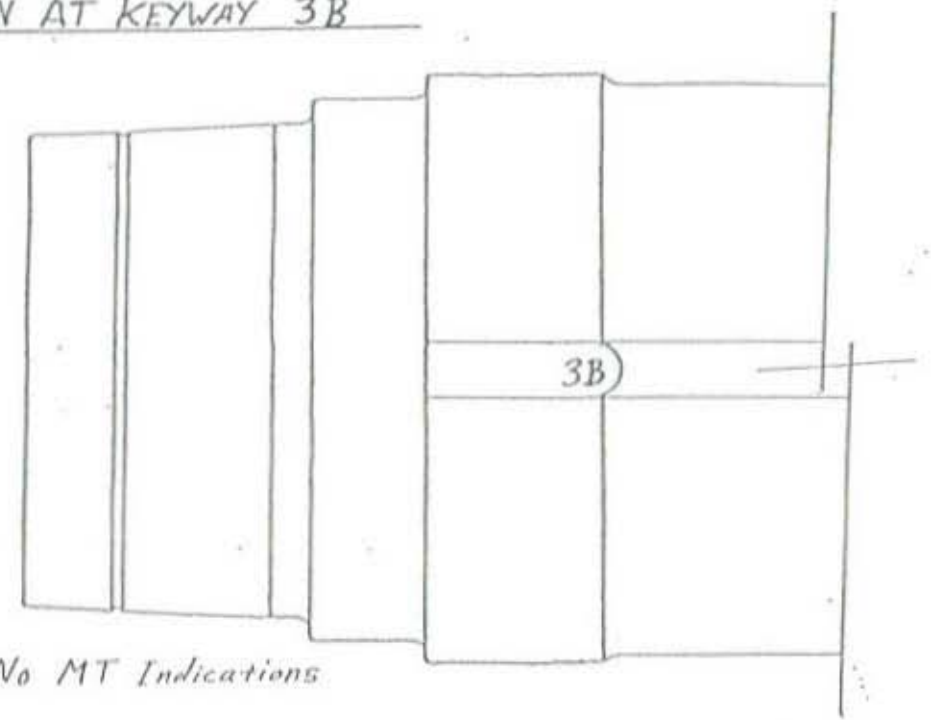
0° UT DUAL PROBE	
A	0.37 deep
B	0.43 deep
C	0.29-0.35 deep
D	0.13-0.22



SECTION AT KEYWAY 3B

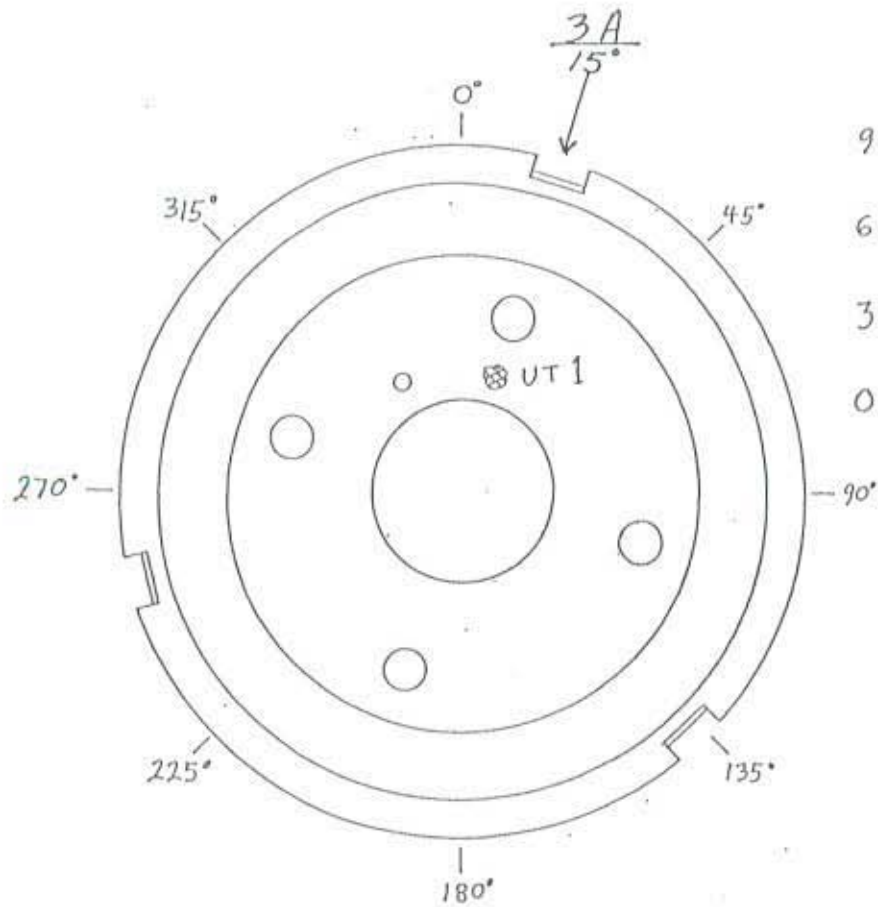


WEST END



SURFACE AT KEYWAY 3B (WEST END)

COUNTERWEIGHT SHEAVE TRUNNION



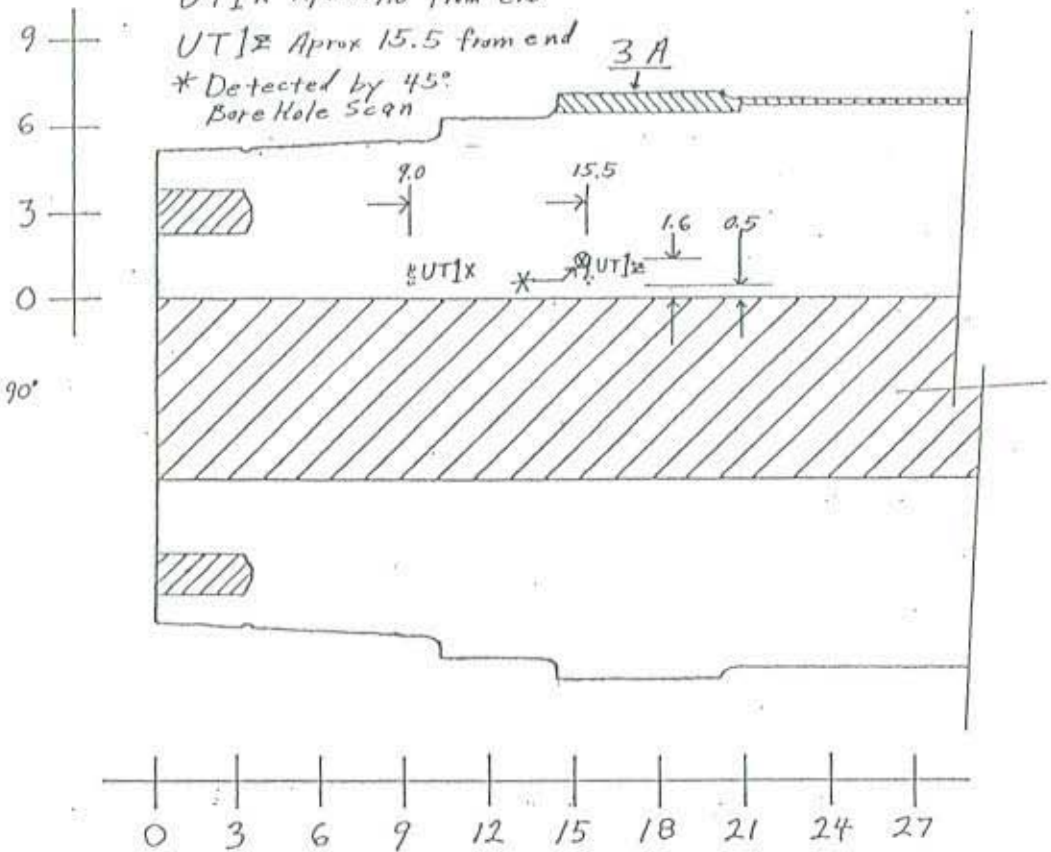
EAST END

Discontinuities located by UT Axial Scan

UT1X Aprox 9.0 from end

UT1Z Aprox 15.5 from end

* Detected by 45°
Bore Hole Scan

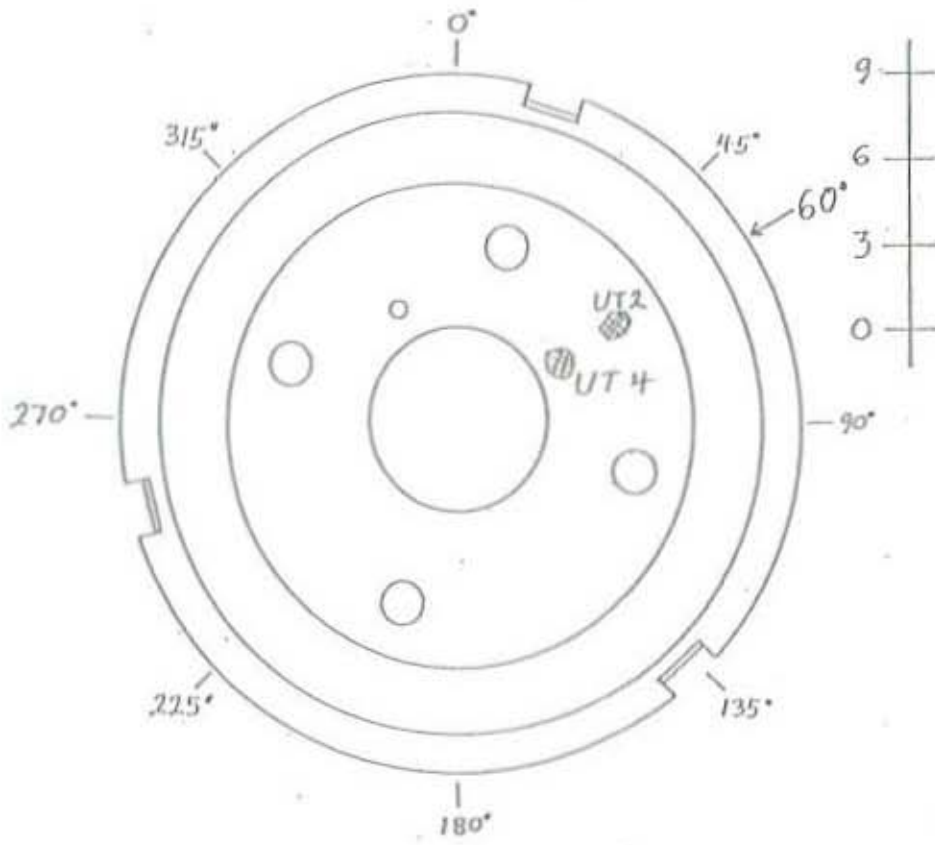
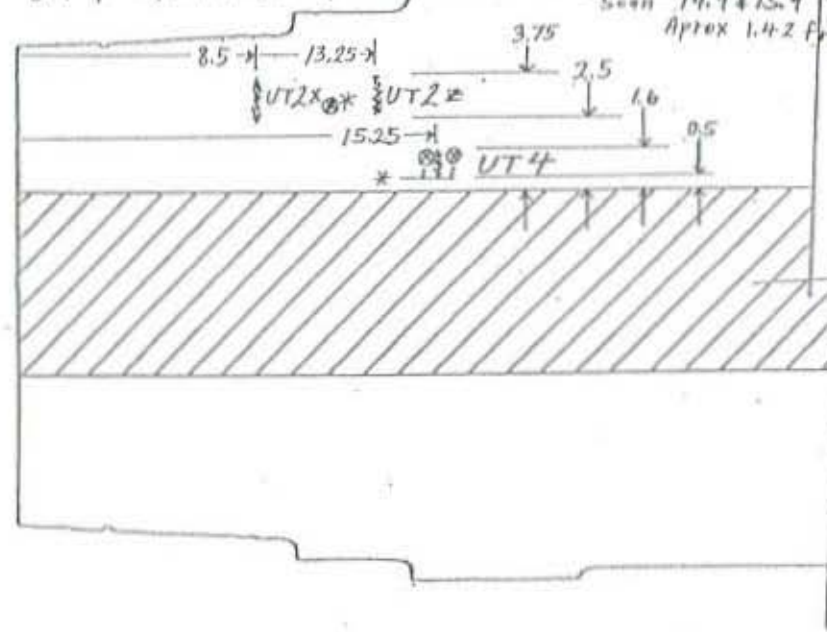


CROSS SECTION - EAST END (T.C. 15°)

COUNTERWEIGHT SHEAVE TRUNNION

Discontinuities located by UT Axial Scan

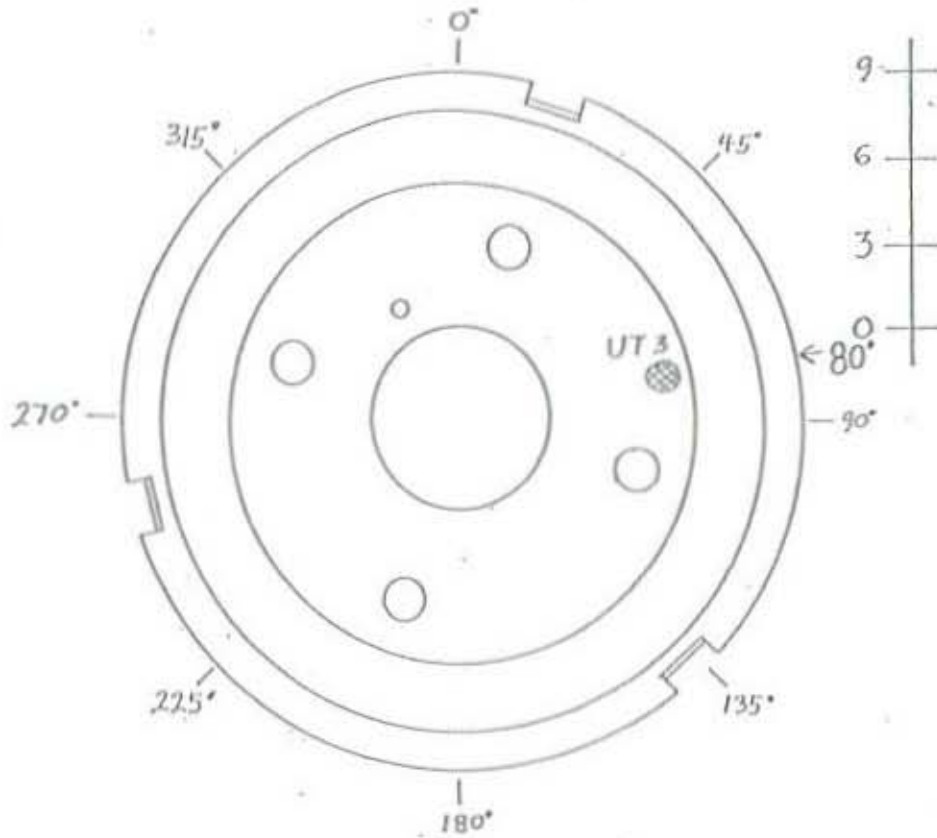
UT 2X Approx 8.5 from end } * Detected by 45° Bore Hole Scan
 UT 2Z Approx 13.25 from end } 11.4 ± from end 2.87 from bore surface
 UT 4 Approx 15.25 from end * Detected by 45° Bore Hole Scan
 Scan 14.9 & 15.9 from end
 Approx 1.42 from bore surface



EAST END

CROSS SECTION - EAST END (T.C. 60°)

COUNTERWEIGHT SHEAVE TRUNNION

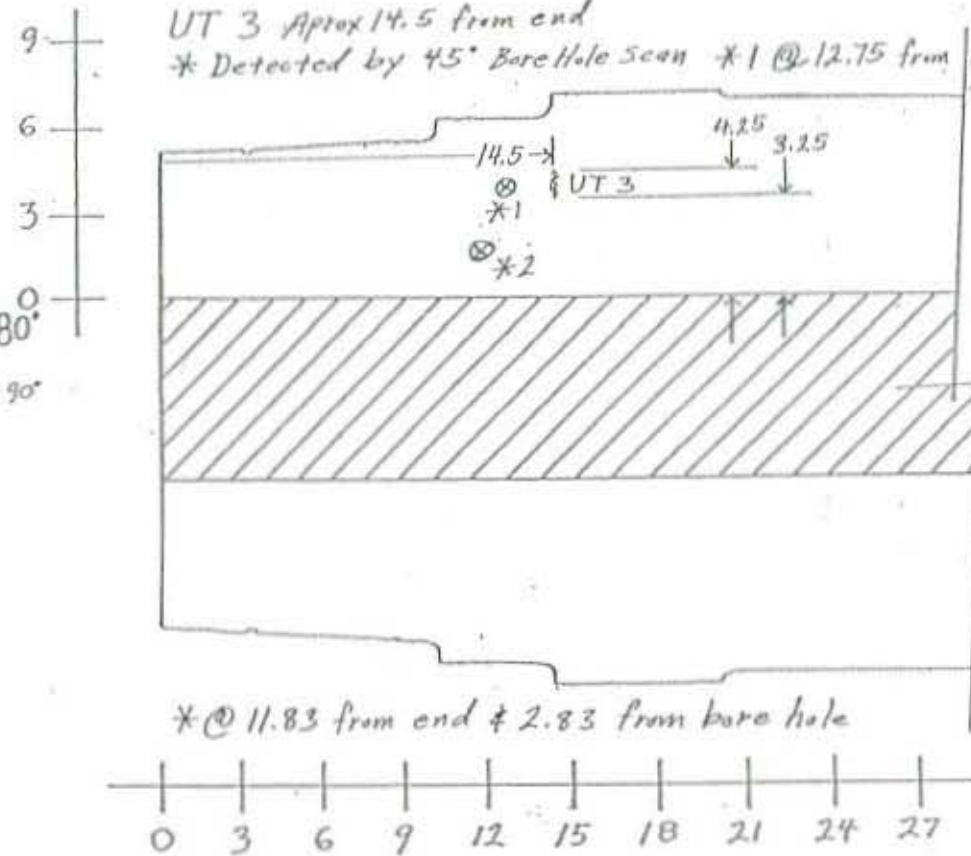


EAST END

Discontinuities located by UT Axial Scan

UT 3 Approx 14.5 from end

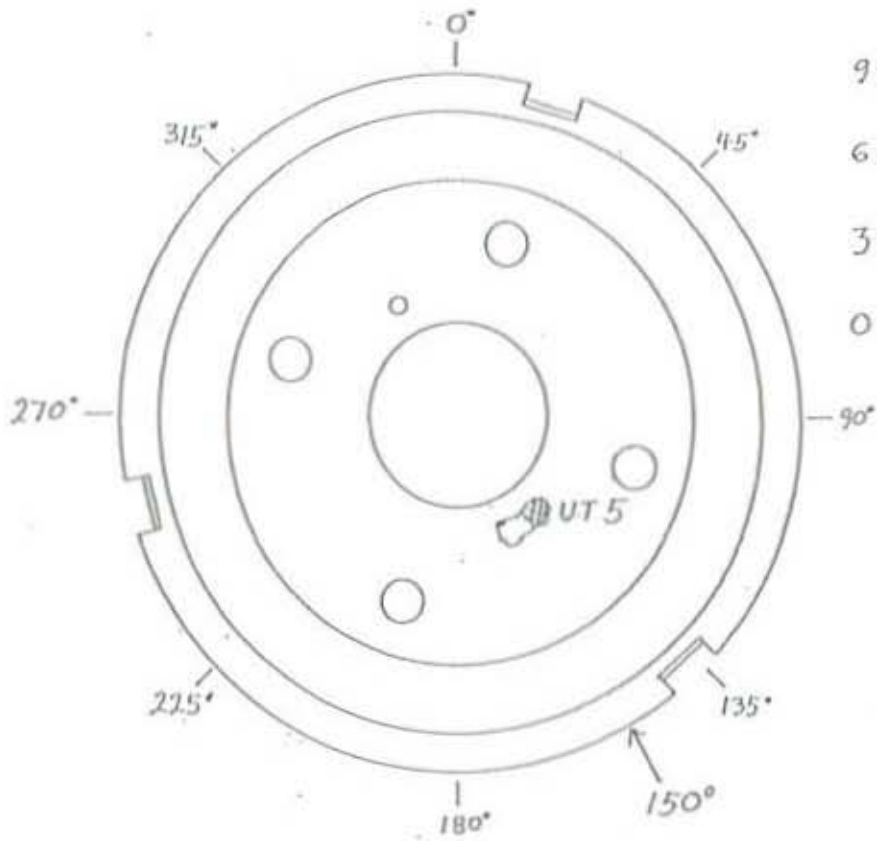
* Detected by 45° Borehole Scan *1 @ 12.75 from end & 2.83 from bore hole



* @ 11.83 from end & 2.83 from bore hole

CROSS SECTION - EAST END (T.C. 80°)

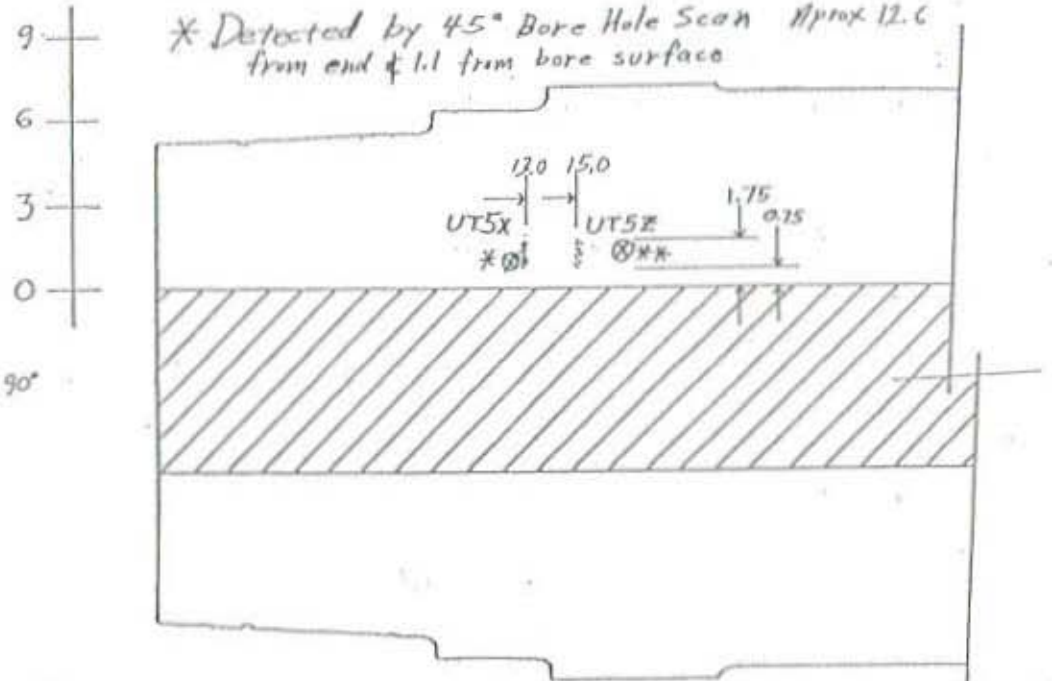
COUNTERWEIGHT SHEAVE TRUNNION



EAST END

Discontinuities located by UT Axial Scan
 UT 5X Aprox 13.0 from end
 UT 5Z Aprox 15.0 from end

* Detected by 45° Bore Hole Scan Aprox 12.6 from end & 1.1 from bore surface

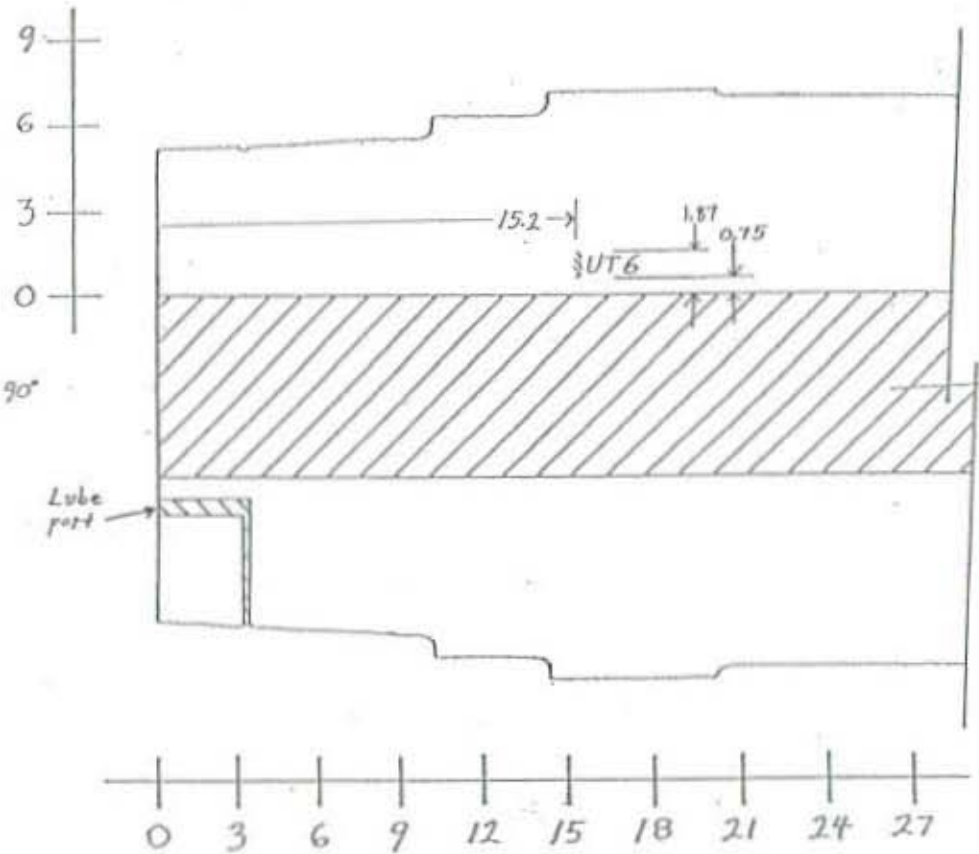
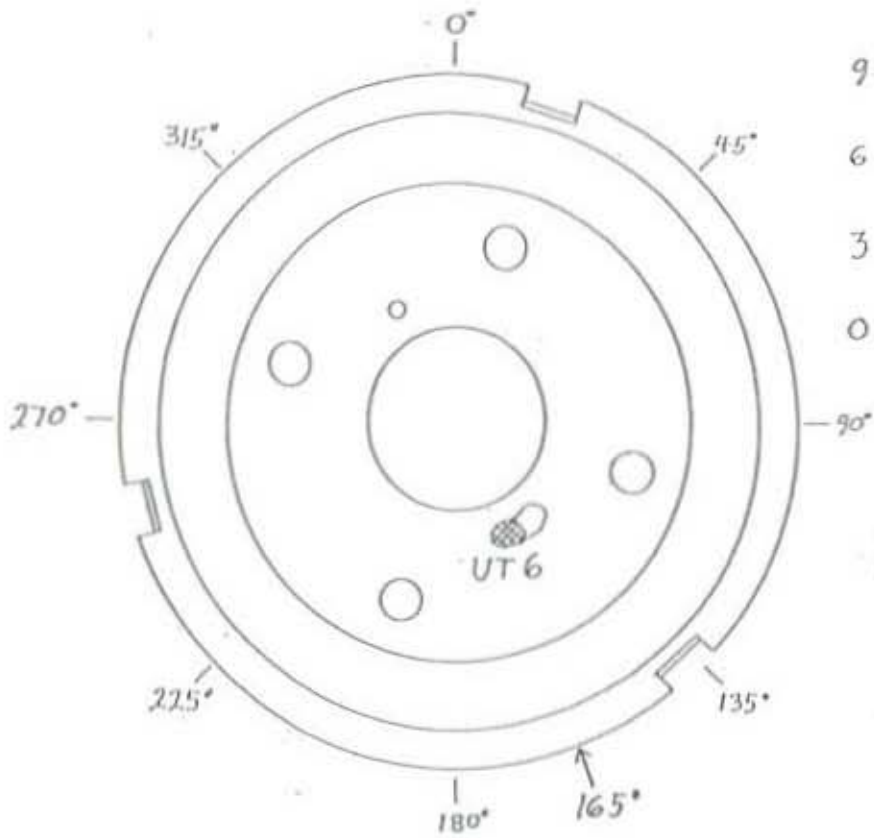


** Detected by 45° Bore Hole Scan (in general vicinity of UT 5)
 Aprox. 16.95 from end & 1.7 from bore hole

CROSS SECTION - EAST END (T.C. 150°)

COUNTERWEIGHT SHEAVE TRUNNION

Discontinuities located by UT Axial Scan
 UT6 Aprx 15.2 from end

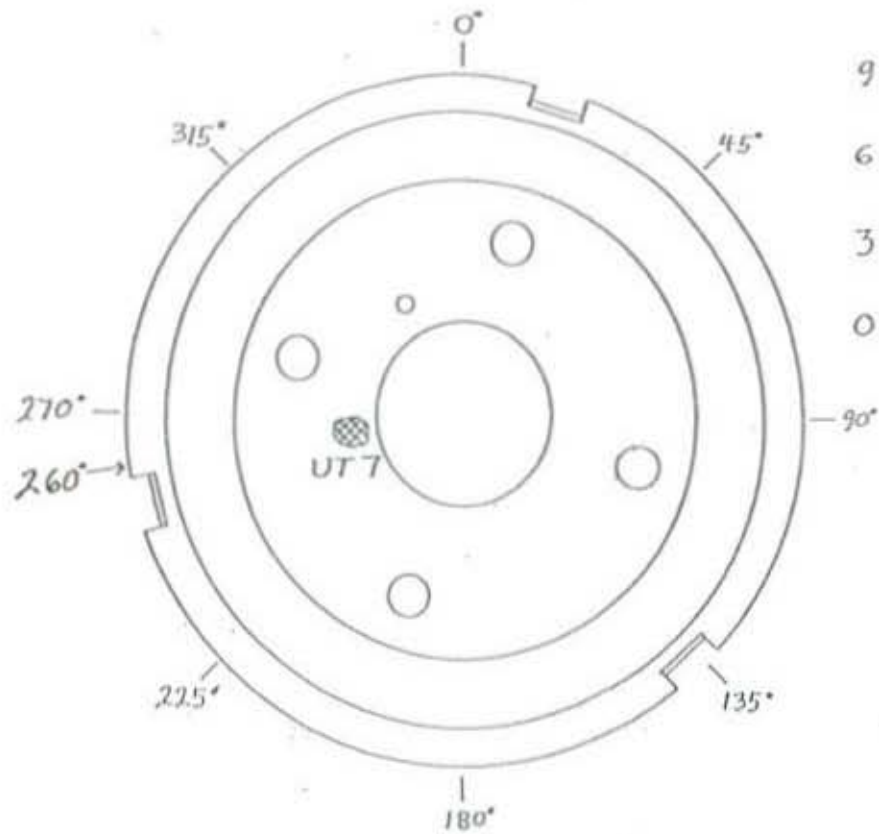


EAST END

CROSS SECTION - EAST END (T.C.165°)

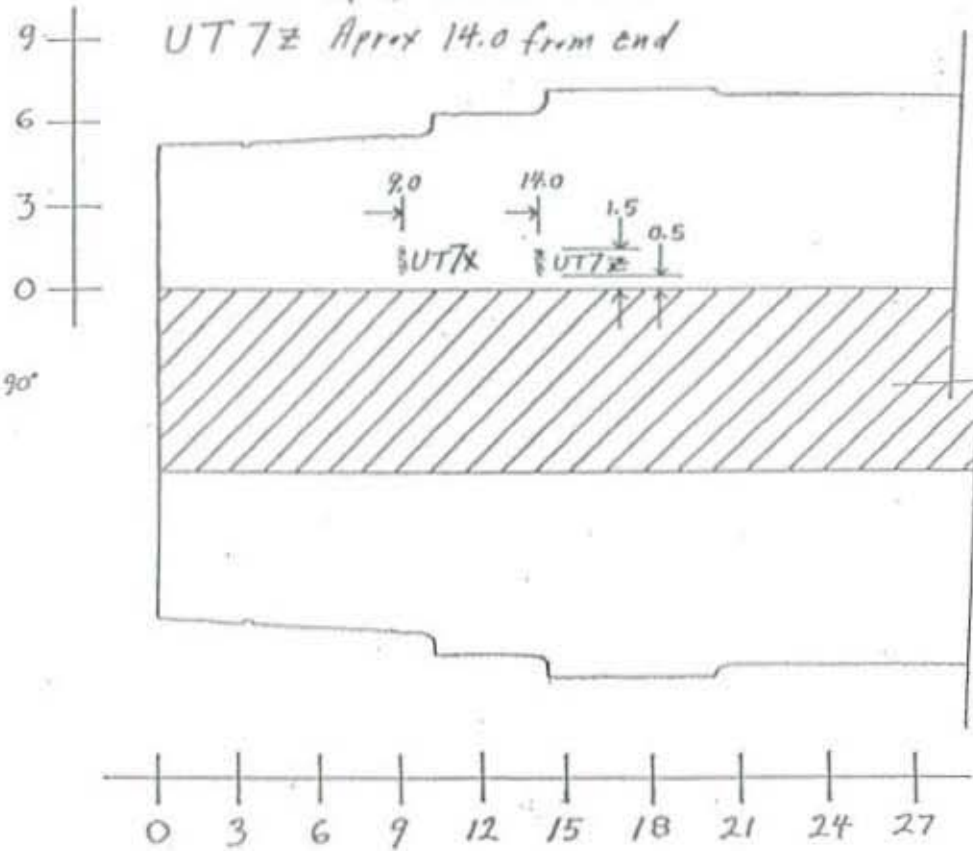
COUNTERWEIGHT SHEAVE TRUNNION

SHEET 11



EAST END

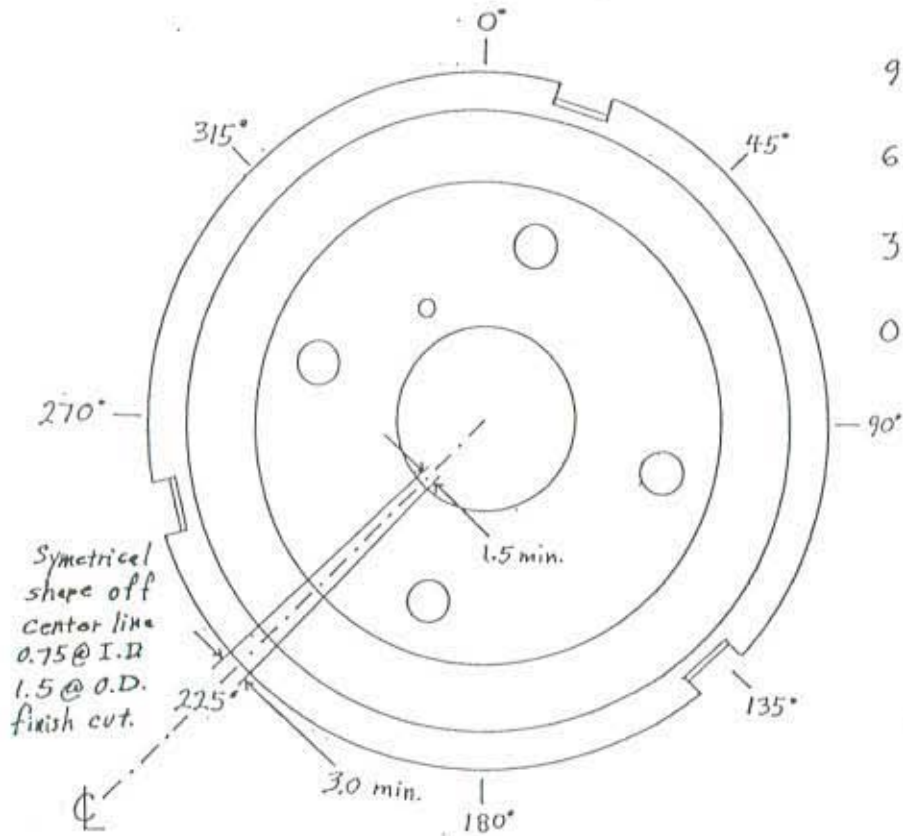
Discontinuities located by UT Axial Scan
 UT 7X Approx 9.0 from end
 UT 7Z Approx 14.0 from end



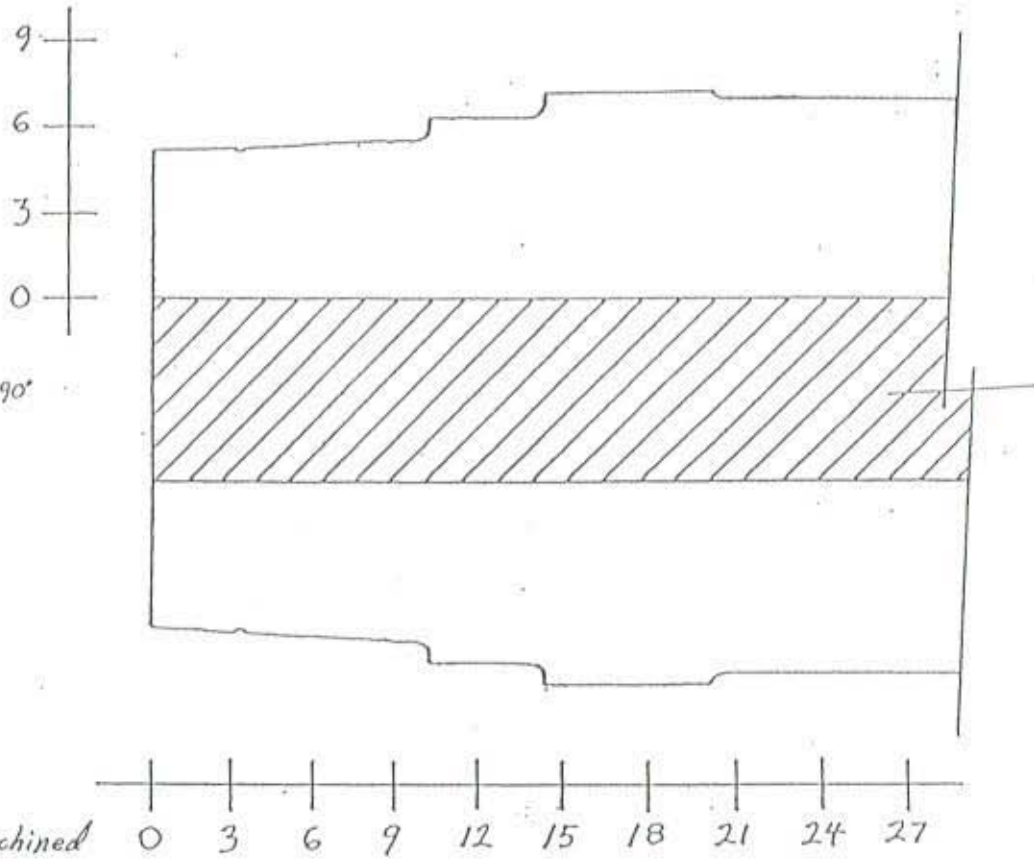
CROSS SECTION - EAST END (T.C. 270°)

COUNTERWEIGHT SHEAVE TRUNNION

Section Cut for Standard Fabrication



Symmetrical
shape off
center line
0.75 @ I.D.
1.5 @ O.D.
finish cut.



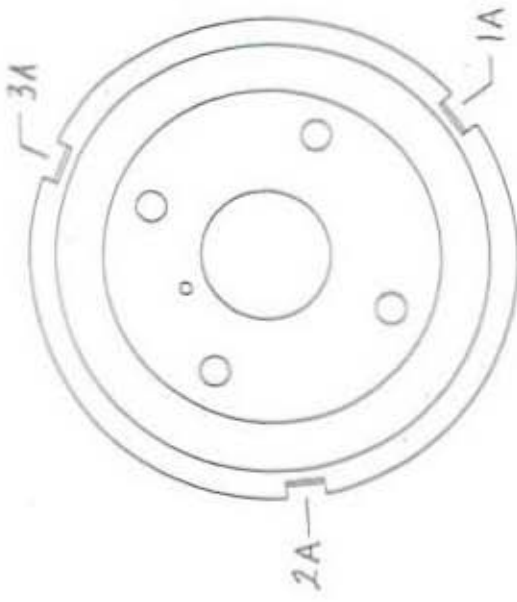
Cut sufficient matl. for finished machined surface to meet minimum dimmensions as shown.

Scribe center line at end, and on surface along trunnion axis at outside radius prior to cutting.

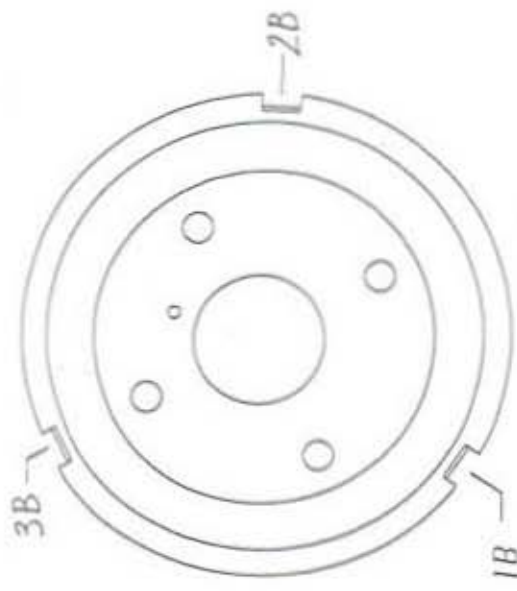
EAST END

CROSS SECTION - EAST END (T.C..25°)

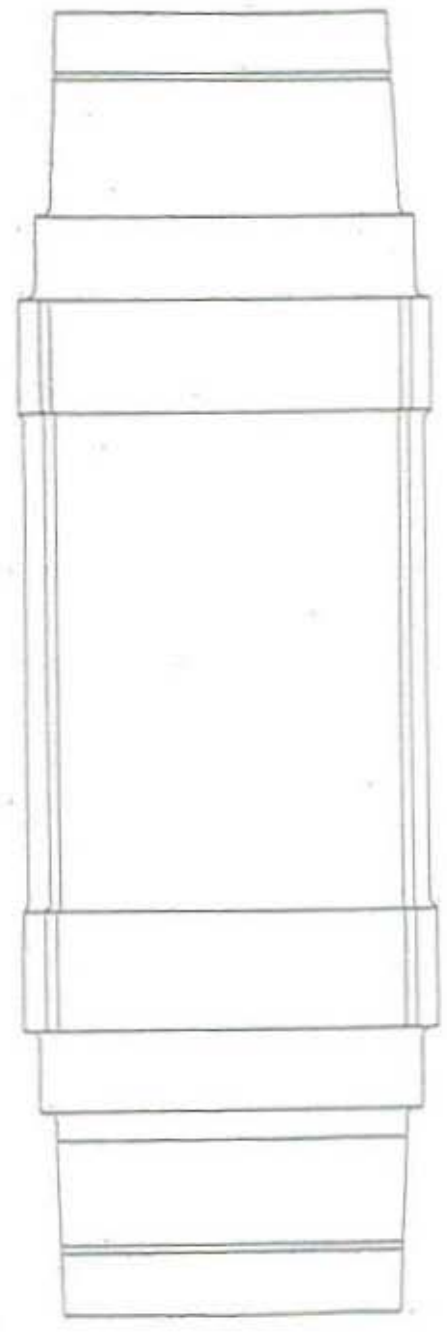
COUNTERWEIGHT SHEAVE TRUNNION



EAST END



WEST END



COUNTERWEIGHT SHEAVE TRUNION

APPENDIX B - DEFECT EVALUATION AND MATERIAL TESTING BY ATSS

ENGINEERING RESEARCH CENTER, LEHIGH UNIVERSITY

**Evaluation of Material Properties, Defects, and Service Life Estimate of the
Counterweight Sheave/Trunnion Assembly of the I-5 Columbia River Bridge**

E.J. Kaufmann
J.W. Fisher

Final Report

Prepared for

Wiss, Janney, Elstner Associates, Inc.
330 Pfingsten Road
Northbrook, Illinois 60062

June 2000

ATLSS Engineering Research Center
Lehigh University
117 ATLSS Drive, Imbt Laboratories
Bethlehem, PA 18015-4729

I. INTRODUCTION

As part of a fitness for purpose evaluation of the counterweight sheave/trunnion assembly of the I-5 Columbia River Bridge for the Oregon Department of Transportation by Wiss, Janney, Elstner Associates Inc. and the ATLSS Engineering Research Center at Lehigh University, a detailed characterization was performed of the material properties of one of two sheave/trunnion assemblies removed from the bridge in 1997. The material tests included standard tensile and Charpy V-notch toughness tests, chemical composition and microstructural analyses of the material as well as standard fracture mechanics tests to measure fatigue crack growth rates and fracture toughness of the materials. Representative defect indications detected by NDE methods during service and after removal from the bridge were also evaluated to characterize their origin and evidence of extension by fatigue. Based upon the measured material properties, available stress and loading history data, and defect evaluation, an assessment of the remaining fatigue life of two similar sheave/trunnion assemblies still in-service was also performed.

II. SHEAVE/TRUNNION DEFECT EVALUATION

II.1 Trunnion Defect Indications

Based upon a re-inspection of the trunnion performed by WJE after removal of the sheave/trunnion from the bridge and disassembly, a detailed NDE evaluation of defect indications in the trunnion was prepared for subsequent sectioning to visually identify and characterize the indications. A general view of the disassembled trunnion as it was received at the ATLSS laboratories is shown in Figure 1. For identification the three east end trunnion keyways were labeled 1A, 2A, and 3A. West end keyways were identified as 1B, 2B, and 3B. Identification, descriptions, and location sketches of defect indications detected by UT and MT during the re-inspection are included in Appendix A for reference. Two principal types of defect indications were detected in the trunnion; 1) Surface crack-like discontinuities or sub-surface discontinuities oilway repair welds; and 2) internal discontinuities in the vicinity of the inner bore of the trunnion. Several defect indications representative of both types were selected for evaluation. Table 1 provides a summary of the defect indications selected.

Surface and sub-surface defect indications detected both ultrasonically and visually by magnetic particle testing were all located near keyways where six weld repairs had been performed to fill exposed internal oil passageways during an earlier renovation of the trunnion bearing assemblies. Surface defect indications were detected by MT at two keyway weld repair areas at the east end of the pin (1A and 3A). A similar surface defect indication was detected at the west end of the pin at the oilway weld repair at keyway 1B. Sub-surface indications were detected by UT at keyways 3A and 2A at various locations along the length of the repair weld.

Figures 2 through 4 show detailed views of keyway regions where surface discontinuities were detected. The crack-like indications can be clearly seen outlined by the reddish colored MT particles. The outline of the repair weld metal can also be seen in the photographs as a strip of material with a lighter tint. In all but one oilway repair the crack-like discontinuities appeared to be confined entirely to the weld metal suggesting they may be weld cracks. Only at keyway location 1B did the weld metal indication appear to extend beyond the weld fusion line into the trunnion base material suggesting the possibility that fatigue crack growth may have extended the crack beyond the weld metal into the parent material (see Figure 4).

In addition to the oilway repair weld metal indications seven internal discontinuities were also detected in the trunnion base metal by axial and/or borehole UT scanning of the pin (UT1 through UT7). These defect indications appeared to be largely grouped in one area near the east end of the trunnion near the center bore suggesting they may have similar origin. Manufacturing defects such as slag inclusions or gas pores often form in clusters and would not be uncommon to find near the center of a large forging.

During visual inspections of the trunnion prior to disassembly it was noted that tack welds added to the outer ends of the keys as retainers were cracked at all six keyways. The cracks all appeared to be weld throat cracks as shown in Figure 5. The tack welds in each case were small and of poor quality and may have developed cracks after welding due to weld contraction strains. No NDE indications of cracking from the weld root or weld toe into the trunnion were detected at any of the six keyway fillet welds. Fillet weld throat cracks would not be expected to propagate into the trunnion since the inherent lack of fusion at the weld root between the key and the pin would arrest further propagation of a weld metal crack into the trunnion. To verify these findings these cracks were also included in the trunnion defect evaluation.

II.2 Sheave Defect Indications

Two core samples were removed from the cast steel sheave wheel for evaluation where NDE located defect indications. A sketch showing the locations of the two core samples is included in Appendix A for reference. Both samples were removed from spoke areas near the wheel hub and showed crack-like defect indications. The two core samples are shown in Figures 6 and 7.

II.3 Trunnion Sectioning

Initially the pin was saw cut through the diameter 22 inches from the east end and 26 inches from the west end. The two end pieces were then saw cut radially into wedges to isolate the four keyway area containing defect indications and the trunnion internal discontinuities. Figure 8 shows the sectioning layout at both ends of the trunnion. After the wedge pieces were

separated the defect indication areas were then saw-cut from the smaller wedge pieces. An extra wedge piece was also cut from a defect free area of the east end of the trunnion for latter development as an ultrasonic test standard.

II.4 Trunnion Defect Evaluation

II.4.1 Oilway Weld Repair Defect Indications

The defect indications at keyway locations 1A and 1B were selected for fractographic examination since the largest surface MT indications were observed at these two locations and in the case of 1B appeared to show possible evidence of stable crack propagation beyond the repair weld metal. The defect indications at keyway location 3A was selected for metallographic cross-sectioning to obtain additional information on the nature of the surface cracks and the sub-surface UT indication detected at this location.

Keyway 2A and 3A

The oilway weld repair at keyway 2A and 3A were cross-sectioned by saw-cutting longitudinally along the centerline of the weld. Figure 9 shows polished and etched views of the cross-sections. Figure 10 shows an enlarged view of the weld termination in Keyway 3A. The multi-pass weld was found to contain numerous weld defects including incomplete fusion defects and slag inclusions particularly at the termination of the oilway groove. This is consistent with the UT analysis which also showed several sub-surface defect indications along the length of the weld. The largest slag inclusion measured 1/8" in width. The incomplete fusion defect at the root of the groove measured 1/2" in length. Viewed microscopically, discontinuous cracks were also observed within the heat-affected-zone of the weld (see Figure 11) which appeared to be hydrogen induced cracks or hot cracking. Considering the possibility of oil contamination within the former oilway, the groove geometry, and likelihood that low preheats were used it would not be surprising that hydrogen cracks might develop at these repairs and that the general weld quality is poor.

Evidence of crack extension by fatigue was observed close to the weld surface at the same location that MT detected a short surface discontinuity. A magnified view of the crack is shown in Figure 12. The crack appeared to have extended to the surface from a small slag inclusion 1/16" below the weld surface. No other indication of fatigue crack propagation was observed at the other weld metal defects detected in the cross-section.

Keyway 1A and 1B

The crack-like surface discontinuities observed at keyway 1A and 1B (see Figures 2 and 4) were exposed by fracturing at low temperature. Figures 13 and 14 show the crack surfaces as they appeared after exposure. The original crack dimensions are clearly delineated by the

blackened crack surfaces. Defect 1A measured 5/8" in width with a maximum depth of 1/2". Defect 1B measured 3/4" in width with a maximum depth of 3/8". The discoloration on the crack surfaces is likely due to exposure to bearing lubricants and air over long periods of time. Views of both crack surfaces after ultrasonically cleaning the surface to remove this film are shown in Figures 15 and 16. Clear evidence of fatigue crack extension is seen on both crack surfaces. Semi-elliptical crack growth is particularly clear in 1B. Figure 17 shows the crack surface of 1B as viewed at low magnification with the SEM where the smooth semi-elliptical crack growth region and initial defect is also clear. Viewed at higher magnification the fatigue nature of the smooth semi-elliptical crack surface (Area "a") was verified by the presence of fatigue striations (see Figure 18). In contrast, the initial defect area (Area "b") showed dendritic solidification structures typical of weld metal hot cracking (see Figure 19).

Fatigue crack extension in Defect 1A was less clear than observed in 1B. Evidence of smooth thumbnail cracks were seen visually at the surface and at an interior location. Several weld metal slag inclusions were also evident. The thumbnail cracks at the surface were more evident when viewed with the SEM (see Figure 20). Viewed at higher magnification these areas appeared fatigue-like although no fatigue striations were observed. Evidence of hot cracking was also observed in Defect 1A near the center of the defect (Area "b" in Figure 20).

II.4.2 Internal Trunnion Defect Indications

Four defect indications detected in the interior of the trunnion were investigated to confirm their presence and characterize their origin. All four (UT1, UT2x, UT2z, and UT4) were located in one area of the trunnion near its inner bore (see Table 1 and Appendix A for locations). In each case a saw-cut was made in two orthogonal planes at the positions determined by ultrasonic examination. With the exception of UT1 no defect was observed at the positions determined by UT. A defect was observed at UT1 which was identified to be a shrinkage cavity left from the original cast ingot. (see Figure 21). The diameter of the cavity was measured to be 3/32". No indication of crack extension from the defect was observed microscopically. Similar defects may have existed at the other positions searched, however, considering the small size of the defect observed at UT1 these could easily have been missed or eliminated in saw-cutting.

II.4.3. Keyway Retainer Fillet Weld Cracks

To verify that crack propagation into the trunnion had not developed from the weld throat cracks observed at key retainer tack welds a cross-section of one weld (Keyway 1B) was examined metallographically. The cross-section is shown in Figure 22 where the weld throat crack is clearly seen. The weld metal was also verified to be austenitic stainless steel weld metal as was earlier suspected. No evidence of crack extension from the weld root or weld toe was observed which is consistent with the NDE examination of these areas.

II.5 Sheave Defect Evaluation

The two core samples (Sample #1 and #2, see Figures 6 and 7) removed from the sheave wheel were cross-sectioned through the diameter and examined metallographically. The cross-section through Sample #1, seen in Figure 23, showed multiple surface cracks surrounding a large internal shrinkage cavity. The void measured about 1 inch in length. The surface cracks measured between 3/16" and 1/4" in depth. The cracks were likely caused by hot tearing occurring during cooling and shrinkage of the casting in the vicinity of the large internal cavity. Microscopic examination of the crack tip regions did not show any indication of crack extension by fatigue. Surface cracks with depths as large as measured here would be expected to have a low threshold stress range for fatigue crack propagation. Since no crack extension developed at these cracks over the long service life of the sheave indicates that stress ranges in this area were very low.

Sample #2 was cross-sectioned similarly and is shown in Figure 24. Grinding of the surface crack detected in this core prior to removing the core apparently eliminated whatever defect had been detected in the core. A small shrinkage cavity close to this area is seen in the cross-section which may have been associated with a larger cavity similar to Sample #1.

III. MATERIAL PROPERTIES

III.1 Chemical Composition and Weldability

A chemical analysis of the trunnion and sheave were obtained to characterize the composition of the materials and also to assess their weldability. Since a gradient in properties can be expected in a large forging an analysis of the composition of the trunnion was obtained near the outside surface and near the inner bore. The properties of the sheave were determined from the two samples removed from two different locations in the casting. The locations are shown in the sheave sampling sketch in Appendix A. Sample #3 was removed from a spoke area of the wheel. Sample #4 was removed from a juncture of a spoke and the outer rim of the wheel. The thickness of the material at the two locations was about 1-3/8" and 1-1/2", respectively.

Chemical composition analyses of the trunnion and sheave samples were performed by a commercial testing laboratory by standard optical emission spectroscopy (OES) methods. The lab test report is included in Appendix B. The compositions of the trunnion at the two test locations were generally the same although the carbon content at the inner test location was slightly higher due to alloy segregation (0.39 wt% vs. 0.35 wt%). The overall composition is similar to a modern day 1040 carbon steel composition often used in forgings.

The weldability of the trunnion material would not be expected to be good for several reasons. The carbon content is high which increases susceptibility to hydrogen cracking. An

often used measure of the susceptibility of a steel composition to hydrogen cracking is the carbon equivalent (CE), calculated as $CE = C + Mn/6 + (Cr+Mo+V)/5 + (Ni+Cr)/15$. Based upon the analysis the carbon equivalent of the trunnion near its outside surface is 0.44. Avoidance of hydrogen cracking at this carbon and CE level requires careful control of hydrogen and high preheat temperatures. Another factor to be considered is the relatively high sulfur content measured (0.034 wt%) and low manganese content (0.51 wt%). Steels with high carbon levels and low Mn/S ratios have been found to have increased susceptibility to HAZ hot cracking. Studies have indicated that Mn/S ratios as high as 35 are necessary to reduce hot cracking risks in these cases. The Mn/S ratio of the trunnion is about 15. An increased susceptibility to weld metal hot cracking would also be expected from sulfur pickup and is consistent with the hot cracking evidence found fractographically at the oilway weld repairs.

The composition of the sheave measured at the two sample locations were similar and consistent with a modern day 1030 carbon steel composition commonly used in steel castings today. Although welding of steel castings requires care the sheave wheel could be welded successfully based upon its composition.

III.2 Microstructure

Etched microstructures of the trunnion near the outside surface and near the inner bore are shown in Figure 25. The microstructure at both locations is ferrite-pearlite with a slightly larger ferrite grain size and pearlite fraction at the inner location consistent with the higher carbon content measured in this region. The microstructure was generally uniform with some areas of proeutectoid ferrite veining. A portion of a ferrite vein is seen in the inner trunnion microstructure.

The microstructures of the cast steel sheave at the two sample locations are shown in Figure 26. The microstructures are also ferrite-pearlitic. The ferrite grain size is coarse as would be expected in a large casting.

III.2 Tensile Properties

Standard 0.505 inch round tensile specimens were fabricated from the trunnion material at the inner and outer diameter test locations. The specimens were oriented longitudinal to the trunnion axis. The same standard test specimens were also fabricated from the two sheave samples. Table 2 provides a summary of the tensile properties measured for the two components. The trunnion yield point ranged from 34-38 ksi at the two test locations. Tensile strengths ranged from 72-80 ksi.

The strength properties of the cast sheave wheel were found to be similar to the trunnion. Yield and tensile strengths measured at the two sample locations were both similar with an

average yield point of 36.75 ksi and tensile strength of 72.0 ksi. The tensile ductility measured in the test specimens from Sample #3 were found to be low due to the presence of small casting defects in the specimen cross-section. Where these defects were absent (Sample #4) tensile elongations exceeding 20% were measured.

III.3 Charpy V-Notch Tests

Standard Charpy-V notch test specimens were fabricated from the trunnion at the two test locations. Eighteen specimens were fabricated at each location to permit tests to be performed over a range of test temperatures covering the transition temperature range. A similar number of specimens were fabricated from each of the sheave samples. Tables 3 and 4 provide a tabulation of the test results. The test data is shown plotted in Figures 27 and 28.

Both components showed similar levels of notch toughness. The room temperature CVN energy in both materials was about 7 ft-lbs with upper shelf energies of 40 and 60 ft-lbs at a temperature of 275 F. Only a small reduction in toughness was measured between the inner and outer trunnion test specimen location which suggests that the toughness of the trunnion throughout its cross-section is fairly uniform. Test data acquired from another lift bridge trunnion removed from service in Duluth, MN is also shown in Figure 27 for comparison. The test specimen location was similar to the outer surface location used in the current tests. The test data shows that the subject trunnion has similar and a marginally higher level of toughness than measured in the Duluth trunnion.

An estimate of the static fracture toughness of the trunnion can be made using the Barsom-Rolfe CVN- K_{ID} correlation temperature shifted to account for strain rate effects. The temperature shift can be calculated as

$$T_{\text{shift}} = 215 - 1.5\sigma_{ys} \quad (1)$$

resulting in a dynamic to static temperature shift for the trunnion material ($\sigma_{ys} = 36$ ksi)

$$T_{\text{shift}} = 160 \text{ F}$$

The static fracture toughness of the trunnion material at the minimum service temperature of -10 F can therefore be represented by its dynamic toughness at 150 F.

Using the correlation relation

$$K_{ID} = [5E(\text{CVN})]^{1/2} \quad (2)$$

and the average CVN energy measured at 150 F (24 ft-lbs) results in a dynamic fracture toughness $K_{ID} = 60 \text{ ksi-in}^{1/2}$. This will correspond to a static fracture toughness, $K_{IC} = 60 \text{ ksi-in}^{1/2}$

at the minimum anticipated service temperature of the bridge.

III.4 J_{IC} Fracture Toughness Tests

Standard J_{IC} (K_{IC}) fracture toughness tests were performed on the trunnion and sheave material to obtain a more direct measure of the static fracture toughness than estimated from CVN tests. Since CVN tests indicated that the trunnion toughness was nearly uniform throughout its cross-section, fracture toughness tests were performed at only one test location near the outside diameter. Standard compact tension specimens were fabricated from trunnion material (ASTM E813) with the notch oriented in a plane through the diameter, the same orientation as used for the CVN specimens. Four 1.5 inch thick specimens were fabricated to provide duplicate test specimens to be tested at the minimum service temperature of -10F and at room temperature. Four test specimens were also fabricated from sheave material (Sample #4). The specimen thickness was limited to ~1.25 inches, equivalent to the full thickness of the material available.

Figures 29 through 44 show load-clip gauge displacement traces for the eight specimens tested along with the appearance of the fractures. The behavior of both the trunnion and sheave specimens were surprisingly similarly considering their different metallurgical condition (ie. forged vs. cast). All of the specimens tested at the minimum service temperature fractured brittly with only a small amount of crack tip plasticity. All of the specimens tested at room temperature (68 F) showed increased plasticity, however, fracture also occurred by cleavage without any evidence of ductile stable crack extension prior to fracture. Multiple brittle crack extensions or "pop-ins" were observed in the sheave material tested at room temperature (Specimens S1 and S2, see Figures 37 and 39) prior to a large brittle crack extension. The final crack extension is seen on the fracture surfaces after heat tinting.

Table 5 provides a summary of the fracture toughness test results. Since fracture in all cases occurred non-linearly by cleavage extension a J value was computed at fracture or at the first pop-in recorded as

$$J = J_{\text{elastic}} + J_{\text{plastic}}$$

$$J = K^2(1-\nu^2)/E + 2A_{\text{plastic}}/Bb_0$$

The resulting J is also shown in the table converted to an approximate K_{IC}. At the minimum service temperature (-10F) the trunnion toughness was measured to be 57 ksi-in^{1/2}. The sheave toughness was measured to be 47.6-52.8 ksi-in^{1/2}. The fracture toughness estimated from the lower bound CVN test data (Eq. 2) was 60 ksi-in^{1/2} and 47.4 ksi-in^{1/2}, respectively, which is in good agreement. At room temperature the trunnion fracture toughness ranged from 93.7 - 131.7 ksi-in^{1/2}. The sheave fracture toughness range from 68.4-78.5 ksi-in^{1/2} which are also in reasonable agreement with the CVN determined toughness.

III.5 Fatigue Crack Growth Rate Tests

Standard fatigue crack growth rate tests (ASTM E647) were performed on both the trunnion and sheave material using automated PC controlled testing software. Duplicate test specimens were prepared from each material to establish their crack growth rate behavior (da/dN vs. ΔK). To generate growth rate test data similar to full reversal conditions specimens were tested at a low stress ratio ($R=0.1$).

Figure 45a shows da/dN vs. ΔK plots for the trunnion and sheave material. Also shown are Paris law constants computed by regression analysis. Data for both materials suggested a slope of 3.6-3.8 which is greater than the value of 3 generally used for steels. Regression analysis of the data in the threshold region indicated $\Delta K_{th} \sim 10-11 \text{ ksi-in}^{1/2}$ (see Figure 45b), however, data at the lower growth rates were problematic due to crack closer effects. Actual thresholds are likely below this value.

IV. SERVICE LIFE ESTIMATE

IV.1 Sheave/Trunnion Defects

Evaluation of the trunnion defects showed that oilway weld repair defects at the keyway regions were the only defects which exhibited indications of fatigue crack extension. This is reasonable considering the close proximity of these defects to the trunnion surface where maximum bending stresses develop and compounded by their close proximity to the machined radius and keyway by stress concentration effects. No evidence was found that any of the internal trunnion defects detected had propagated by fatigue and would not be expected to considering the small size of the defects observed and their location. The analysis of the remaining life of the trunnion therefore focused on the weld repair defects 1A and 1B for which evidence of crack extension was observed.

IV.2 Stress Analysis and Loading History

Based upon the bridge service log it is estimated that 500 to 700 lifts per year occurred since renovation of the trunnion in 1960 and its removal in 1997. Estimating that each 90 ft. lift requires the sheave/trunnion to rotate an average of six revolutions (3 revolutions up and 3 down), the number of load cycles applied each year is between 3000 and 4200 cycles. Therefore, over the 37 year service life of the weld repaired trunnion it is estimated that a total of 111,000 to 155,400 load cycles were applied resulting in the observed fatigue crack growth at the oilway weld repair defects.

Stress computations have indicated a maximum stress range in the trunnion $S_r = 9.8$ ksi or $9.8 \text{ ksi} \times 2 = 19.6$ ksi for the full load cycle. The full stress range is applicable as high residual tensile stresses will exist from the weld repair. The machined radius at the shoulder ($r = 1/2$ ") increases this by the stress concentration factor $K_t \sim 2.2$.

IV.3 Estimate of Stress Intensity Range, ΔK

Since fatigue striations were observed on the crack surface of Defect 1B (see Figure 18) the stress intensity range, ΔK , at this location on the crack surface can be estimated using the measured striation spacing and a general crack growth relationship for steel

$$da/dN = 3.6 \times 10^{-10} \Delta K^3 \quad (3)$$

The striations were detected on the crack surface near the initial crack tip and measured 3×10^{-4} mm (1.18×10^{-5} inches). Substituting into Eq. 3 yields a stress intensity range, $\Delta K = 32.0$ ksi-in^{1/2}.

IV.4 Crack Model

Fractographic analysis of the defect crack surfaces at keyways 1A and 1B indicated one or more initial fabrication weld defects. Defect 1B contained a single weld metal hot crack which extended to the surface. The initial edge crack measured 1/4 inch deep with a length measured at the surface of 5/16 inch. Fatigue crack extension of the initial crack resulted in a final crack depth of 3/8 inch and surface length of 5/8 inch. Modeling the crack as a semi-elliptical edge crack is reasonable considering the observed shape of the crack extension.

Defect 1A was more complex since several initial fabrication defects were present (two slag inclusions and a hot crack). Treating the weld root slag inclusion and adjacent weld hot crack as a single defect results in an initial nearly circular embedded defect with a diameter of 5/16 inch. Extension of the crack by fatigue resulted in a surface crack with a final depth of 1/2 inch and surface length of 3/4 inch.

The stress intensity factor range, ΔK , for the semi-elliptical surface crack can be expressed as

$$\Delta K = F_s F_g S_r \sqrt{\pi a} \quad (4)$$

where F_s is the crack shape correction factor and F_g is the stress gradient correction factor. The factors are applied to correct for the shape of the semi-elliptical crack and stress gradient in the vicinity of the crack due to the machined radius, respectively. Determination of stress gradient correction factors, F_g , for specific geometries is generally very complex requiring finite element

analysis. An indication of the magnitude of F_g can be inferred from ΔK estimated from striation spacings observed at a crack depth, $a = 5/16$ inch, in Sec. IV.3. Substituting $\Delta K = 32 \text{ ksi-in}^{1/2}$ and $a = 5/16$ " into Eq. 4 with $S_r = 19.6 \text{ ksi}$ yields a value of $F_g F_g = 1.64$. This seems in agreement with the stress concentration at the shoulder of the trunnion of 2.2.

Integrating the crack growth relationship (Eq.3) to estimate the cycles required to grow the fatigue crack observed at Defect 1B from its initial defect size of 0.25 inch to its final size of 0.375 inch

$$N = \int_{0.25}^{0.375} \frac{da}{(3.6 \times 10^{-10}) \Delta K^3} \quad (5)$$

where $\Delta K = (19.6)F_g F_g \sqrt{\pi a}$ and $F_g F_g = 1.64$ results in a fatigue life, $N = 11,000$ cycles. Assuming no stress gradient and shape correction (ie. $F_g F_g = 1$) results in a fatigue life, $N = 49,000$ cycles. Comparing to the estimated number of cycles applied to the trunnion (Sec. IV.2) suggests that the stress gradient decays rapidly as the crack extends and that the initial weld defect likely required cycles to initiate fatigue cracking.

IV.5 Fatigue Life Estimate

As the crack grows out of the machined radius region and the stress gradient decays, the correction factors $F_g F_g$ will eventually approach the known edge crack relationship

$$\Delta K = 1.12 S_r \sqrt{\pi a} \quad (6)$$

Evidence of this tendency was observed in another lift bridge trunnion which developed a larger fatigue crack in the machined radius of the shoulder (see Figure 46). The depth of the crack in this case was 1.5 inches. Equation 6 can be used to estimate the number of cycles needed to extend the 3/8 inch deep crack at keyway 1B to a depth of 1 inch. Substituting into Eq. 5 provides

$$N = \int_{0.375}^{1.0} \frac{da}{(3.6 \times 10^{-10}) (1.12 S_r \sqrt{\pi a})^3} \quad (7)$$

$$N = [2 \times 10^{10} / (1.12)^3 (3.6) (\pi)^{3/2} S_r^3] [1/\sqrt{0.375} - 1/\sqrt{1.0}]$$

$$N = 62,720 \text{ cycles}$$

This would require 15-21 years of additional service at the frequency indicated in Sec. IV.2. If the stress range were taken as 15 ksi as estimated by WJE, the cycle life would increase to 140,000 cycles or 33-47 years of additional service.

At a crack depth of 1 inch the maximum applied stress intensity factor, K_{max} , in tension is

$$K_{max} = 1.12\sigma_{max}\sqrt{\pi a} \quad (8)$$

where $\sigma_{max} = 9.8$ ksi. This yields a maximum stress intensity of $19 \text{ ksi-in}^{1/2}$. The fracture toughness, K_{IC} , of the trunnion material is estimated from CVN test data (see Sec. III.3) to be near $60 \text{ ksi-in}^{1/2}$ at the lowest anticipated service temperature. Static fracture toughness of the trunnion pin from J_{IC} tests yielded an average value of $57.5 \text{ ksi-in}^{1/2}$ which is comparable. Hence, the factor of safety against crack instability is near 3 when the crack extension reaches 1 in. depth. Hence, there is no near term concern with the performance of other trunnions if they have comparable conditions.

V. REVIEW OF CRACKING IN TRUNNION SHAFTS

In recent years a number of shafts and trunnions used in lift bridges that were designed and built prior to the 1960's have developed fatigue cracks and occasionally fractured the shaft. Cracks have developed at keyways and at changes in the shaft diameter when the trunnions experienced several reversal stress cycles during each lift and return of the structure. Rotations of more than 180° results in a complete reversal in the stress cycle.

The specifications used to design movable bridges were evolved from the AREA Specifications. The allowable bending stresses for trunnions up to 1983 were taken as 15 ksi for ASTM A608 Class G steel when the rotation was more than 180° . In the structures that experienced cracking, the tension design stress was between 9.8 and 17 ksi.

Table 6 provides a tabulation of the stress and rotations experienced by structures that developed cracks in the trunnion at the radius. These components are also plotted in S-N form in Figure 47 and compared to Categories A and C. Note that two of the sheaves had the trunnion welded to the shaft. Those welds were on the major diameter of the shafts.

It can be seen that the I-5 trunnion crack is consistent with the general behavior observed in other structures. Fatigue cracking has developed at a weld repair and exceeds Category C for the Columbia River Bridge. However, based on the experience with these other structures, significant residual life should exist as the stress range will decrease as the crack extends out of the high stress concentration region.

Finally, it should be noted that only two of these structures experienced complete failure of the trunnion shaft. One was the Valleyfield structure and the second was St. Lambert over the St. Lawrence Seaway.

VI. CONCLUSIONS

1. Evaluation of representative defect indications detected in the trunnion verified the presence of weld defects at oilway weld repairs which included weld cracks, slag inclusions, and incomplete fusion. Evidence of fatigue crack extension of defects located near the weld surface was observed at three oilway repair locations examined. Although small internal defects were observed in the trunnion which originated during its manufacture these were observed to be small volumetric defects and showed no evidence of extension by fatigue. The sheave wheel defect examined was found to have originated during manufacture of the casting and although containing crack-like discontinuities showed no indication of extension by fatigue.
2. The mechanical properties of the trunnion and sheave were found to be consistent with properties expected of forged and cast components from the period of manufacture and component size and consistent with other lift bridge components which have been evaluated.
3. Estimates of the remaining service life of the trunnion examined based upon the observed defect sizes and extension by fatigue over its service life suggests that additional crack growth corresponding to 15 to 20 years of service if the stress range is taken as 19.6 ksi, or 33 to 47 years if the stress range is taken as 15 ksi. This would be applicable to the remaining two trunnions in service assuming similar sized defects exist. This indicates that crack growth can be monitored by periodic inspections and will provide further assurance of long term performance.
4. To date no detectable crack growth has been observed in the cast sheaves. Its fracture toughness is only slightly lower than the trunnion pin at the minimum anticipated service temperature. Comparable performance should be expected with the sheave wheels.

TABLE 1 SUMMARY OF TRUNNION DEFECT INDICATIONS

Defect Indication ID	Location	Description	Reference Sketch
1A	Keyway @ 1A (East End)	Transverse surface crack in oilway repair weld metal (MT)	Sheet 16
1B	Keyway @ 1B (West End)	Transverse surface crack in oilway repair weld metal (MT)	Sheet 17
3A	Keyway @ 3A (East End)	Transverse surface crack in oilway repair weld metal (MT). Embedded Weld Metal Indications (UT)	Sheet 18
UT1	Trunnion Near Inner Bore 15.5" from East End	Embedded Discontinuity (UT)	Sheet 19
UT2x UT2z	Trunnion Near Inner Bore; 8.5" and 13.25" from East End	Embedded Discontinuity (UT)	Sheet 20
UT4	Trunnion Near Inner Bore; 15.25" from East End	Embedded Discontinuity (UT)	Sheet 20
2A	Keyway @ 2A (East End)	Embedded Weld Metal Indications (UT)	Sheet 21

TABLE 2 SHEAVE/TRUNNION MECHANICAL PROPERTIES

	Sample Location	Yld. (ksi)	U.T.S. (ksi)	Elong. (2") (%)	R.A. (%)
Trunnion Pin	Outer Diameter	36.03	76.12	22.6	43.8
		37.88	79.70	18.3	23.8
	Innner Diameter	33.83	71.95	29.6	37.2
		34.78	72.37	30.0	35.2
Sheave Wheel	Spoke (Sample #3)	36.99	73.04	10.9	14.2
		37.88	65.38	6.4	7.8
	Spoke/Rim (Sample #4)	38.15	75.58	21.3	43.7
		34.00	73.97	21.9	44.4

TABLE 3 TRUNNION CHARPY V-NOTCH TEST RESULTS

<u>Outside Surface</u>		<u>Inside Surface</u>	
<u>Temperature, F</u>	<u>CVN Energy, ft-lbs</u>	<u>Temperature, F</u>	<u>CVN Energy, ft-lbs</u>
40	4.5	40	3.0
	5.0		4.0
	5.0		3.5
71	7.0	71	7.0
	7.5		8.0
	8.5		9.0
110	17.0	110	15.0
	23.0		16.5
	15.0		11.5
150	24.0	150	31.0
	35.0		25.0
	29.0		21.0
204	38.5	204	40.0
	53.0		44.5
	48.5		41.0
275	56.0	275	53.0
	65.5		49.5
	60.0		55.0

TABLE 4 SHEAVE WHEEL CHARPY V-NOTCH TEST RESULTS

<u>Sample #3 (Spoke Area)</u>		<u>Sample #4 (Rim Area)</u>	
<u>Temperature, F</u>	<u>CVN Energy, ft-lbs</u>	<u>Temperature, F</u>	<u>CVN Energy, ft-lbs</u>
40	6.0	40	4.0
	5.0		6.5
	3.5		5.0
71	6.5	71	9.0
	6.5		8.0
	8.0		6.0
110	12.0	110	14.0
	12.0		13.5
	10.0		14.0
150	20.0	150	20.0
	15.0		17.0
	16.0		33.0
206	26.0	206	24.5
	25.0		38.0
	24.5		34.5
275	39.0	275	46.0
	36.0		38.5
	38.0		51.5

TABLE 5 SUMMARY OF FRACTURE TOUGHNESS TESTS

Spec. No.	Test Temp. (°F)	B (in.)	W (in.)	a/W	P _{max} (lbs.)	K _{max} (ksi-in ^{1/2})	J = J _{elastic} + J _{plastic} (in-lbs/in ²)	K _c = (JE) ^{1/2} (ksi-in ^{1/2})	K _{IC,CVN} = (SE[CVN]) ^{1/2} (ksi-in ^{1/2})
P1	-10 F	1.500	2.997	0.625	9,722	56.61	109.5	57.3	60.0
P2	-10 F	1.500	2.995	0.619	9,805	55.82	111.6	57.8	(24 ft-lbs)
P3	68 F	1.500	2.995	0.682	6,557	49.58	578.0	131.7	77.5
P4	68 F	1.500	2.993	0.607	11,168	60.55	292.6	93.7	(40 ft-lbs)
S1	68 F	1.282	2.996	0.618	8,556*	56.76	156.0	68.4	64.8
S2	68 F	1.254	2.999	0.609	8,994*	58.73	205.6	78.5	(28 ft-lbs)
S3	-10 F	1.282	2.997	0.615	8,780	57.32	93.1	52.8	47.4
S4	-10 F	1.281	2.999	0.614	7,682	49.93	75.5	47.6	(15 ft-lbs)

P = Trunnion Pin

S = Sheave Wheel

*1st pop-in

TABLE 6 SUMMARY OF CRACKS AT RADIUS OF TRUNNION AND FATIGUE LIFE

Bridge	Design Stress (ksi)	Stress Concentration K_t	Stress Range ksi = $k_t S_r$	Life Cycles
1. Valleyfield East St. Louis, IL	13.5	1.70	47.0	900,000
2. Caughmawaga St. Laurence Seaway	10.3	1.72	35.4	600,000
3. St. Lambert St. Laurence Seaway	13.0	1.75	45.5	700,000
4. Shippings Port New Jersey	16.0	1.75	56.0	600,000
5. Carleton Maine	17.0	2.18	74.0	450,000
6. Hackensack River Br. New Jersey	9.7	2.15	41.7	1,170,000
7. Newark Bay Bridge New Jersey	9.7	2.15	41.7	1,170,000
8. Duluth Minnesota	12.8	2.05	52.5	1,000,000
9. I-5 Columbia River	9.8 or (7.5)	2.20	43.0 (33.0)	155,000*

* Estimated cycles up to 1997

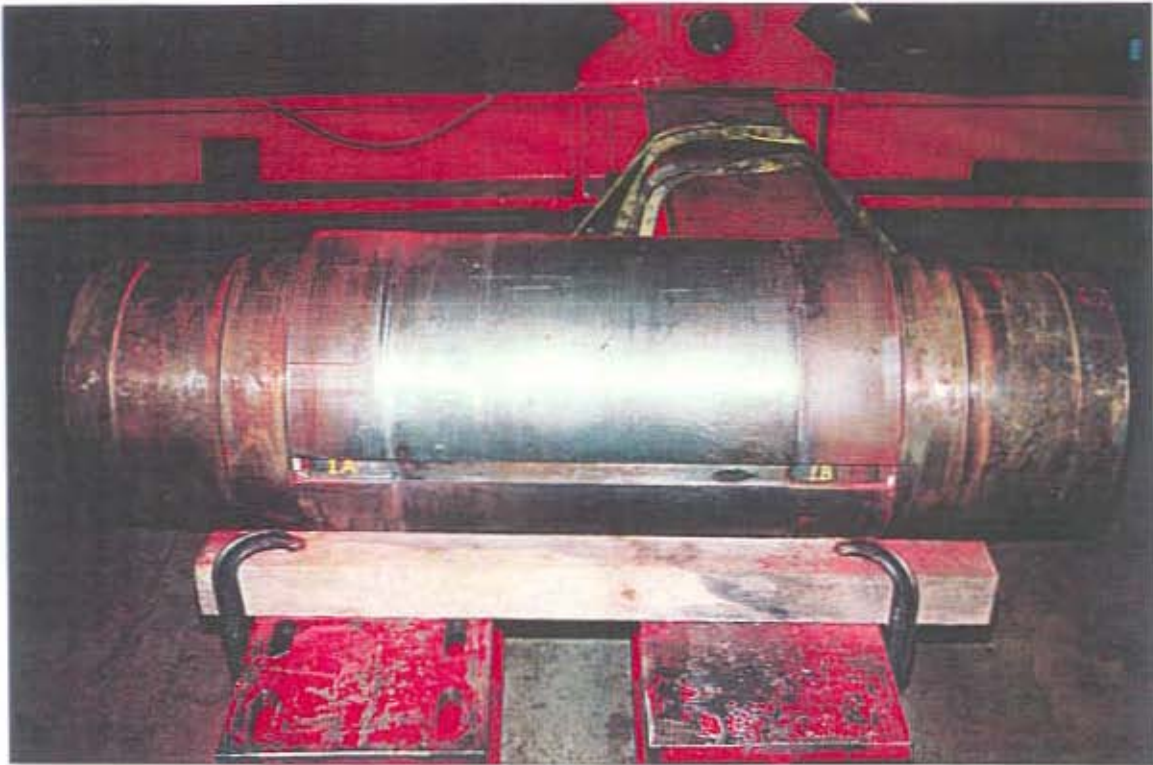


Figure 1 - General Views of the Disassembled Trunnion As-Received at the ATLSS Laboratories.
(Photos Courtesy of WJE)



Figure 2 - Surface Discontinuity Detected by MT at Oilway Weld Repair Near Keyway 1A.
(Photo Courtesy of WJE)



Figure 3 - Surface Discontinuity Detected by MT at Oilway Weld Repair Near Keyway 3A.
(Photo Courtesy of WJE)



Figure 4 - Surface Discontinuity Detected by MT at Oilway Weld Repair Near Keyway 1B.
(Photo Courtesy of WJE)



Figure 5 - Typical Key Retainer Fillet Weld Crack Throat Crack (Keyway 1B).
(6/99/2-3)



Figure 6 - Sheave Wheel Core Sample #1. Note Surface Crack Indicated by Arrow.
(4/99/14-11)



Figure 7 - Sheave Wheel Core Sample #2. The Surface Crack Detected Was Ground to Gauge Crack Depth Prior to Coring.
(4/99/14-8)

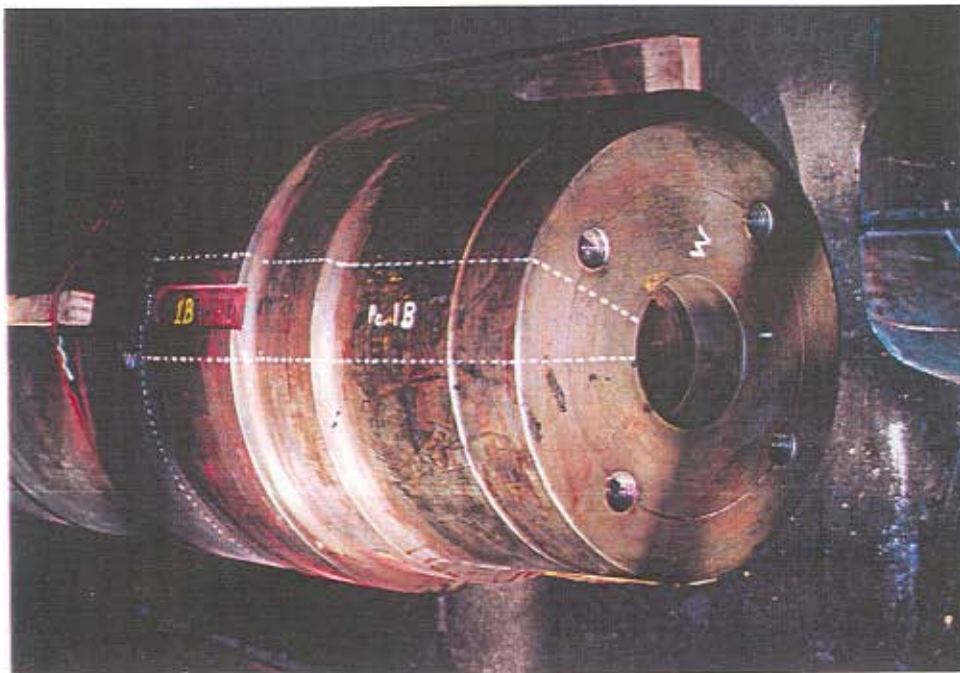
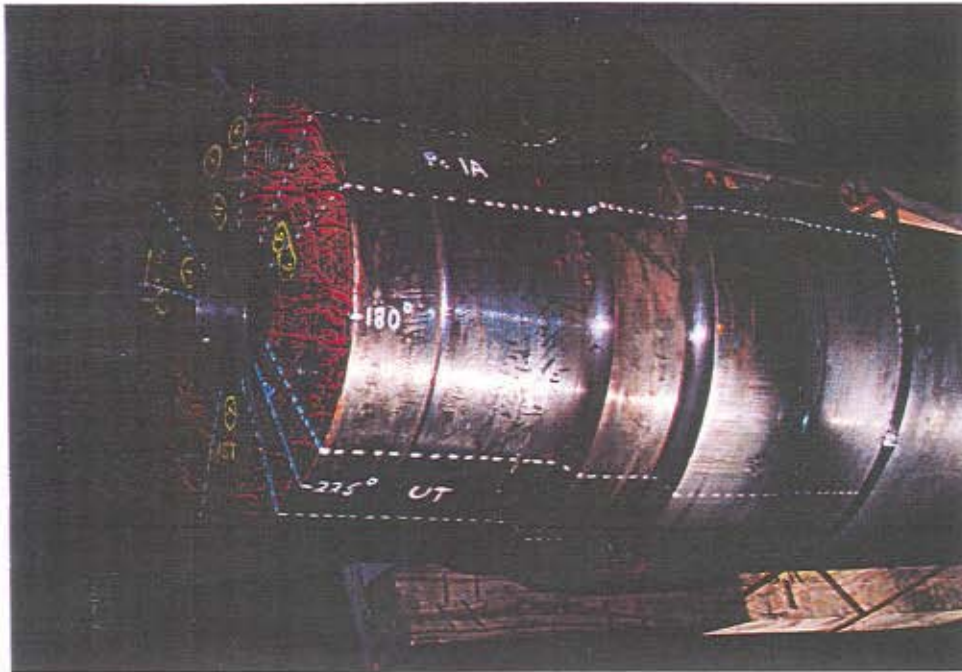


Figure 8 - Layout for Saw-Cutting the Trunnion to Remove the Defect Indication Areas.
Top: East End (11/98/1-6) Bottom: West End (11/98/1-4)

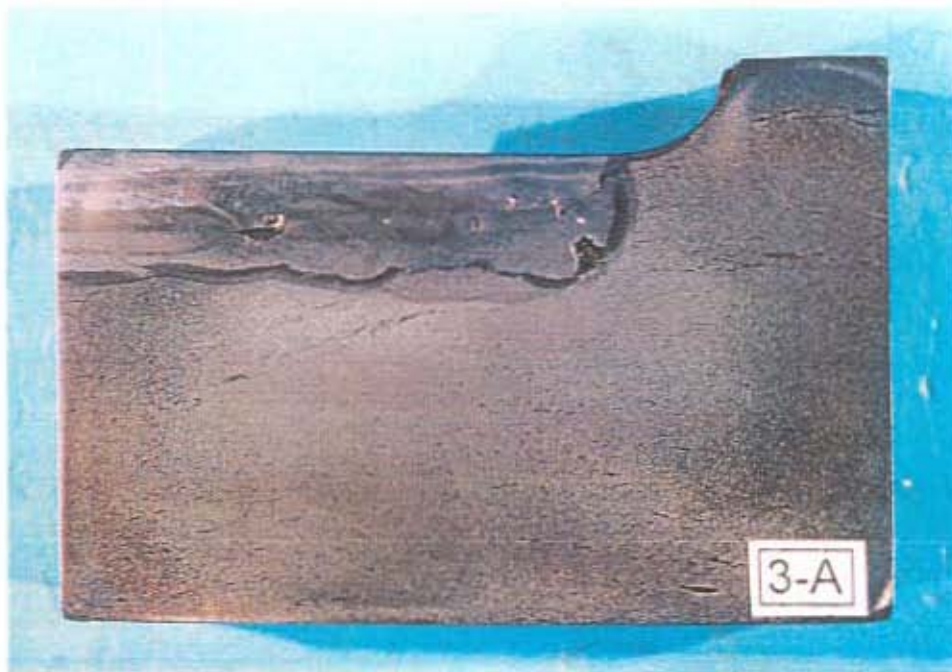


Figure 9 - Etched Cross-Sections of the Oilway Repair Weld at Keyway 2A and 3A Showing Multiple Weld Defects.
(1/00/5-2, 4/99/16-2)

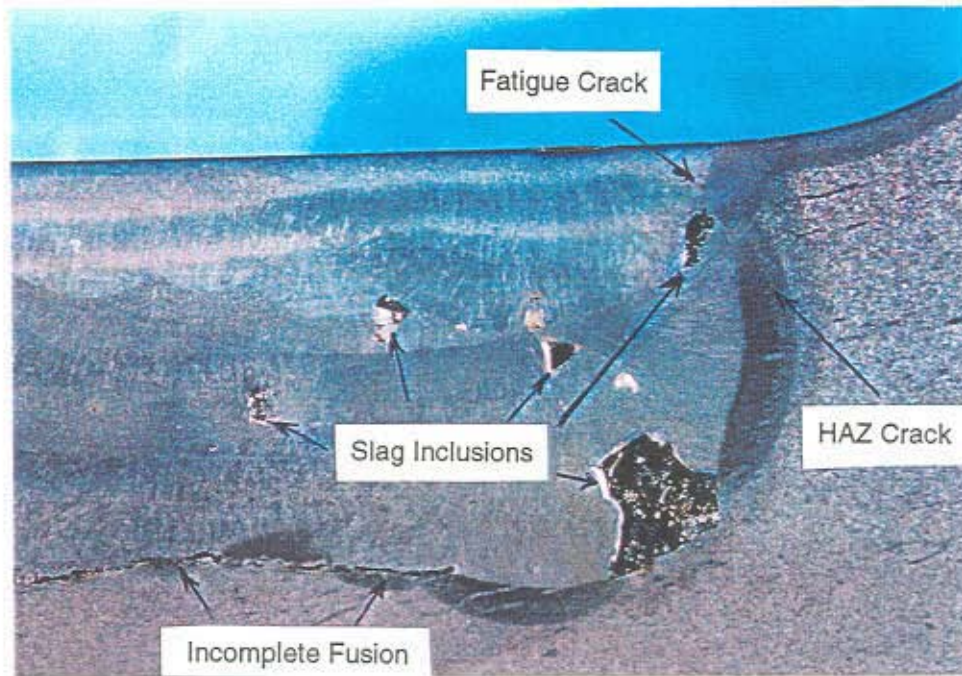


Figure 10 - Enlarged View of the Weld Defects at the Termination of the Oilway Groove Weld Showing Slag Inclusions, Incomplete Fusion and Cracks.
(4/99/16-8)



Figure 11 - Hydrogen Induced Crack Observed in the Weld HAZ at Keyway 3A.
[Mag. 100X]



Figure 12 - Fatigue Crack Extension From a Near Surface Slag Inclusion Observed at Keyway 3A. [Mag. 100X]

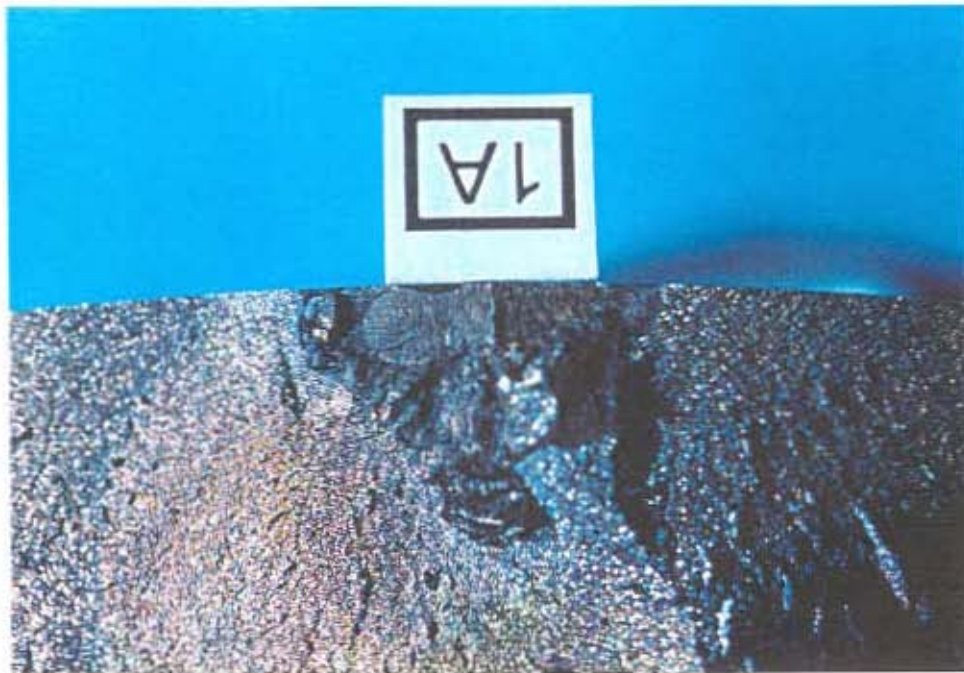
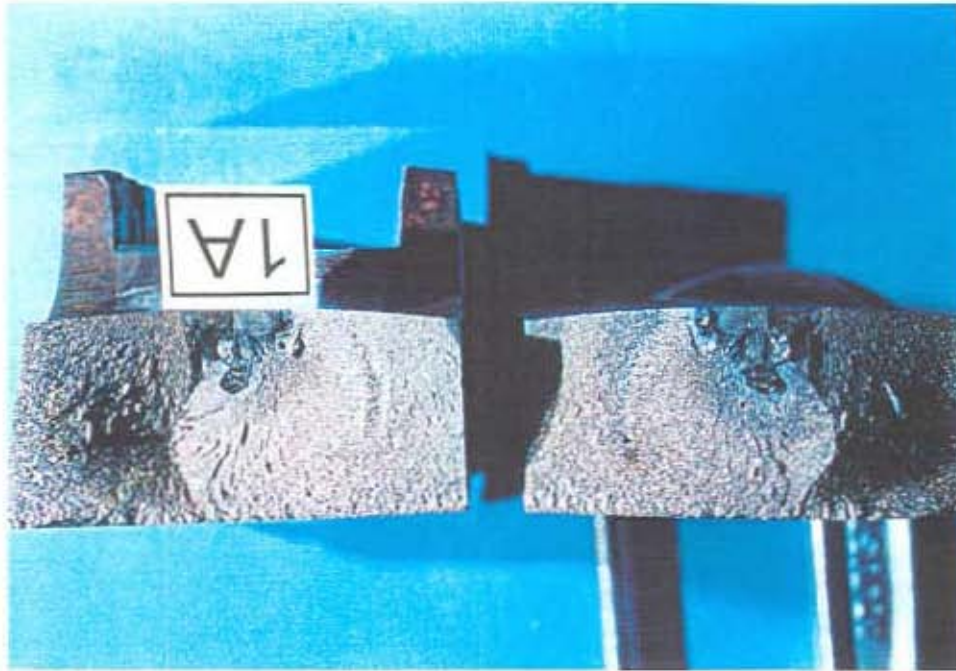


Figure 13 - Exposed Crack Surfaces of the Defect Detected In the Weld Repair at Keyway 1A.
(Top: 6/99/2-10, Bottom: 6/99/2-11)

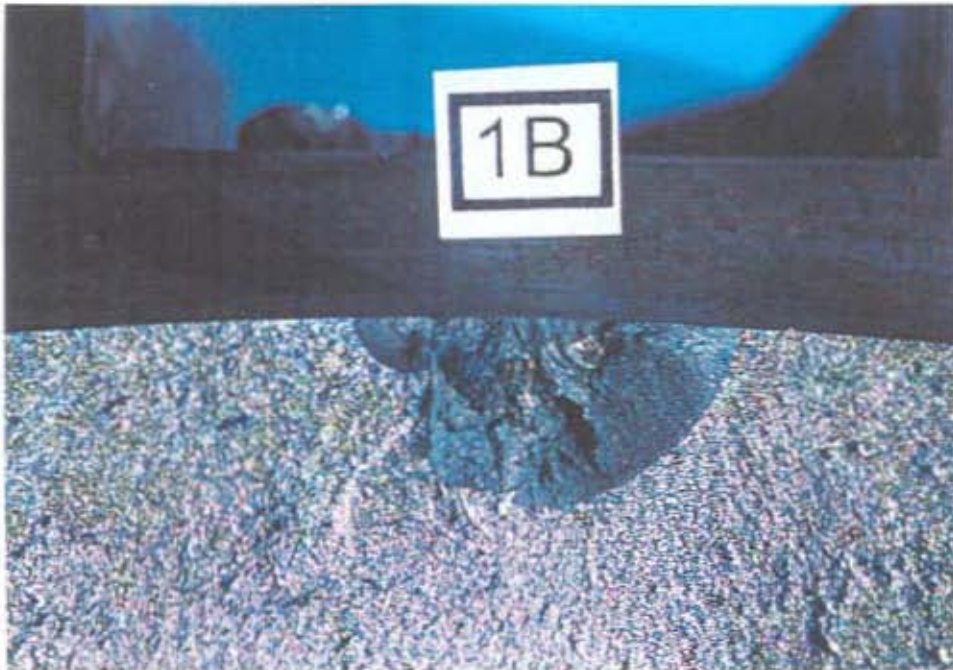
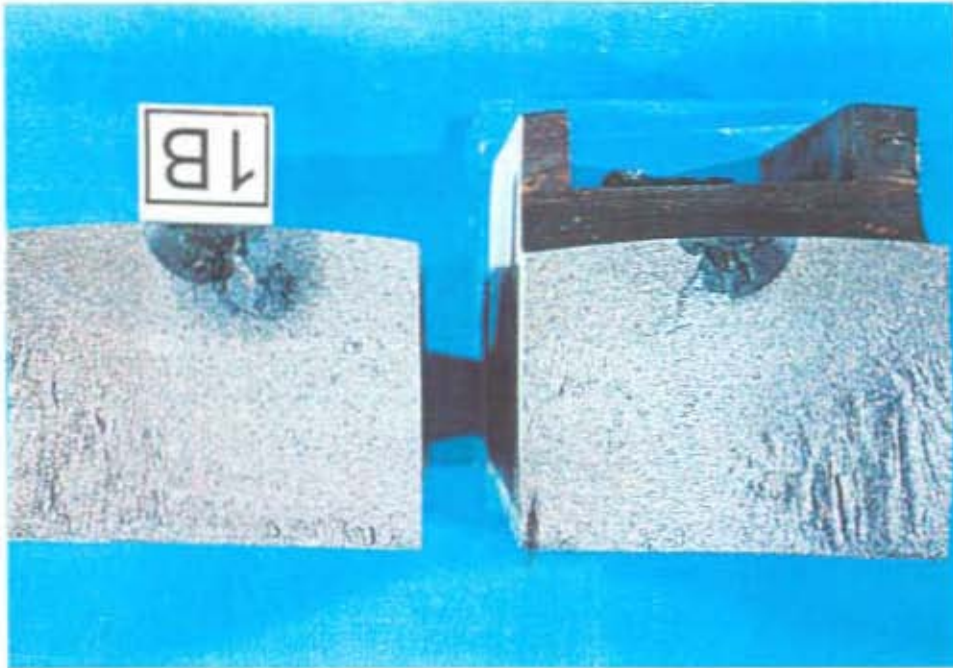


Figure 14 - Exposed Crack Surfaces of the Defect Detected in the Weld Repair at Keyway 1B.
(Top: 6/99/2-5, Bottom: 6/99/2-7)

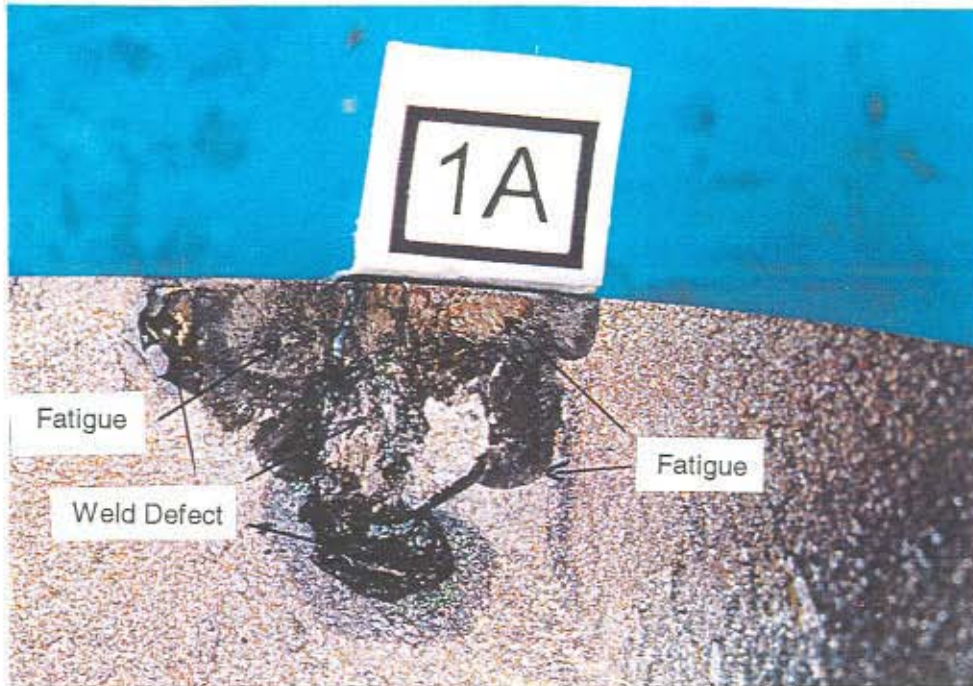


Figure 15 - Crack Surface From Keyway 1A After Ultrasonic Cleaning of the Surface.
Evidence of Fatigue Crack Extension is Seen in Several Areas.
(6/99/3-3)

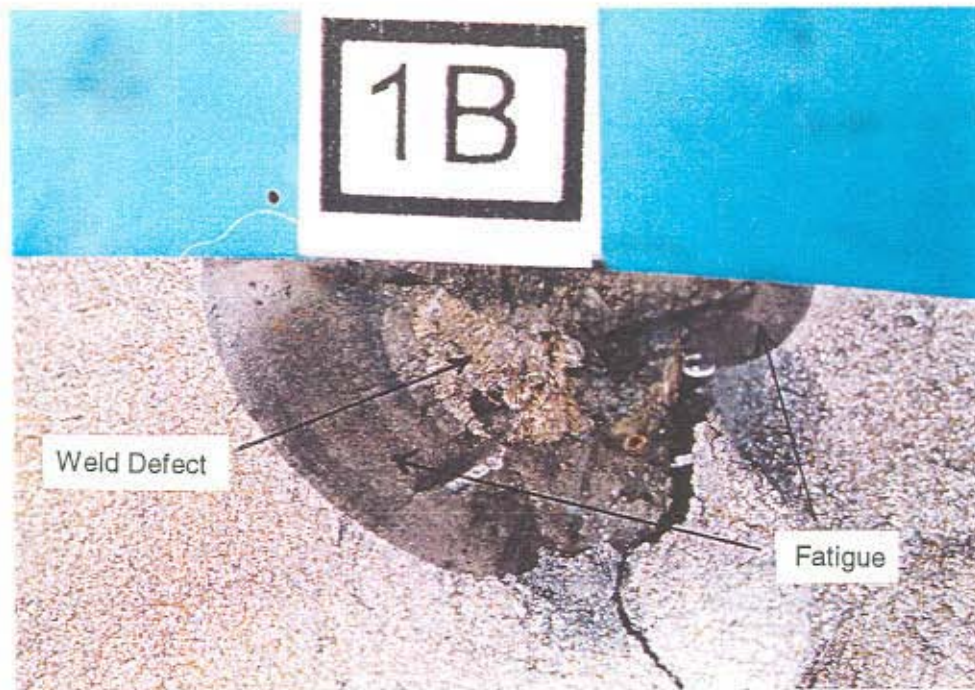


Figure 16 - Crack Surface From Keyway 1B After Ultrasonic Cleaning of the Surface.
Fatigue Crack Extension From an Initial Weld Defect is Clearly Evident.
(6/99/3-1)

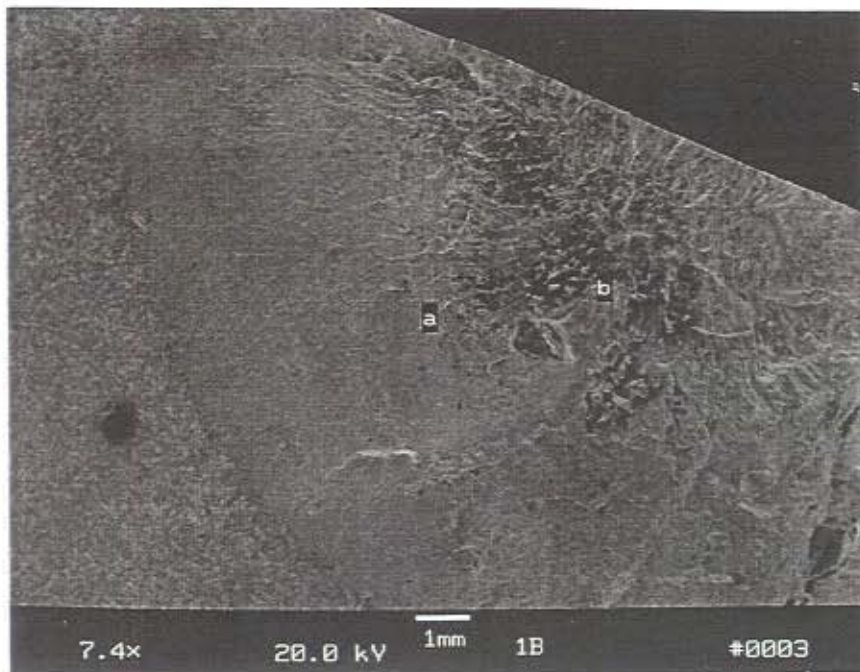


Figure 17 - SEM Micrograph of the Crack Surface of Defect 1B Showing the Initial Weld Defect and Fatigue Extension. [Mag. 7.4X]

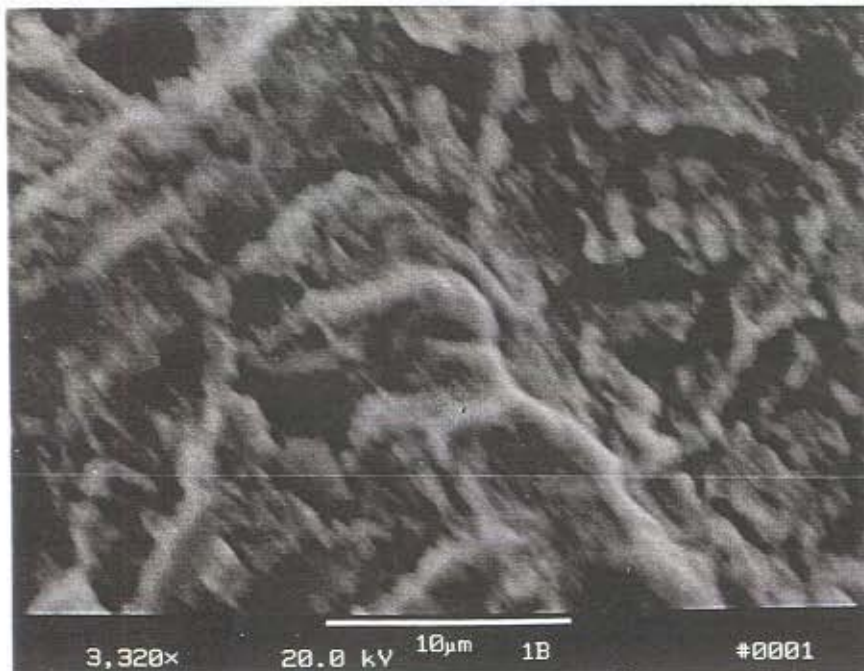


Figure 18 - High Magnification SEM Micrograph Showing Fatigue Striations in the Smooth Semi-elliptical Crack Growth Area (Area "a" in Figure 17).[Mag.3,320X]

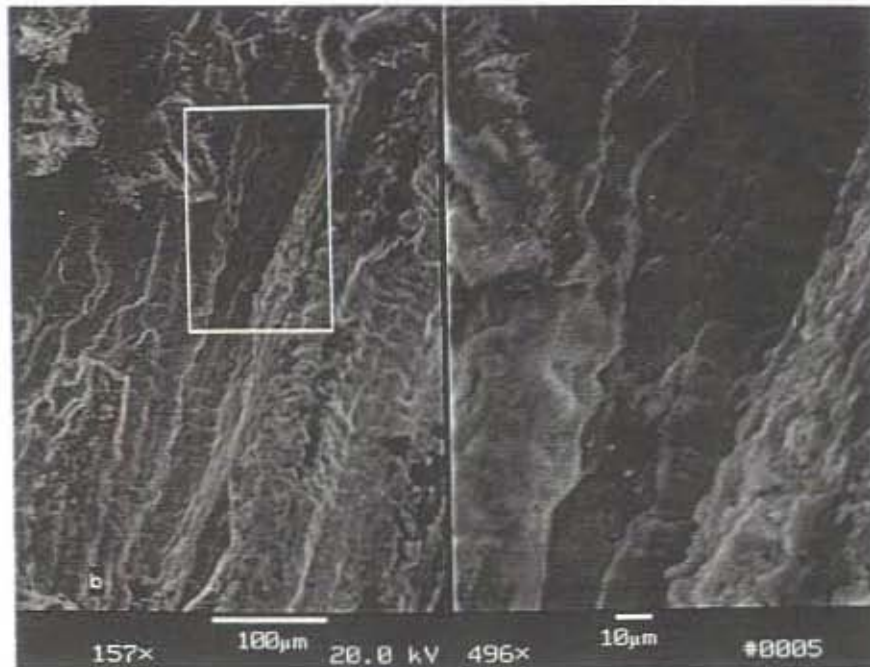


Figure 19 - Crack Surface of Defect 1B Obtained in the Initial Defect Region (Area "b" in Figure 17) Showing Solidification Structures Typical of Hot Cracking in Weld Metal. [Mag. 157X & 496X]

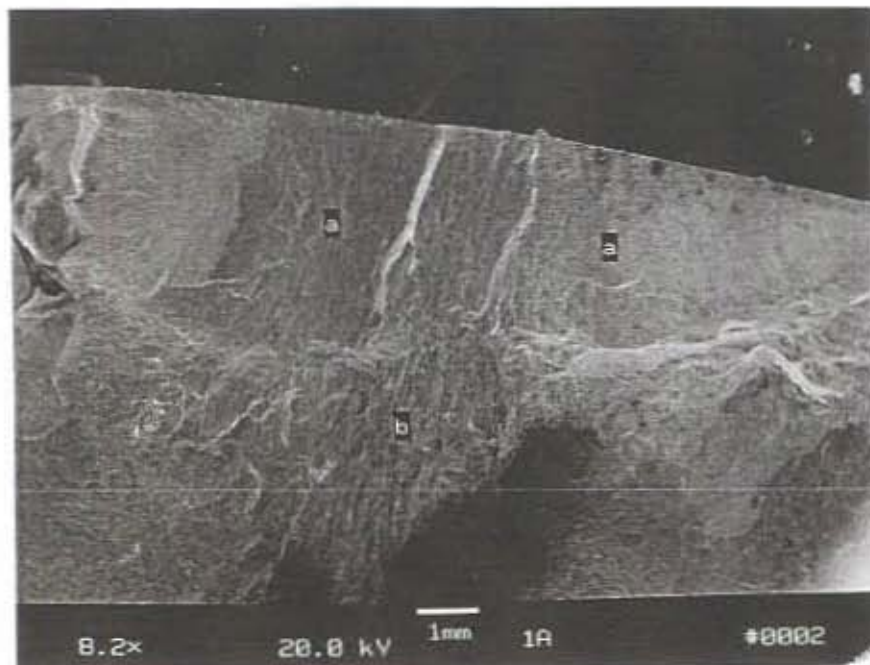


Figure 20 - Low Magnification SEM Micrograph of the Crack Surface of Defect 1A. Evidence of Thumbnail Fatigue Cracks (Areas "a") and Hot Cracking Were Observed (Area "b"). [Mag. 8.2X]



Figure 21 - Internal Trunnion Defect Detected By Ultrasonic Inspection (UT1).
(12/99/7-4)

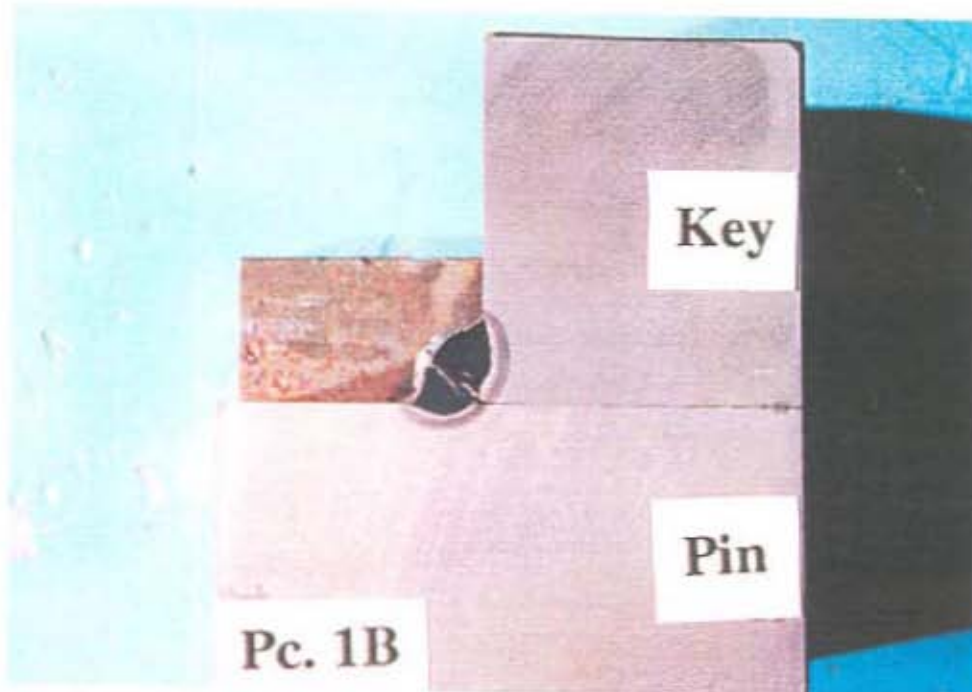


Figure 22 - Cross-section of Cracked Trunnion Key Retainer Fillet Weld (Keyway 1B).
(12/99/7-2)

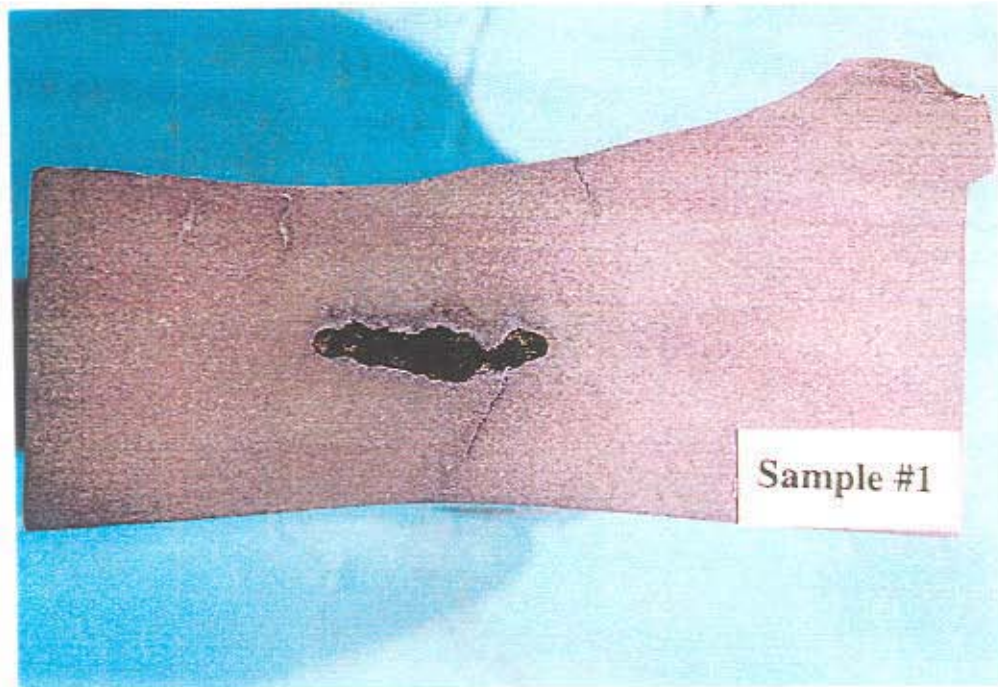


Figure 23 - Cross-Section Through Sheave Core Sample #1. A Large Shrinkage Cavity Is Seen at the Mid-Thickness With Surrounding Hot Tears.
(12/99/7-8)

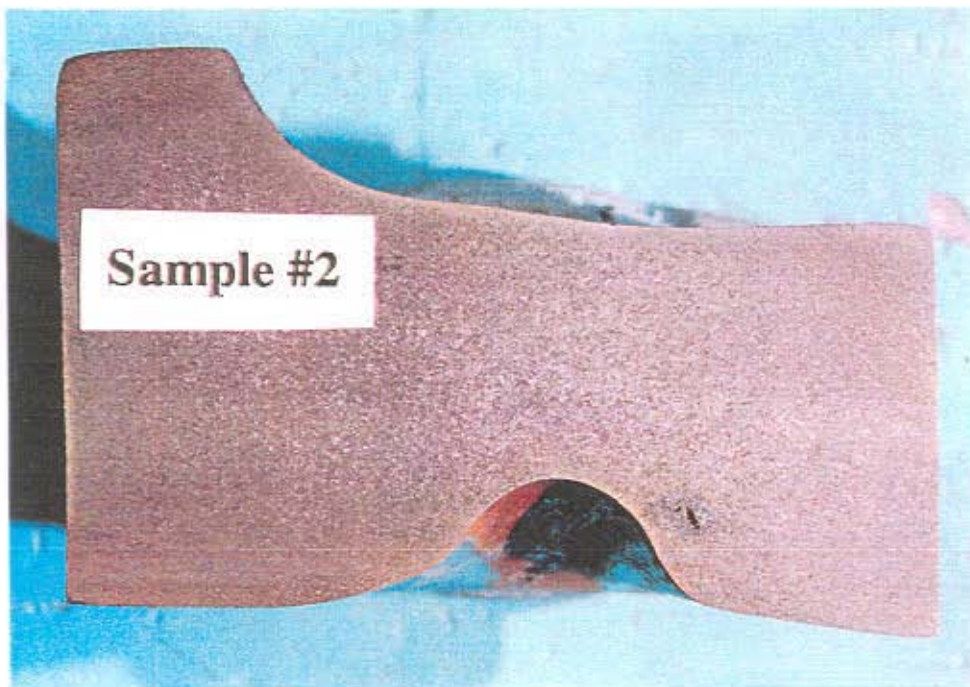


Figure 24 - Cross-Section Through Sheave Core Sample #2. No Primary Defect Was Remaining After Grinding the Surface. A Small Casting Void Is Seen Adjacent to the Ground Area.
(12/99/7-9)

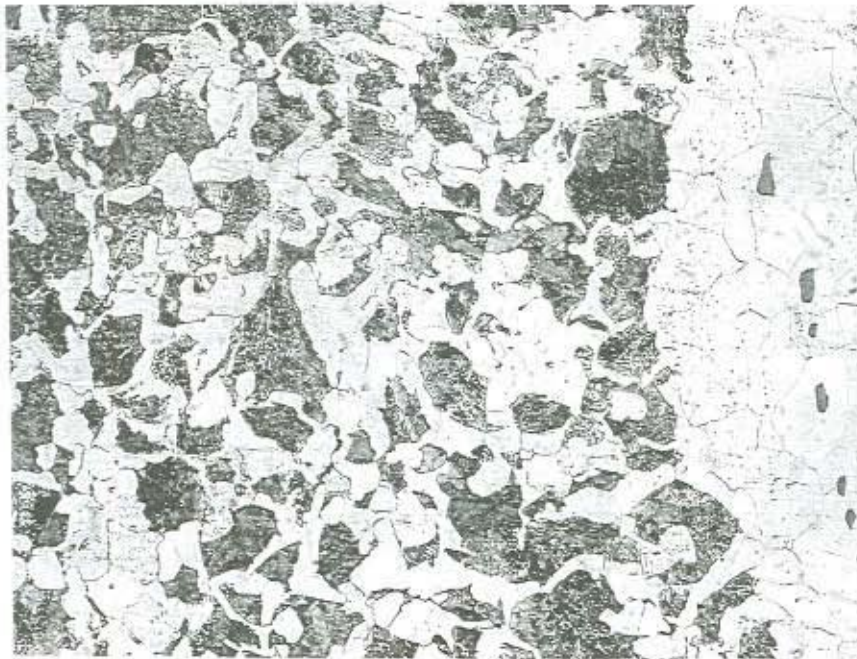
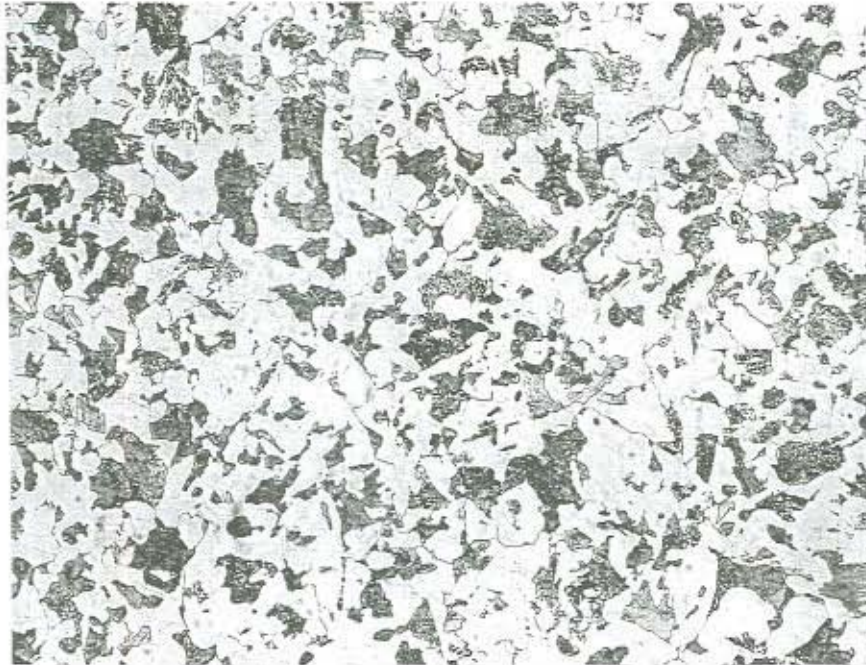


Figure 25 - Microstructure of the Trunnion. [Mag. 200X]
Top) Near Outer Diameter Bottom) Near Inner Diameter



Figure 26 - Microstructure of the Sheave. [Mag. 200X]
Top) Sample #3 Bottom) Sample #4

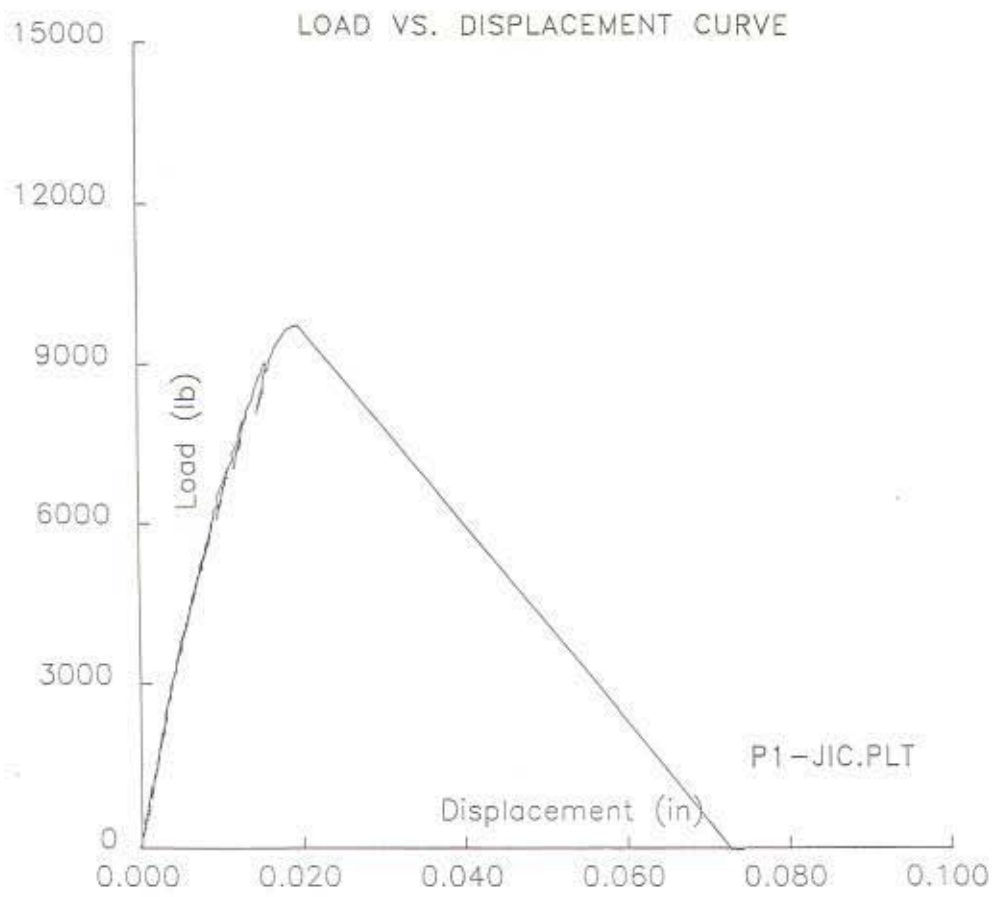


Figure 29 - Load-Clip Gauge Displacement Plot for Test Specimen P1 (T = -10F).

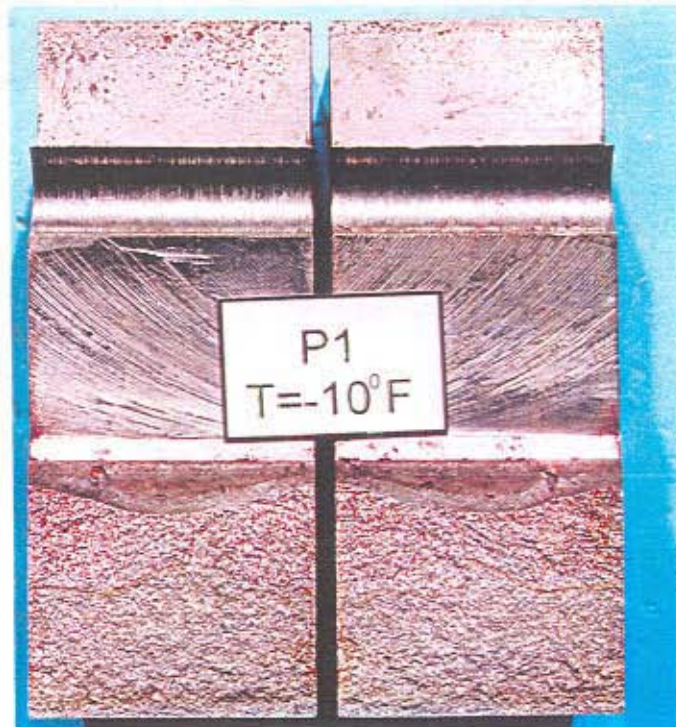


Figure 30 - Fracture Surfaces of Test Specimen P1. (6/00/3-4)

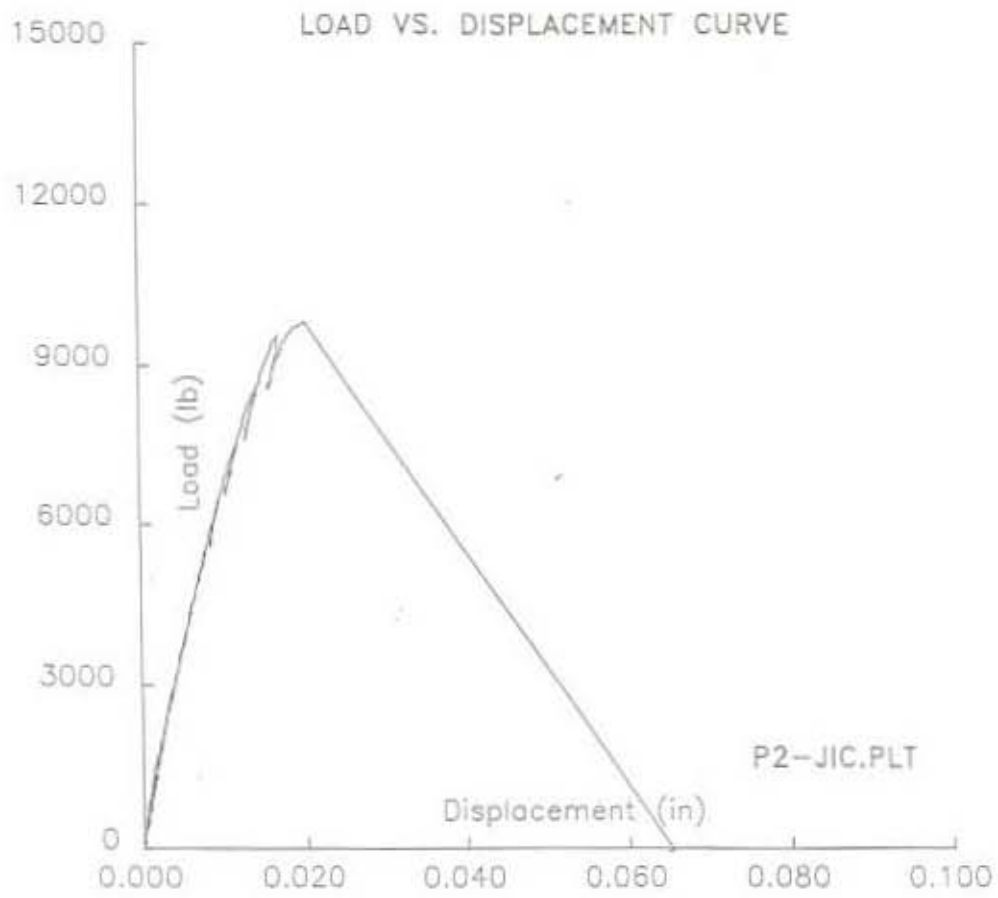


Figure 31 - Load-Clip Gauge Displacement Plot for Test Specimen P2 (T = -10F).



Figure 32 - Fracture Surfaces of Test Specimen P2. (6/00/3-5)

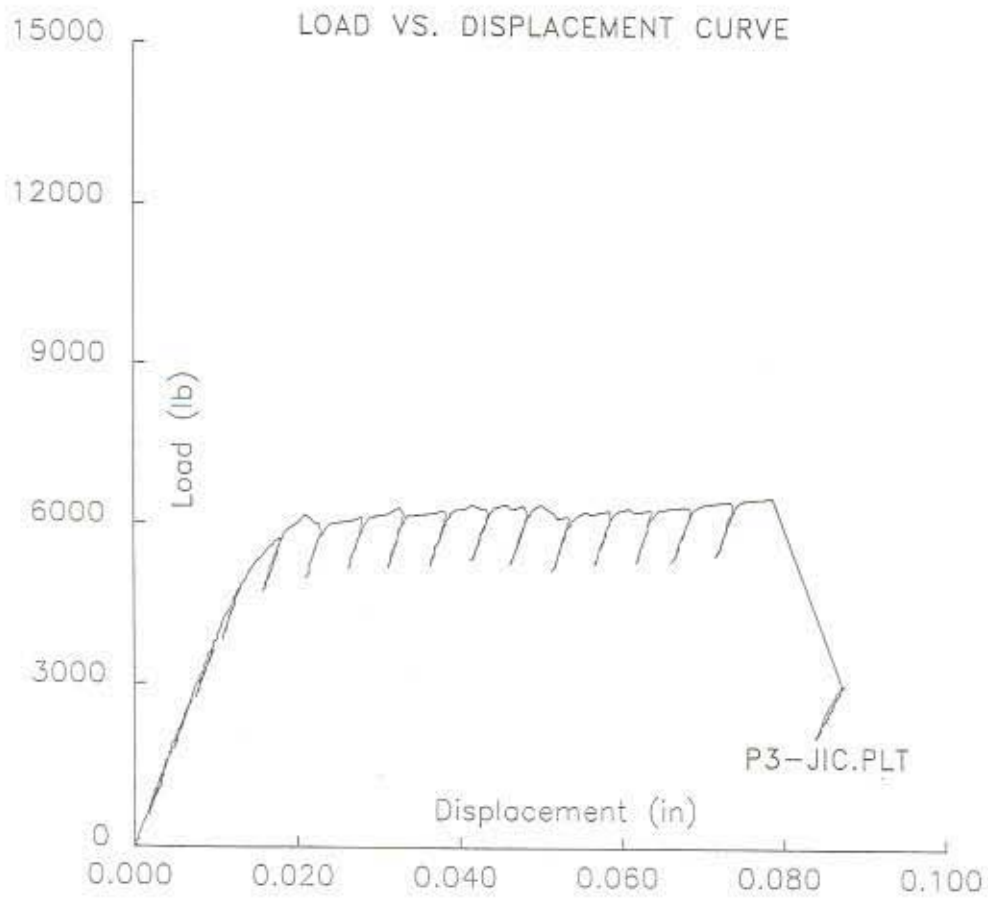


Figure 33 - Load-Clip Gauge Displacement Plot for Test Specimen P3 (T = 68F).

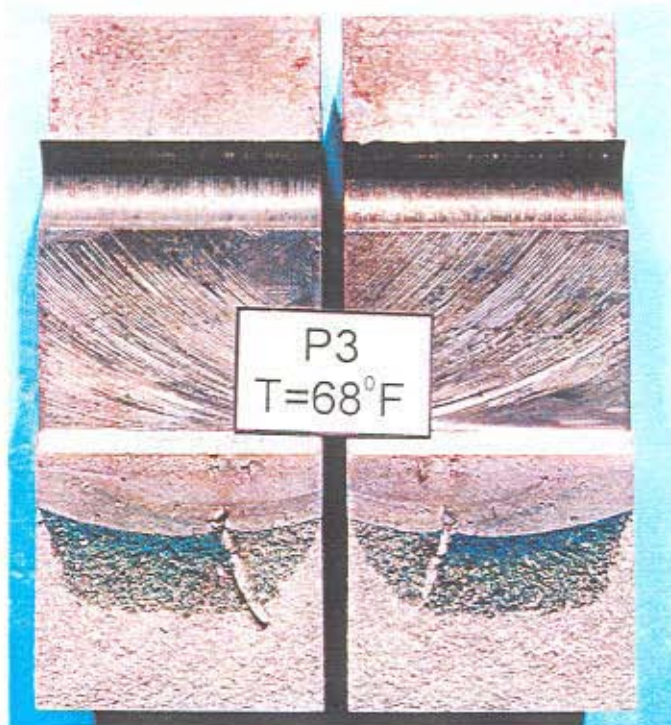


Figure 34 - Fracture Surfaces of Test Specimen P3. (6/00/2-10)

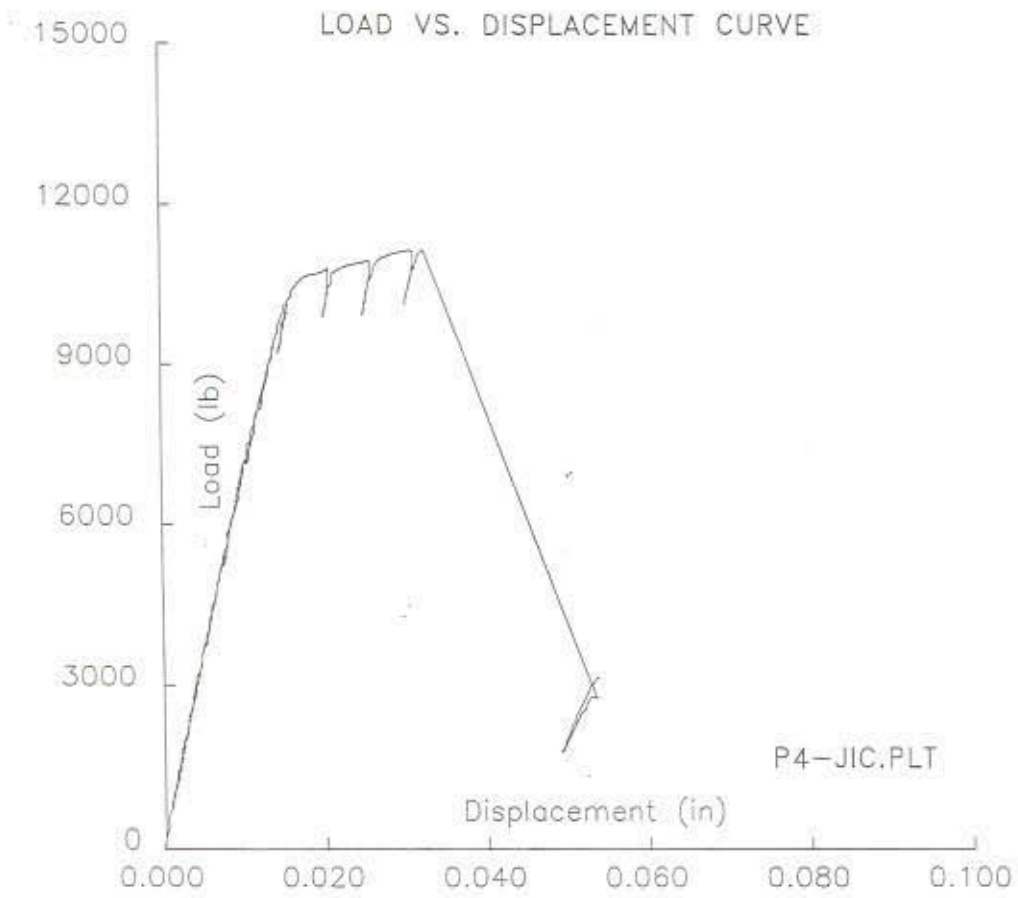


Figure 35 - Load-Clip Gauge Displacement Plot for Test Specimen P4 (T = 68F).

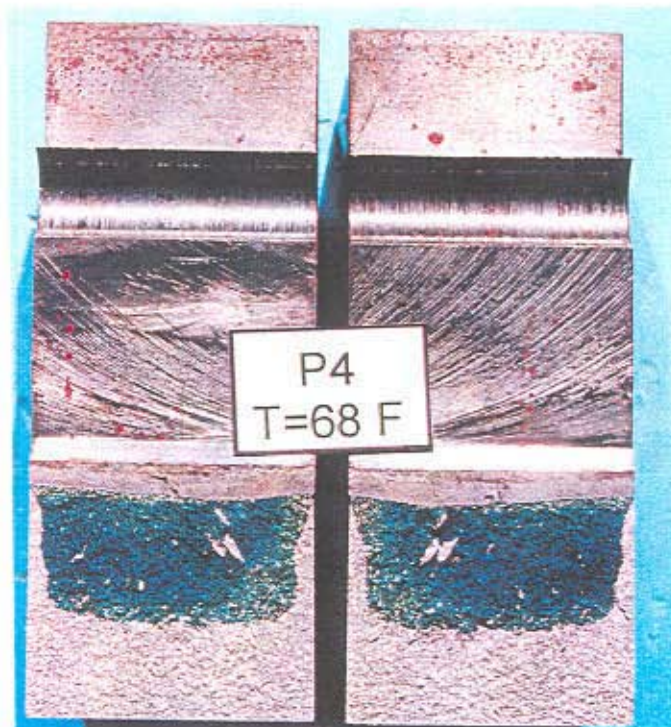


Figure 36 - Fracture Surfaces of Test Specimen P4. (6/00/3-1)

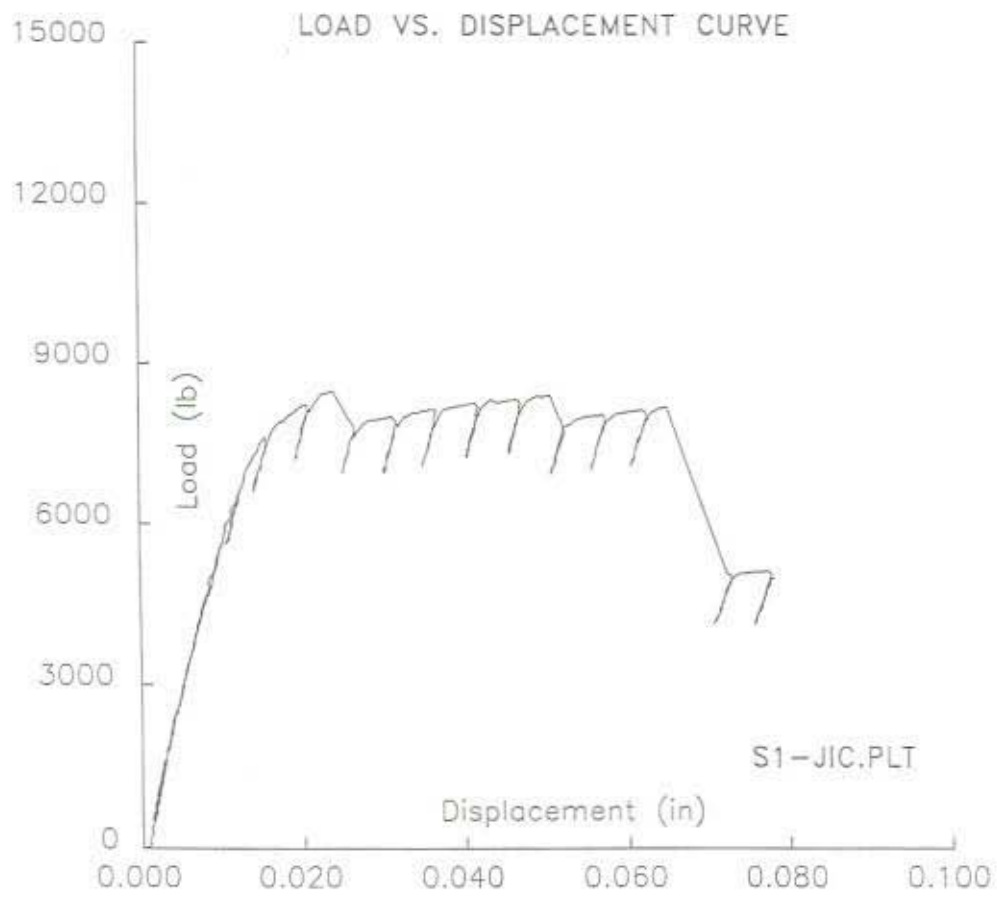


Figure 37 - Load-Clip Gauge Displacement Plot for Test Specimen S1 (T = 68F).

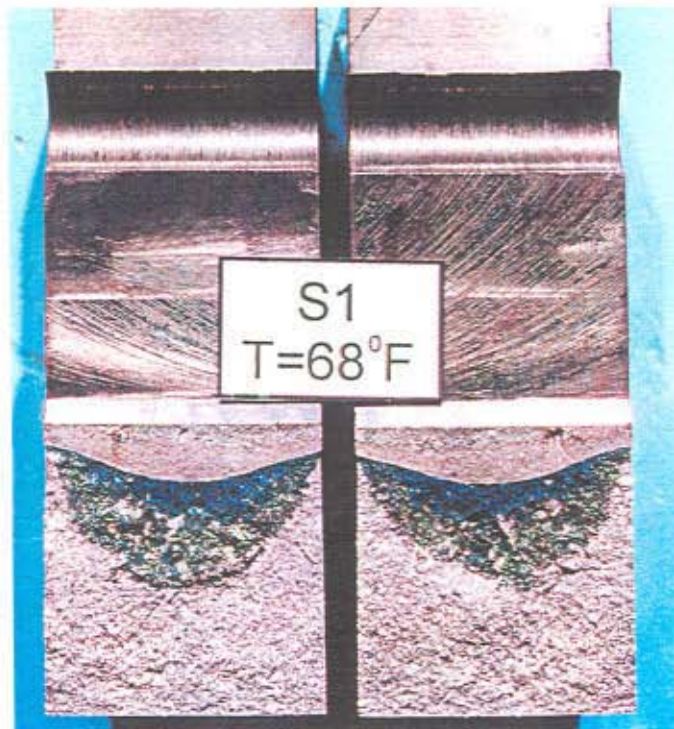


Figure 38 - Fracture Surfaces of Test Specimen S1. (6/00/2-5)

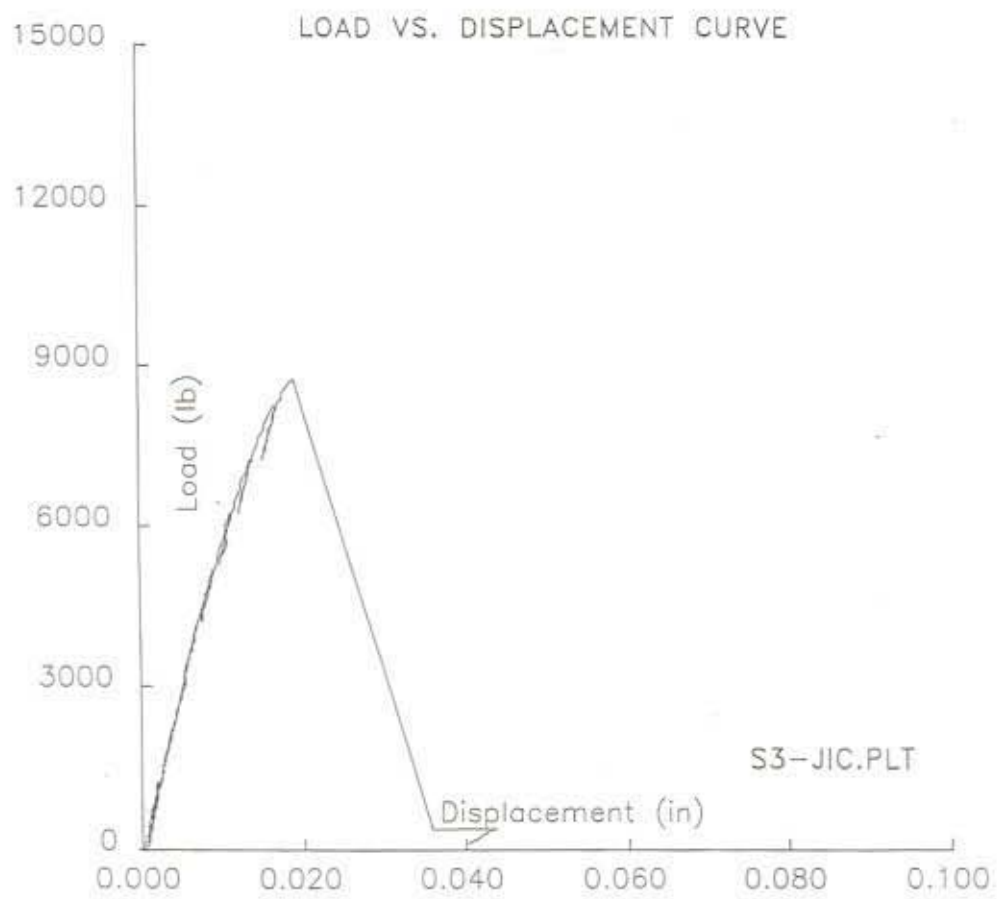


Figure 41 - Load-Clip Gauge Displacement Plot for Test Specimen S3 (T = -10F).



Figure 42 - Fracture Surfaces of Test Specimen S3. (6/00/3-7)

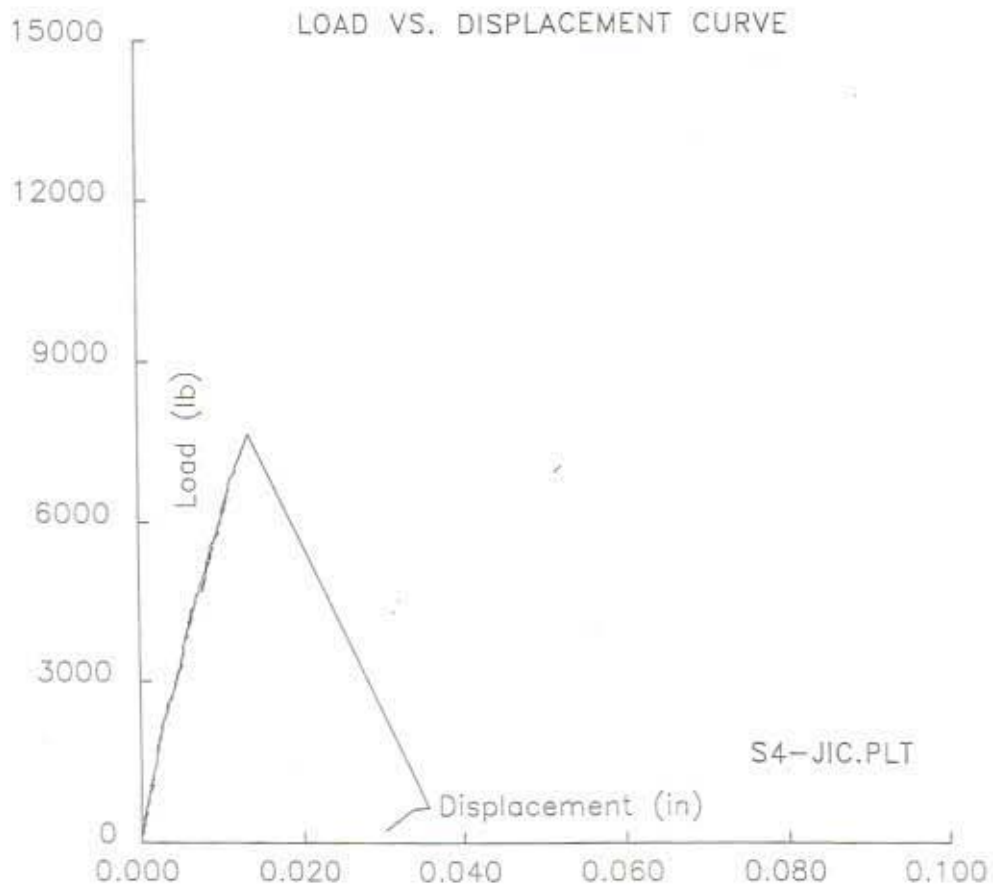


Figure 43 - Load-Clip Gauge Displacement Plot for Test Specimen S4 (T = -10F).

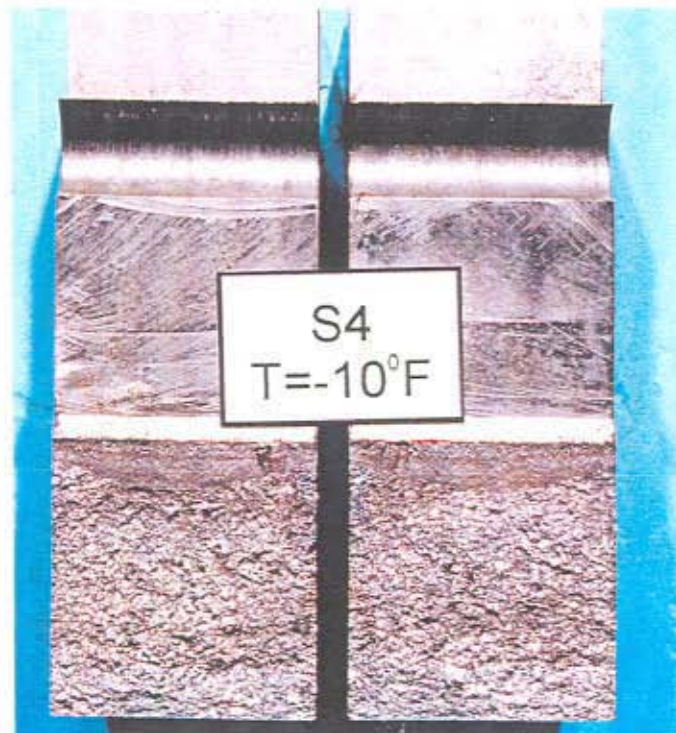


Figure 44 - Fracture Surfaces of Test Specimen S4. (6/00/3-9)

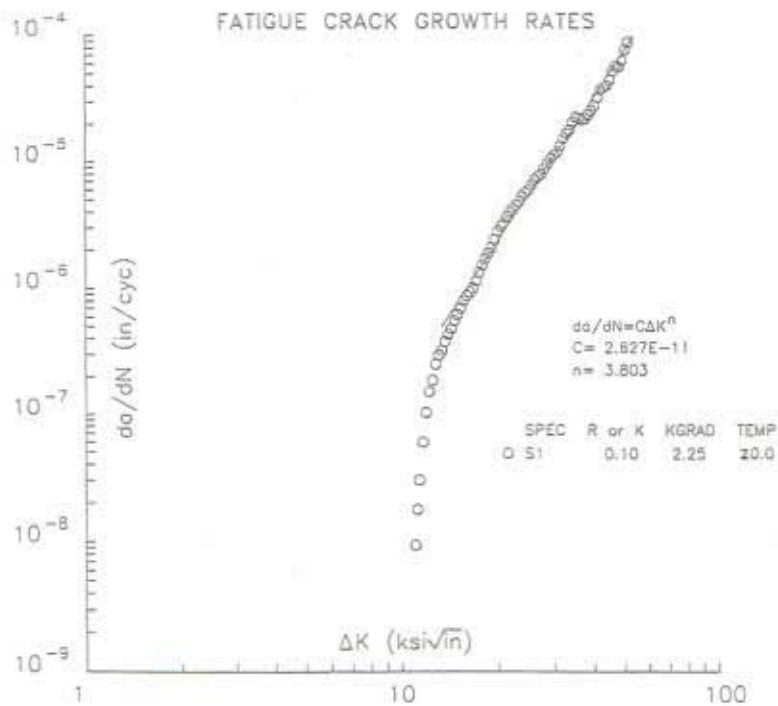
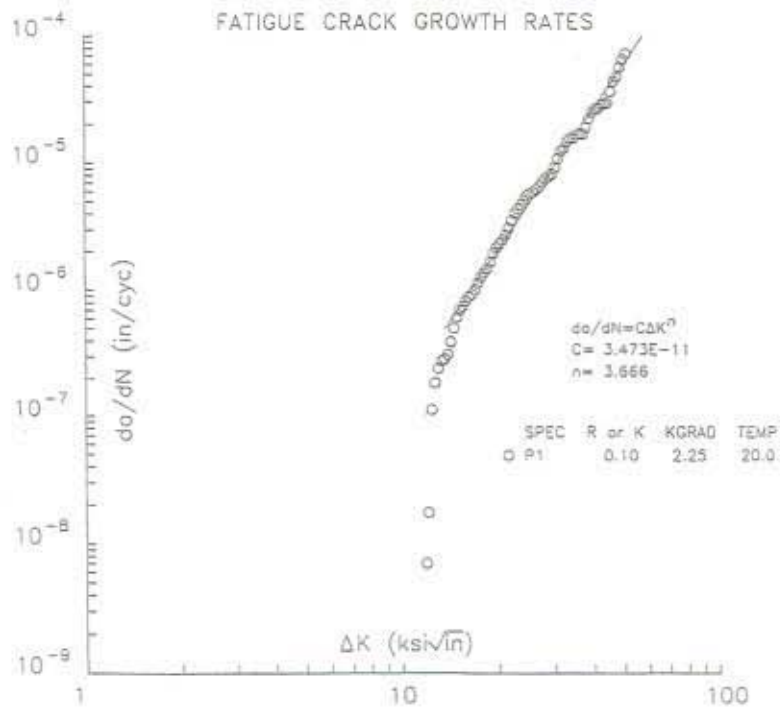


Figure 45a - da/dN vs. ΔK plots for the trunnion (top) and sheave (bottom) material.

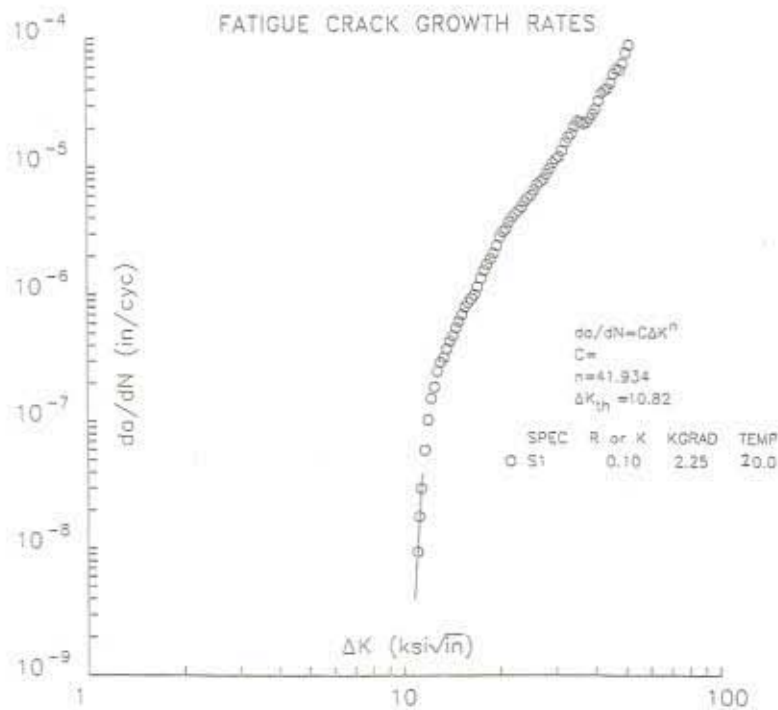
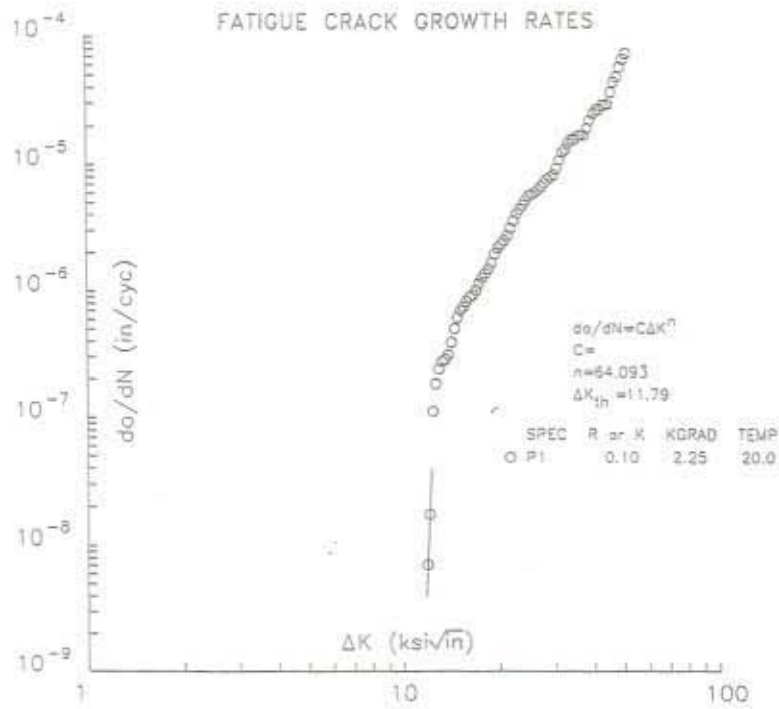
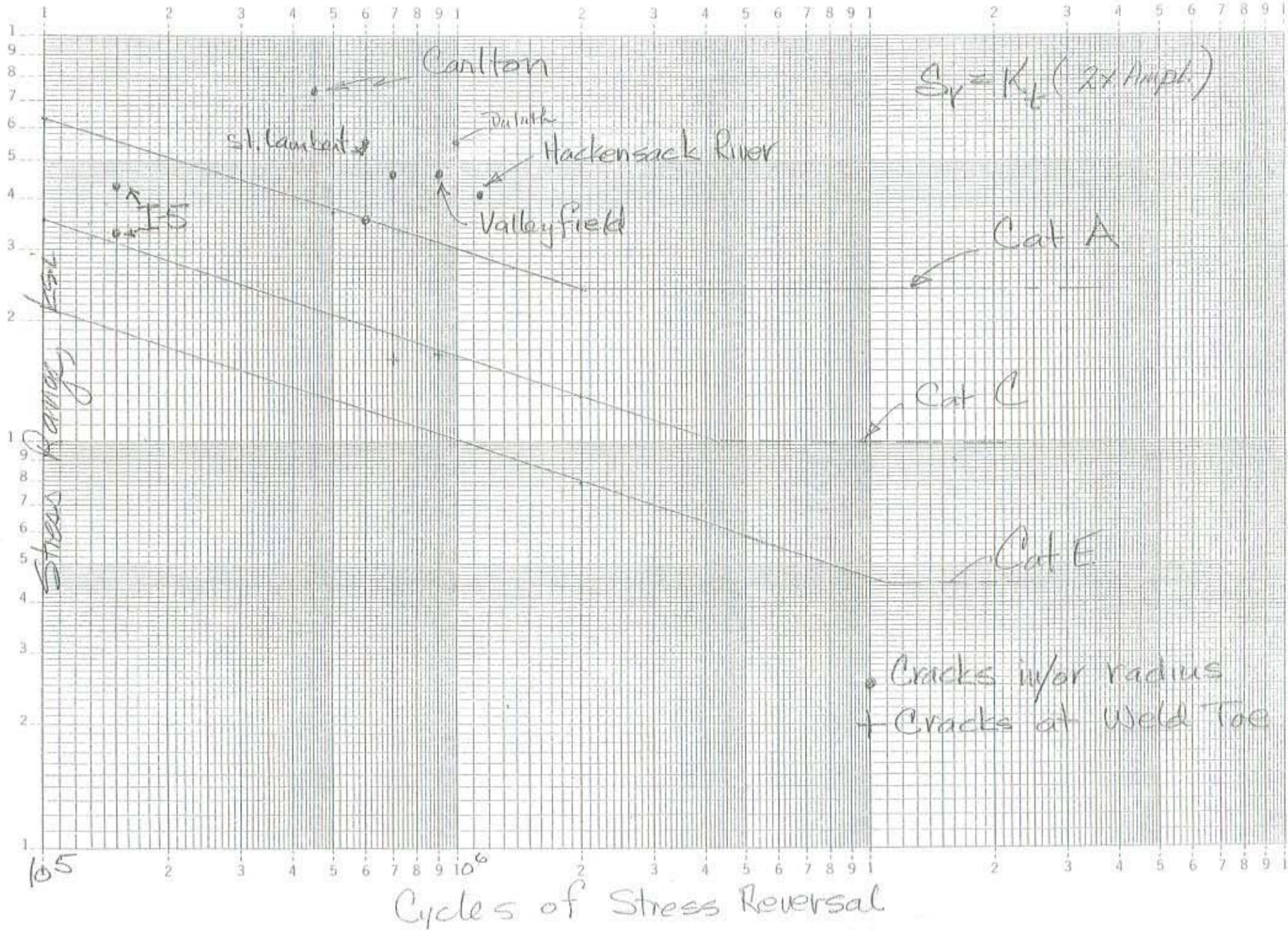


Figure 45b - Regression analysis results for the threshold region for the trunnion (top) and sheave (bottom) material.



Figure 46 - Semi-elliptical fatigue crack extension from machined radius at trunnion shoulder
(City of Duluth, MN Lift Bridge)
(5/97/15-7)



Appendix A

WJE	Wiss, Janney, Elstner Associates, Inc. 83 South King Street, Suite 820, Seattle, Washington 98104	MADE BY	RDG	SHEET NUMBER	5-1
		CHECKED BY		PROJ. NUMBER	973010
Oregon State D.O.T. I-5 Trunion Study		DATE	10-19-98		

Summary of Representative Conditions
Selected for Analysis

Item No.	Description
① @ 1A Keyway (Crack)	- Linear indication detected using MT (Crack) - Surface breaking discontinuity oriented transverse to former oil way filled with weld metal Indication appears to extend into base metal Reference: Sheet 16 & Photo's UT 1-5 & 1-17
② @ 1A Keyway (fillet base)	- Base metal, where fillet joined the key to the keyway surface Reference: Sheet 16 & Photo's UT 1-5 & 1-17
③ @ 1B Keyway (Crack)	- Linear indication detected using MT (Crack) - Surface breaking discontinuity oriented transverse to former oilway, filled with weld metal Reference: Sheet 17 & Photo's UT 1-8 & 1-10
④ @ 1B Keyway (fillet base)	- Remaining fillet and base metal where key was joined to the keyway Reference: Sheet 17 & Photo's UT 1-8 & 1-10
⑤ @ 3A Keyway (oilway filler weld & keyway fillet)	- Root of oilway with filler weld, as well as cross sectional area of key/keyway fillet weld (Approx 8" long sample with longitudinal section) Reference: Sheet 18 & Photo's UT 1-3 & 1-20

WJE	Wiss, Janney, Elstner Associates, Inc. 83 South King Street, Suite 820, Seattle, Washington 98104	MADE BY RPG	SHEET NUMBER 5-2
		CHECKED BY	PROJ. NUMBER 973010
Oregon State D.O.T. I-5 Trunion Study		DATE 10-19-89	

Continued Summary of Selections for Analysis

<u>Item No.</u>	<u>Description</u>
⑥ Azimuth 15° UT #1 ≡ (Embedded)	Embedded inclusion or discontinuity detected with UT, located 15.5 from trunion East end.

Reference: Sheet 19 & Photo UT 2-2A

⑦ * Azimuth 60° UT #2 ≡ (Embedded)	Embedded inclusion or discontinuity detected with UT, located 13.25 from trunion East end.
---	--

Reference: Sheet 20 & Photo UT 2-2A

⑧ Azimuth 60° UT #4 (Embedded)	Embedded inclusion or discontinuity detected with UT, located 15.25 from trunion East end.
---	--

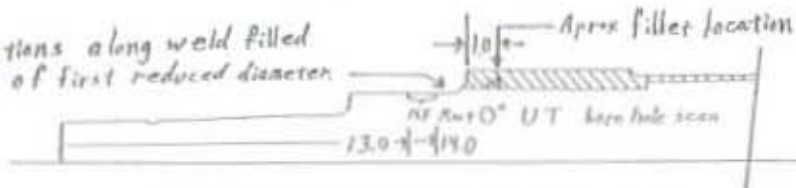
Reference: Sheet 20 & Photo UT 2-2A

⑨ Azimuth 255° (Oilway fusion)	Cross sectional cuts through weld filled oilway.
--------------------------------------	--

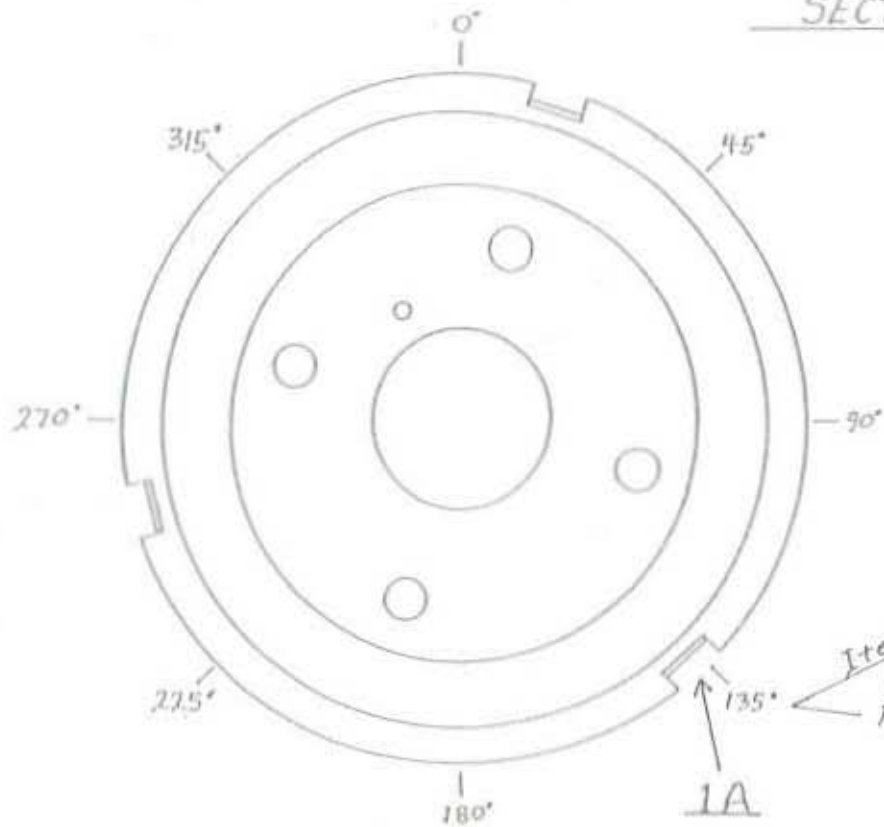
Reference: Sheet 21 & Photo UT 1-21

* One of the indications reported by O-D.A.T.

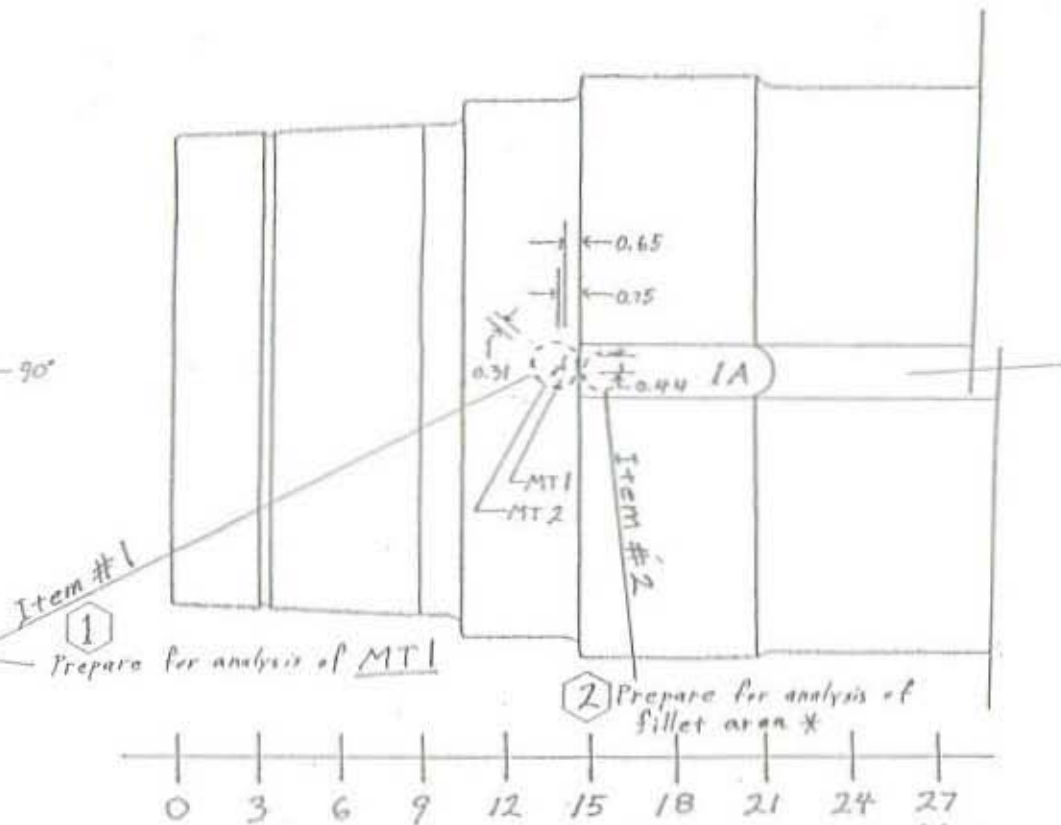
MT Indications along weld filled
oilway of first reduced diameter



SECTION AT KEYWAY 1A



EAST END



Item #1
1 Prepare for analysis of MT1

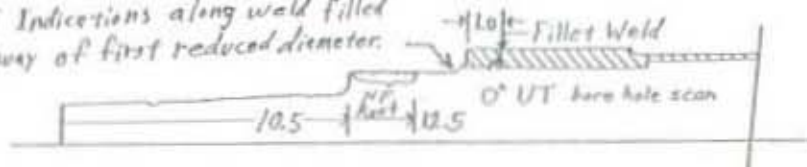
Item #2
2 Prepare for analysis of fillet area *

* Fillet was ground off to facilitate removal of the key from the Keyway. HAZ is believed to be intact. See keyway section, above.

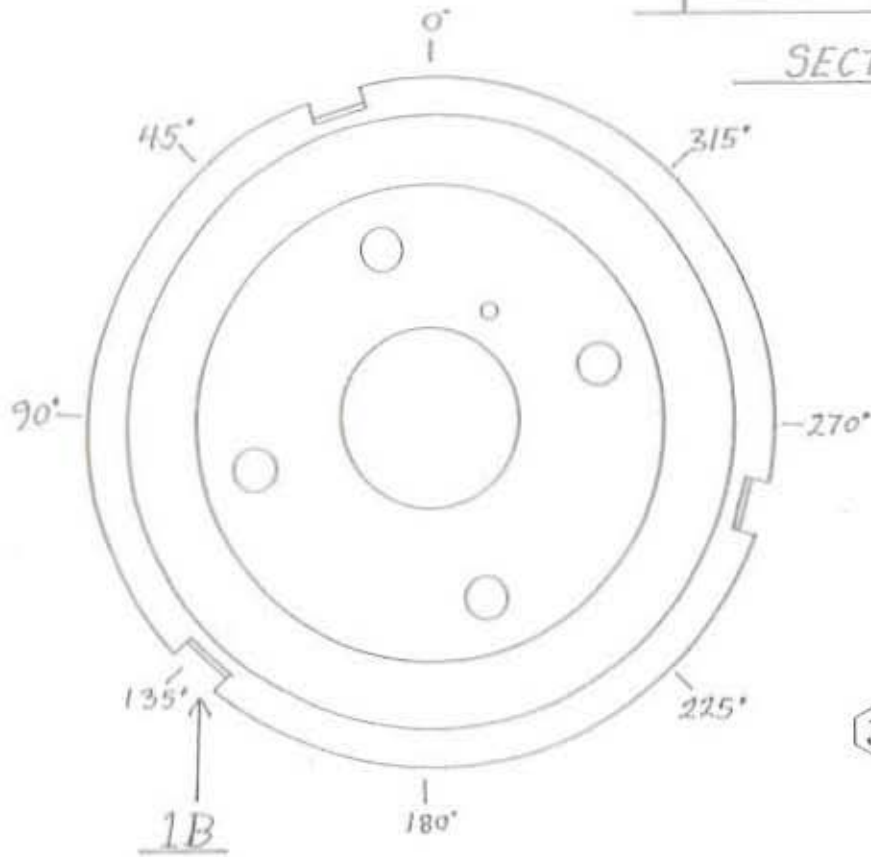
SURFACE AT KEYWAY 1A (EAST END)

COUNTERWEIGHT SHEAVE TRUNNION

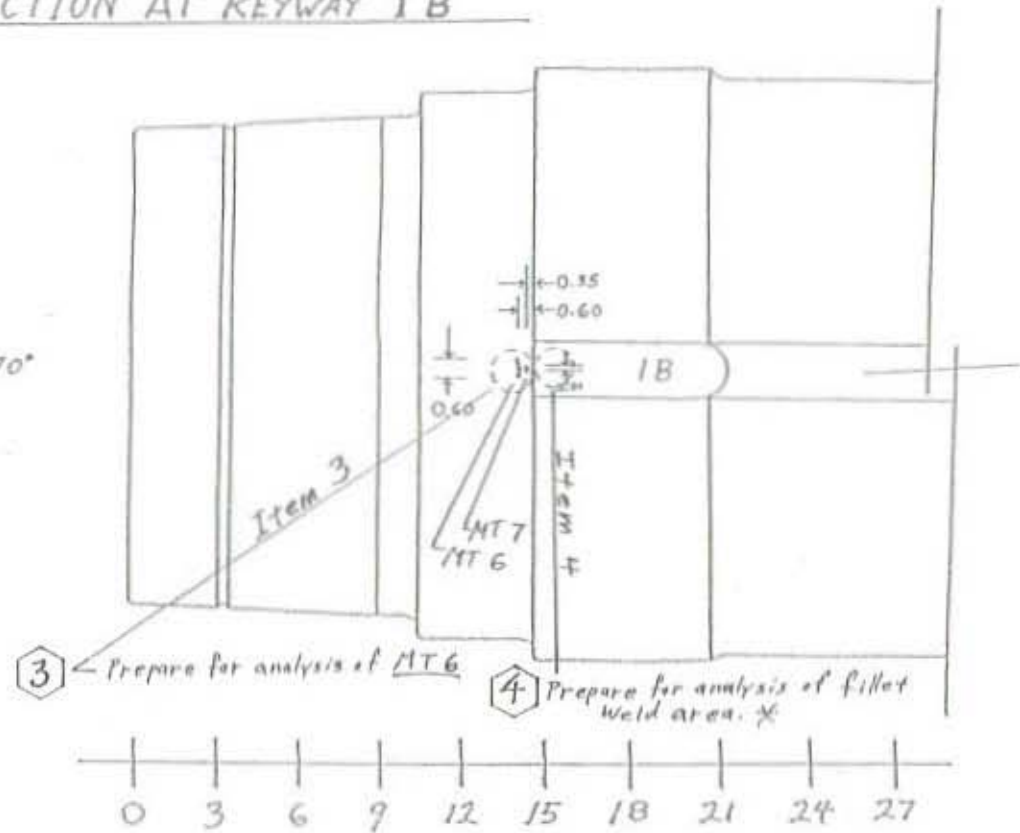
MT Indications along wall filled
oilway of first reduced diameter.



SECTION AT KEYWAY 1B



WEST END



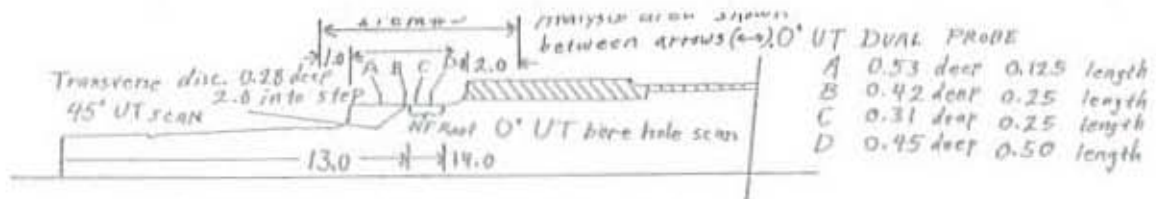
③ Prepare for analysis of MT 6

④ Prepare for analysis of fillet
weld area. *

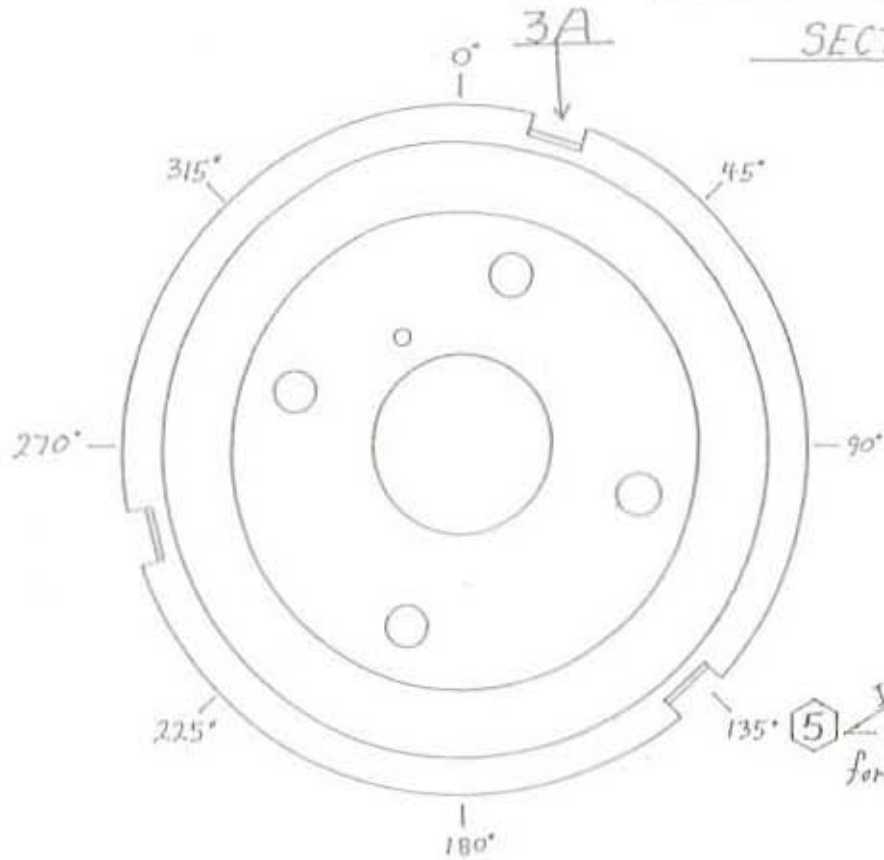
* Fillet is intact as welded. Leg
fusing to Key was previously
fractured. See keyway section, above

SURFACE AT KEYWAY 1B (WEST END)

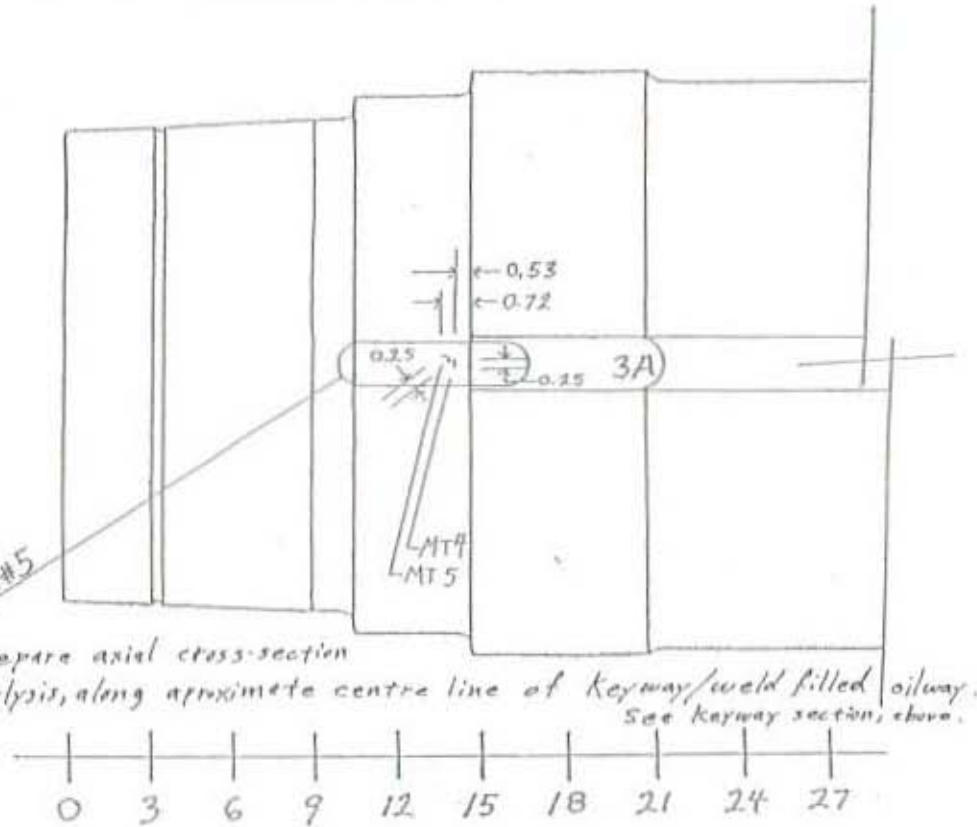
COUNTERWEIGHT SHEAVE TRUNNION



SECTION AT KEYWAY 3A



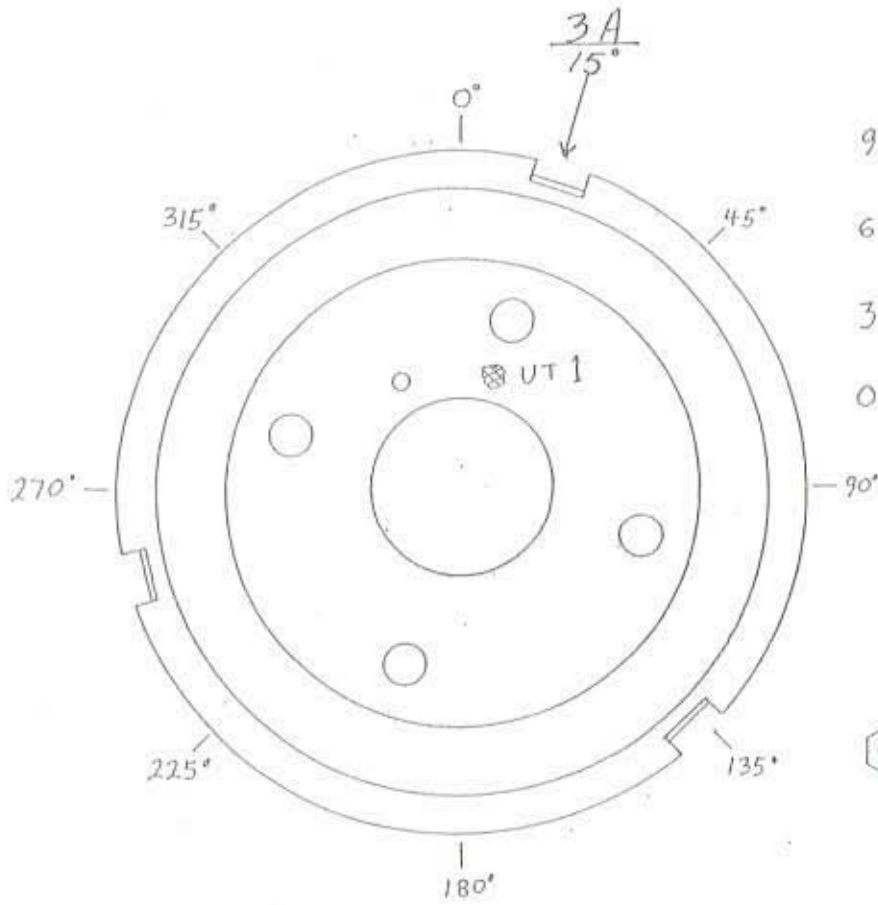
EAST END



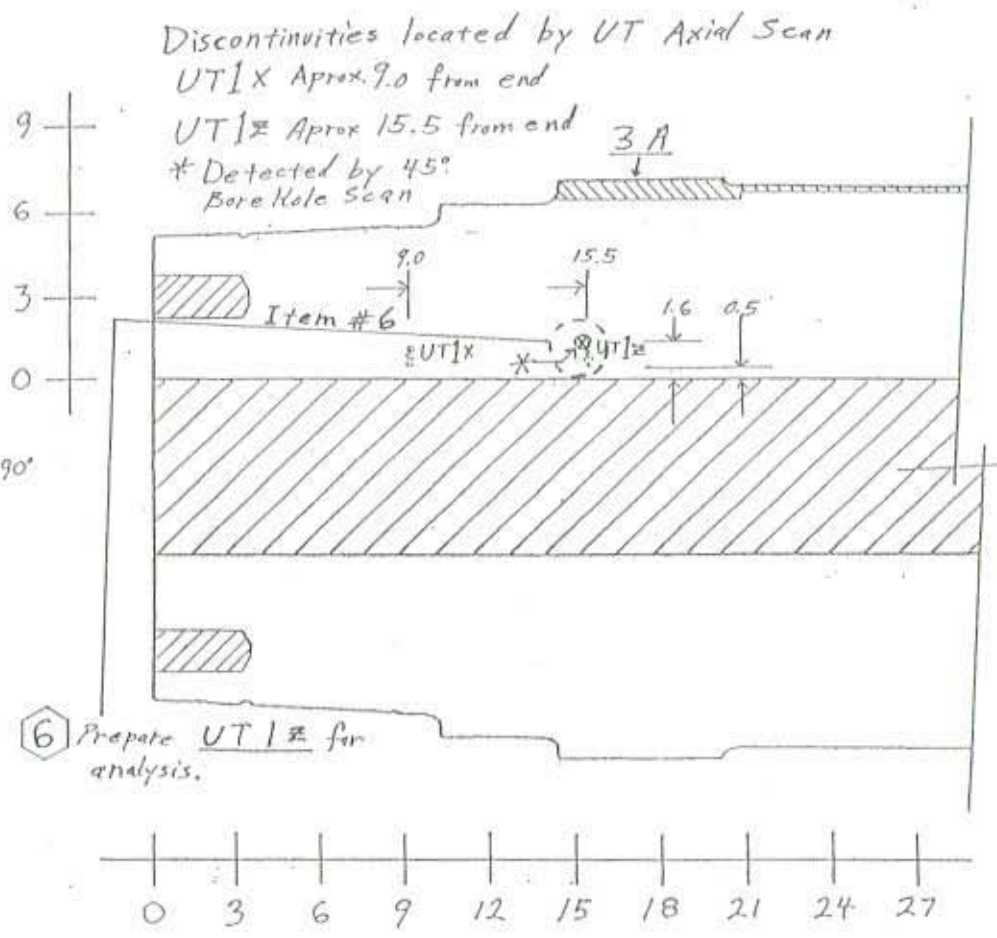
Prepare axial cross-section for analysis, along approximate centre line of keyway/weld filled oilway. See keyway section, above.

SURFACE AT KEYWAY 3A (EAST END)

COUNTERWEIGHT SHEAVE TRUNNION

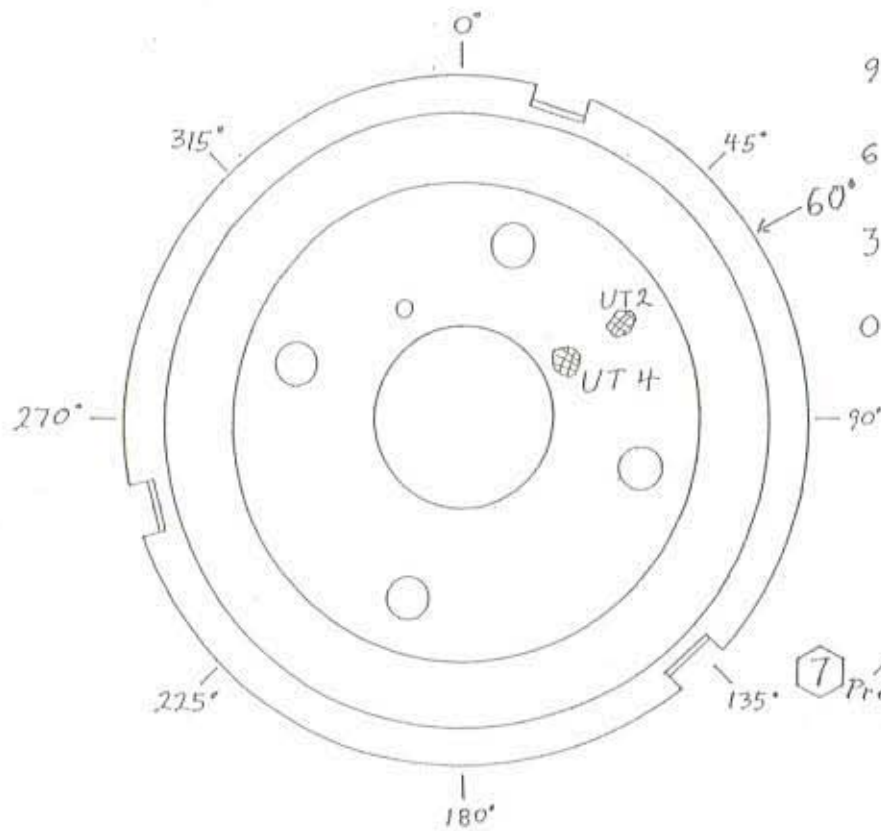


EAST END



CROSS SECTION - EAST END (T.C. 15°)

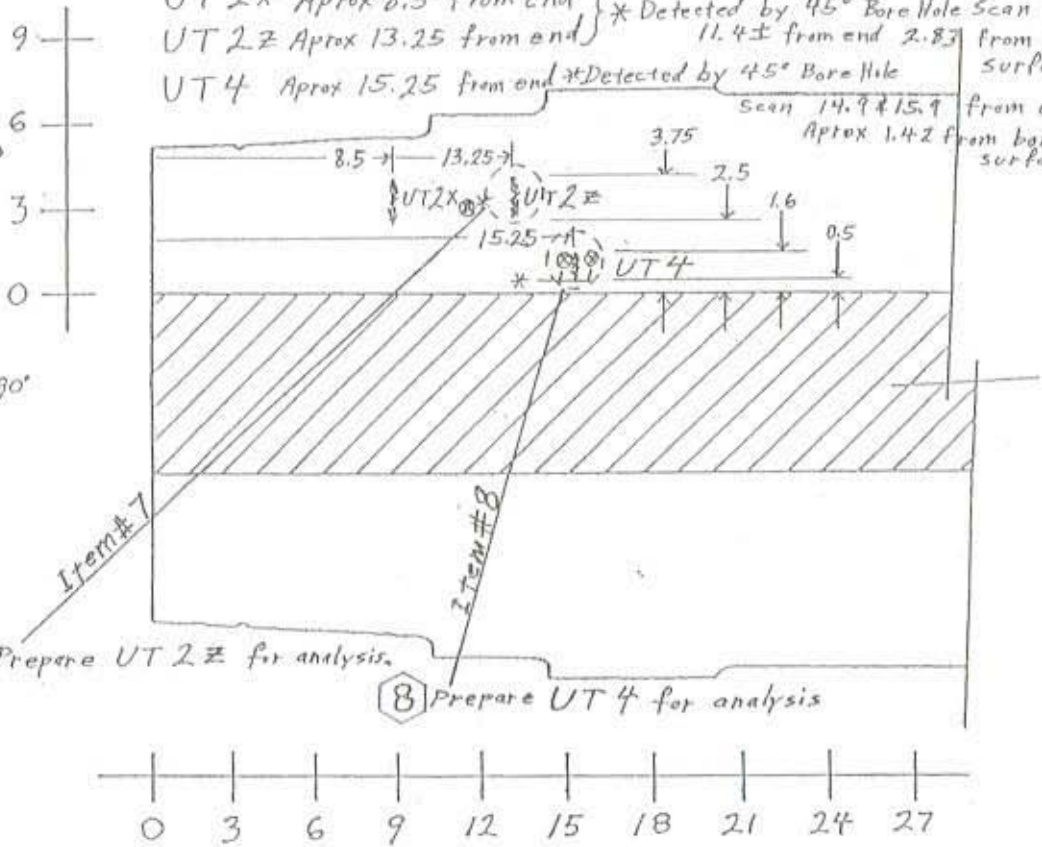
COUNTERWEIGHT SHEAVE TRUNNION



EAST END

Discontinuities located by UT Axial Scan

UT 2X Aprox 8.5 from end } * Detected by 45° Bore Hole Scan
 UT 2Z Aprox 13.25 from end } 11.4 ± from end 2.83 from bore surface
 UT 4 Aprox 15.25 from end * Detected by 45° Bore Hole Scan
 Scan 14.9 & 15.9 from end
 Aprox 1.42 from bore surface



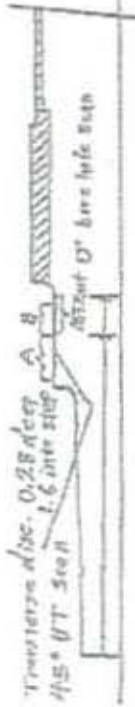
7 Prepare UT 2Z for analysis.

8 Prepare UT 4 for analysis

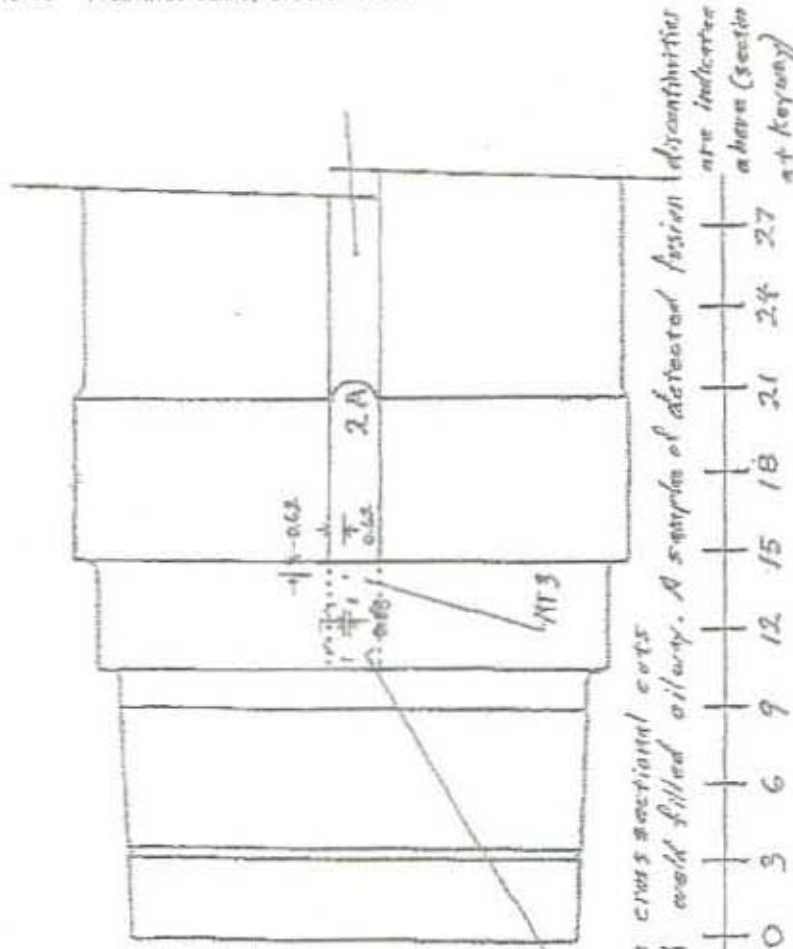
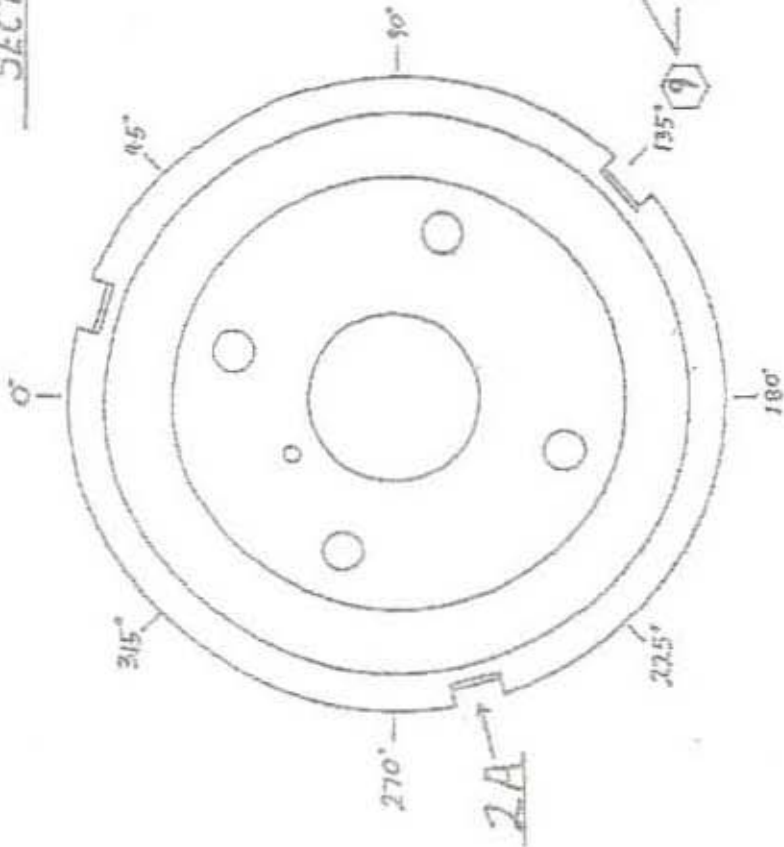
CROSS SECTION - EAST END (T.C. 60°)

COUNTERWEIGHT SHEAVE TRUNNION

DUT DUAL PROBE
A 0.185 to 0.45 depths
B 0.16/0.27/0.36/0.45 sample depths



SECTION AT KEYWAY 2A



EAST END

SURFACE AT KEYWAY 2A (EAST END)

COUNTERWEIGHT SHEAVE TRUNNION

WJE

Wiss, Janney, Elstner Associates, Inc.
330 Pfingsten Rd., Northbrook, Illinois 60062

MADE BY
BSB

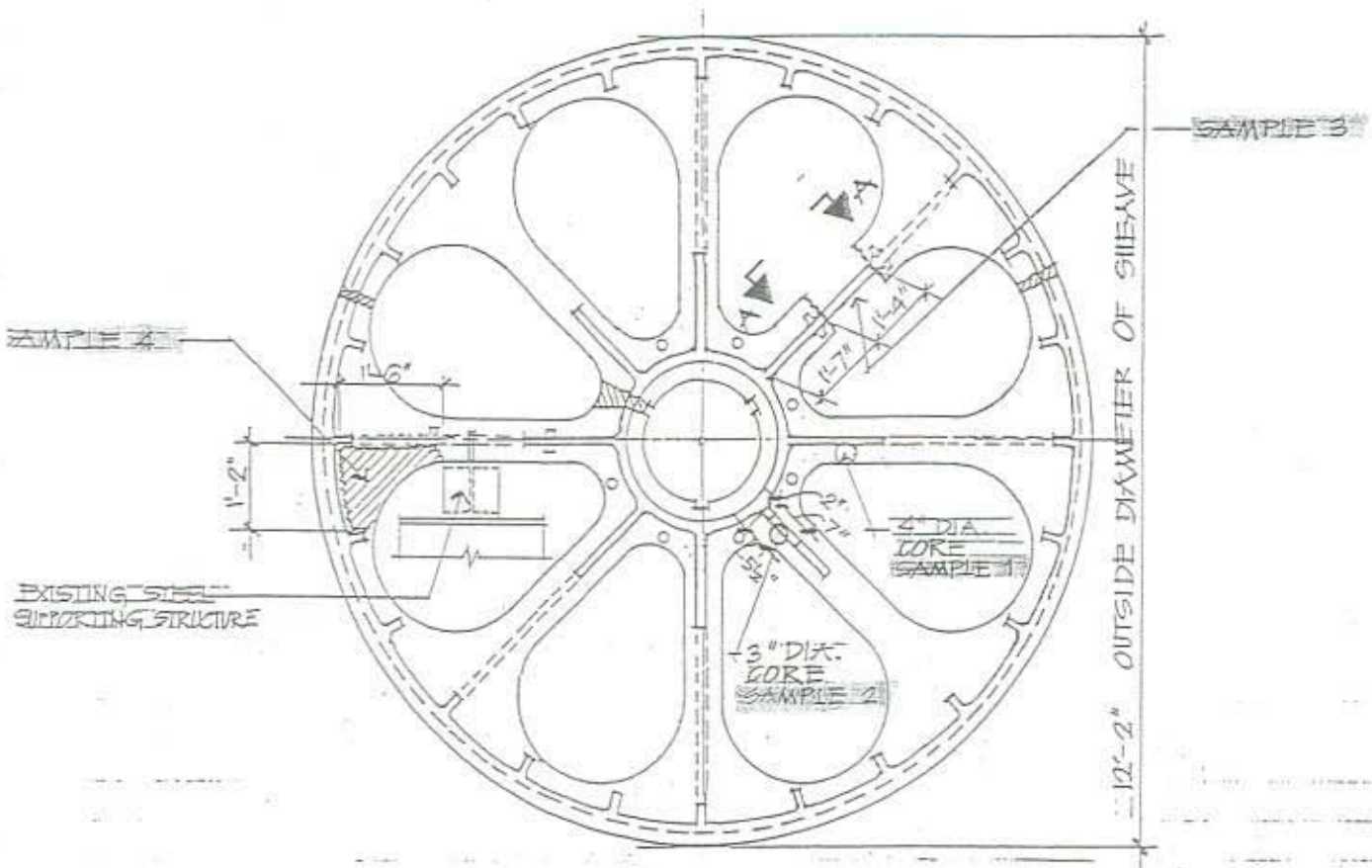
SHEET NUMBER
1

WHEEL SAMPLES FOR MATERIAL TESTING
AND SAMPLES CONTAINING CRACKS

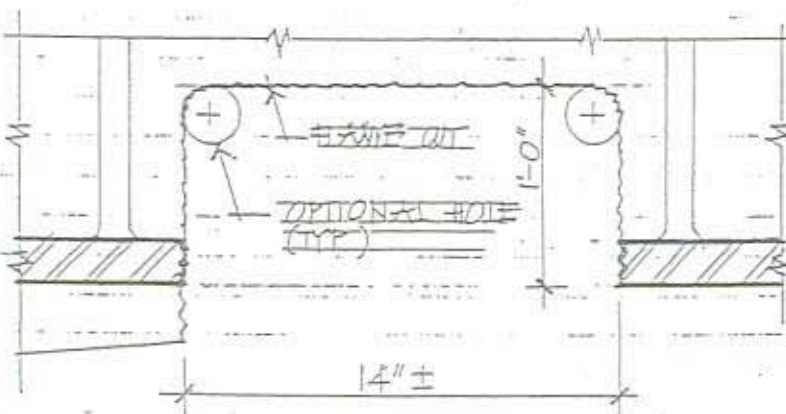
CHECKED BY
MJK

PROJ. NUMBER
973010

DATE
01/04/99



ELEVATION



SECTION A-A

SAMPLE NO.	DESCRIPTION
1	4" DIA. CORE CONTAINING CRACK
2	3" DIA. CORE WITH GROUND CRACK
3	SPOKE & WEB PLATE SAMPLE FOR MATERIAL TESTING
4	SPOKE / RIM SAMPLE FOR MATERIAL TESTING

Appendix B



PO Box 249, 120 Mill St., Dublin, PA 18917
 TEL: 800-627-3966 • FAX: 215-249-9656

Certified Test Report
 LHU001-99-05-09680



SOLD TO

Lehigh University
 Alumni Memorial Building
 27 Memorial Drive West
 Bethlehem, PA 18015-3039

SHIP TO

Lehigh University
 ATLSS Engr. Research Cntr
 Imbt Labs 117 ATLSS Drive
 Bethlehem, PA 18015-3039
ATTN: Eric Kaufmann

CUSTOMER P.O.

22495

CERTIFICATION DATE

5/26/99

SHIP VIA

FAX AND MAIL

DESCRIPTION

4 pcs. Test Pieces, Steel, Identified as PIN-ID, PIN-OD, Sheave Web (#3) and Sheave Rim (#4), Item 1
 Reference: Acct. No. 297061 (AT 8.6), Expense Code 4060

Four pieces of the submitted samples were analyzed in accordance with Customer's Instructions with the following results:

<u>SAMPLE ID</u>	<u>ELEMENT</u>	<u>ACTUAL</u>	<u>SAMPLE ID</u>	<u>ELEMENT</u>	<u>ACTUAL</u>
PIN-ID	C	0.39%	WEB #3	C	0.31%
	Mn	0.48%		Mn	0.77%
	P	0.015%		P	0.029%
	S	0.024%		S	0.024%
	Si	0.20%		Si	0.38%
	Ni	0.040%		Ni	0.11%
	Cr	0.013%		Cr	0.055%
	Mo	0.005%		Mo	0.053%
	Cu	0.037%		Cu	0.084%
	PIN-OD	C		0.35%	RIM #4
Mn		0.51%	Mn	0.77%	
P		0.015%	P	0.030%	
S		0.034%	S	0.025%	
Si		0.21%	Si	0.38%	
Ni		0.032%	Ni	0.11%	
Cr		0.009%	Cr	0.054%	
Mo		0.004%	Mo	0.053%	
Cu		0.038%	Cu	0.084%	

The services performed above were done in accordance with LTI's Quality System Program Manual Revision 13 dated 3/16/98. These results relate only to the items tested and this report shall not be reproduced, except in full, without the written approval of Laboratory Testing, Inc. L.T.I. is accredited by A2LA in the Chemical, Mechanical and Nondestructive Fields of Testing. L.T.I. is accredited by NADCAP in the Material's Testing and NDT, MT, PT, RT and UT.

Sherri L. Lengyel
 QA Coordinator

By 
 Authorized Signature

APPENDIX C - PROCEDURE FOR ULTRASONIC EXAMINATION OF SOUTH TOWER
TRUNNIONS

ULTRASONIC EXAMINATION PROCEDURE FOR SOUTH TOWER TRUNNIONS FOR THE I-5 COLUMBIA RIVER BRIDGE

I. Scope

This procedure provides for the examination of in-service trunnions using ultrasonic methods. Techniques are established primarily for detection of discontinuities that may propagate within critical areas of the trunnion. Ultrasonic waves are introduced for inspection via accessible end, and center bore hole surfaces. Several transducer assembly designs and associated scanning plans are defined for interrogation of critical areas of the trunnion.

The procedure includes both general and specific directives. Test equipment and personnel qualification requirements apply to all inspection techniques defined herein. Instrument and transducer calibrations, scan plans, and reporting procedures are uniquely specified for application with the trunnion examination.

Proposed variations to the procedure shall be submitted to the designated NDT Level III examiner for approval prior to use for inspection. Approval for use shall describe specific alterations in equipment, technique, associated calibrations, and define application in testing of the trunnions. Variations may be implemented only with the signed approval of the designated Level III. The signed approval shall be included with the report of trunnion examination for which the variation applies.

II. General Provisions

A. Inspection Personnel

1. All personnel that perform inspections according to these procedures shall satisfy the requirements of SNT-TC-1A for Level II Inspectors, and shall demonstrate the ability to perform the described calibrations, inspection scans, related calculations, and to discern spurious or non-relevant indications from significant discontinuities.
2. The designated Level III examiner responsible for approval of procedure variations or review of test data must satisfy the requirements of II-A-1, and may also perform inspections of the trunnions.

B. Ultrasonic Equipment

1. Test Instrument

- a. The test instrument shall be a pulse echo type ultrasonic flaw detector designed for use with transducers that oscillate at frequencies inclusive of 1 through 10 MHz.
- b. The instrument display shall be an "A scan" rectified presentation, using a cathode ray tube (CRT), electro-luminescent (EL), or liquid crystal display (LCD).
- c. The horizontal linearity of the test instrument shall be accurate within two percent over the full sound path distance to be used in testing.

- d. The test instrument shall include internal stabilization circuitry so that after warm up, no variation in signal response ± 1 dB will occur throughout the operating duration of the battery charge. There shall be an alarm or meter to indicate a drop in battery voltage prior to instrument shutoff due to battery exhaustion.
- e. The test instrument shall have calibrated gain control (attenuator) adjustable in discrete 1 or 2 dB steps over a range of at least 60 dB. The accuracy of the attenuator settings shall be within ± 1 dB.
- f. The dynamic range of the instrument display shall be capable of discrete presentation of amplitude changes that result with an alteration of 1 dB in gain or attenuator settings.

2. Transducers

- a. The size and shape of ultrasonic search units for inspection of the trunnion shall be defined for the intended scan plan, as described in Section III part A.
- b. Transducers shall operate at a nominal frequency of 2.25 MHz.
- c. All transducers (while disengaged from contoured or angled shoes, if applicable) shall be capable of resolving the three reflectors in the IIW block from position "F", shown in Fig. UT-1.
- d. Search units shall be free of internal reflectors that interfere with accurate interpretation of data.
- e. Search units for scans "SC-3 and SC-5" (described in Section III part C) shall demonstrate the capability to detect each of the sensitivity reference notches in the Trunnion Calibration Standard (as defined in Section II-B-3-a) within the middle half of the ultrasonic beam.

3. Reference Standards

- a. The custom-designed and fabricated Trunnion Calibration Standard (TCS) depicted in Fig. UT-2 shall be used for calibration of instrument horizontal linearity and sensitivity levels. The design of the TCS includes provisions for calibrations of ultrasonic apparatus to be used with designated scan plans established for use with this procedure. The test piece is fabricated from forged material that was cut from an identical trunnion removed in 1997 from the North Tower of the bridge.
- b. An IIW block is required only for resolution qualification of ultrasonic transducers.

4. Couplant

- a. UT-X powdered ultrasound couplant, produced by Sonotech, or suitable equivalent shall be used for ultrasonic test scans. The selected couplant shall be mixed or supplied at a high viscosity (50-90 weight oil equivalent) and shall exhibit characteristics for maintenance of pulse transmission at the transducer contact interface when utilized on vertical surfaces.

- b. The couplant shall not be harmful to trunnion surfaces, or adversely contaminate lubricants that remain on the trunnion bearings.

C. Calibration

1. Initial Calibration - Instrument calibration and settings shall be in accordance with the provisions described in Section III Part B for each ultrasonic scan plan. The custom-designed Trunnion Calibration Standard, described in Section II-B-3 shall be used for calibrations of ultrasonic apparatus as applicable for all tests performed on the trunnions. The test instrument and transducers used in the calibration shall meet the provisions of Section II-B-1 and 2.
2. Re-calibration - Instrument re-calibration for sensitivity and horizontal linearity shall be required at minimum intervals of two hours or following changes of transducers or power source.
3. Provisions for Limited Re-calibration Requirements - A single daily calibration may be permitted with the following provisions:
 - a. The test instrument shall utilize digital circuitry to store the calibration settings for the various scan plans and associated transducer assemblies.
 - b. Substitutes for transducer assemblies that were initially calibrated for applicable test scans shall not be permitted, and couplant shall be maintained at transducer / shoe interfaces, when applicable.
 - c. Stability of the test instrument calibration must be established to demonstrate a maximum change in vertical linearity equal to a variation of 2 dB over an extended period. The ultrasonic instrument shall be monitored for calibration variation in three trial periods of at least 8 hours for qualification of this provision. No alteration of instrument calibration settings shall be permitted during the trial periods. A change of battery shall occur in at least one of the trial periods. With the instrument reverted to initial calibration settings, a change of vertical linearity representing an excess of 2 dB, or discernible variation in horizontal linearity disqualifies the provision. (It is intended that instrument stability qualification be conducted in the course of typical inspection activity. Instrument calibration should be monitored at maximum 2 hour intervals throughout and at the conclusion of the trial period.)
 - d. Verification of horizontal and vertical instrument linearity of ultrasonic test apparatus used for testing of trunnions shall be conducted using the Trunnion Calibration Standard within 2 hours following conclusion of the days testing. Calibration settings used for trunnion inspection shall exhibit linearity response within the variation provisions of Section II-C-3-c.
5. Angle Beam Transducer Calibration - Longitudinal and shear wave angle beam search units must be tested for compliance with the provisions of Section II-B-2 prior to initial calibration for periodic testing of the trunnions. Procedures for angle calibration must be conducted using the TCS as described in Section III Part B.

D. Testing

1. Ultrasonic testing of the trunnions shall be at the direction of the "Engineer in Charge" (EIC), and with the supervision of the designated NDT Level III (L-III).
2. The interval schedule, level, and extent of inspection shall be established by the EIC. Full or limited inspection as defined in this procedure applies to both ends of the trunnion. No alternate plans, additions, or omissions shall be implemented without written description of the variation, approved by the designated L- III. Interim inspection however, as deemed appropriate to monitor specific indications may be implemented for a single end of a trunnion.
 - a. Full inspection requires access to end and center bore hole surfaces of the trunnion for implementation of scan plans designated: SC-1, SC-2, SC-3, SC-4, and SC-5.
 - b. Limited inspection of the trunnion requires access to the end surface for implementation of scans SC-1 and SC-3 only.
3. Ultrasonic examination of trunnions shall be conducted in accordance with specific applicable scanning patterns and transducer configurations as described in Section III.
4. Radial orientation for each trunnion end shall be described by azimuth. The location of the former oilway port shall be the designated zero point. Clockwise and counterclockwise orientations are established respectively for East and West trunnion ends and shall be indicated on inspection forms described in Section II-E-3.
5. Axial orientation shall be based on linear distance measured from the trunnion end subject to inspection.
6. Orientation of keyways are indicated at ends of each trunnion ends by three center punch impressions near the mouth of the center bore, at each location.
7. Scanning contact surfaces shall be sufficiently cleaned and smooth to permit coupling with the ultrasonic search unit. Bore and end surface conditions of the TCS represent appropriate surface preparation for ultrasonic test scans.
8. Ultrasonic sound couplant that satisfies the provisions of Section II-B-4 shall be supplied at the transducer contact interface for all calibrations and testing of trunnions.
9. Ultrasonic couplant and any materials used in the inspection of trunnions shall be removed at the conclusion of testing. No permanent marks shall be made without prior approval of the designated Level III and "Engineer in Charge".

E. Evaluation of Trunnion Examination Test Data

1. Critical areas of the trunnion, indicated in Fig. UT-4-D include: former oilway grooves; keyways; and major section changes located between 8 ½ in. and 17 in. from the end and within 2 in. of the outside diameter.
2. Ultrasonic scans used for evaluation of the trunnions shall comply with the provisions of Section III Part C of this procedure.

3. Inspection scans SC-3 and/or SC-5 as described in Section III Part C shall be the primary source data used in evaluation of the trunnions.
4. The attenuation loss of ultrasonic energy is approximately represented at 2 dB per inch of sound travel in the forged material, within the critical test area of the trunnion.
5. Only reflectors generated within the first leg of the sound path shall be used for primary evaluation of discontinuities within critical areas of the trunnion..
6. Inspection scans SC-2, SC-3, and SC- 4 may be used for supplementary information, as well as additional definition or characterization of the indication.
7. With instrument gain settings at 10 dB over reference level, indications detected in critical areas of the trunnion resulting in signal trace deflections with amplitude equal or greater than achieved at reference level shall be documented.
8. Interpretation of indications shall be based upon;
 - a. Discontinuity location
 - b. Cross-reference with other scans
 - c. Indication magnitude
 - d. Signal characteristics
9. Disposition of the trunnion shall be established from documented ultrasonic data and consideration of trunnion operation, geometric features, and pre-existing discontinuities.

F. Reporting of Trunnion Examinations

1. Reports of ultrasonic examinations shall include the following:
 - a. Trunnion identification.
 - b. Date of testing
 - c. Procedure used
 - d. Scan performed
 - e. Name and professional affiliation of inspector
 - f. Significant indications detected including:
 - 1) Indication level
 - 2) Indication location
 - 3) Transducer scanning location, orientation, and incident beam angle
2. Disposition of each trunnion subjected to examination shall be expressed in written or tabular form, based on a summary of significant ultrasonic indications.

3. Trunnion inspection forms as shown in Fig. UT-3 shall be used for collection of data from ultrasonic tests.
4. Use of sketches for presentation of indication location is optional.
5. Inclusion of the test instrument display presentation is optional.
6. Reports shall clearly identify extent of testing as full or limited as defined in Section II-D-2. Interim tests if applicable, shall be so identified, and shall also define the specific extent and object of tests performed.

III. Specific provisions for ultrasonic examination of in service trunnions.

A. Design of ultrasonic transducers for inspection of trunnions.

1. Straight beam (0 degree) transducer for axial, longitudinal scan (designated A-1).
 - a. The vibrating element shall be round with a nominal diameter of $\frac{3}{4}$ in. to 1 in.
 - b. Operating frequency shall be 2.25 MHz.(nominal)
2. Angle beam (10 to 12 degree) transducer for axial, longitudinal angle beam scan (designated A-2).
 - a. The vibrating element shall be round with a nominal diameter of $\frac{3}{4}$ in. to 1 in. or square with nominal dimensions of $\frac{3}{4}$ in. by $\frac{3}{4}$ in.
 - b. Operating frequency shall be 2.25 MHz (nominal)
 - c. A removable wedge shaped "shoe" shall be fabricated from acrylic plastic or similar material.
 - d. When coupled with the angled wedge, the transducer assembly shall create a longitudinal wave having an incident angle within the TCS of 10 to 12 degrees, inclusive.
 - e. A medium weight lubrication grease or petroleum jelly shall be used for the transducer/angle wedge interface.
3. Straight beam (0 degree) transducer for radial, longitudinal scan from the center bore (designated A-3).
 - a. The vibrating element shall be round with a nominal diameter of $\frac{1}{2}$ in. to $\frac{3}{4}$ in.
 - b. Operating frequency shall be 2.25 MHz (nominal).
 - c. A removable contoured shoe shall be fabricated from acrylic plastic or similar material.
 - d. The contact face of the shoe shall be fitted to match the contour of the center bore surface.

- e. When coupled with the shoe, a straight beam wave with orientation towards the outer radius of the trunnion shall be created.
 - f. The maximum thickness for the sound path of the shoe shall not exceed $\frac{3}{16}$ inch.
 - g. A medium weight lubrication grease or petroleum jelly shall used for the transducer/contoured shoe interface.
4. Angle beam shear wave transducer for radial/axial oriented, center bore inspection (designated A-4).
- a. The vibrating element shall be round with a nominal diameter of $\frac{1}{2}$ in. to $\frac{3}{4}$ in.
 - b. Operating frequency shall be 2.25 MHz (nominal).
 - c. A removable contoured angle wedge shall be fabricated from acrylic plastic or similar material.
 - d. The contact face of the shoe shall be fitted to match the contour of the center bore surface.
 - e. When coupled with the shoe, a shear wave shall be created with radial/ axial orientation having a nominal incident angle of 45 degrees (42 min./47 max.) within the TCS.
 - f. A medium weight lubrication grease or petroleum jelly shall be used for the transducer/contoured and angled shoe interface.
 - g. The shoe shall have a width of 1 in. to $1\frac{1}{2}$ in., and a length of 3 in. to $3\frac{1}{2}$ in.
- B. Calibration of ultrasonic apparatus for testing, using the Trunnion Calibration Standard (TCS) depicted in Fig. 2. Five unique ultrasonic Scan Plan set-up arrangements are employed for tests of the trunnion which use transducers described in Section III Part A. Refer to Fig. 2 for TCS transducer position locations.
- 1. Axial straight beam transducer (A-1) for full-length scanning (SC-1)
 - a. Establish horizontal linearity of the test instrument with a calibrated range of 100 in. presented on the instrument display.
 - b. Couple transducer A-1 at position "A" of the TCS to use ultrasonic multiples of 24 in. (full length of TCS) for distance calibration.
 - c. Scanning reference level shall be based on 100 percent signal trace amplitude from the third back reflection (72 in.) or 24 dB over a 100 percent trace amplitude from the first back reflection.
 - 2. Axial straight beam transducer (A-1) for near end scanning (SC-2).
 - a. Establish horizontal linearity of the test instrument with a calibrated range of 20 in. presented on the instrument display.

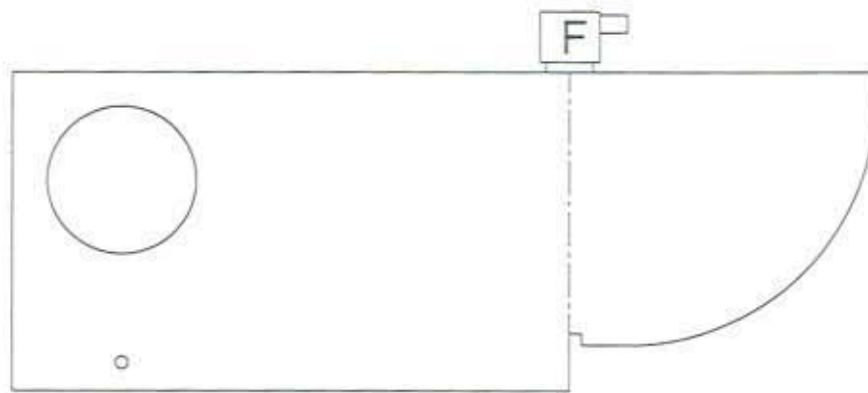
- b. Couple transducer A-1 at position "B" of the TCS to use ultrasonic multiples of 8 in. for distance calibration. The transducer shall subsequently be coupled at position "C" for direct calibration using the 18 in. reference distance near the upper end of the calibrated range.
 - c. Scanning reference level shall be based on 100 percent signal trace amplitude from reflection from the 18 in. reference distance of the TCS.
3. Axial longitudinal angle beam transducer (A-2) for near end axial, outside radius scan (SC-3).
- a. Perform calibration with transducer A-1 according to Section III-B-2-a and b.
 - b. Disconnect transducer A-1 from the instrument and connect transducer A-2.
 - c. Transducer A-2 shall be placed at position "A" of the TCS, with the beam angled toward the angle calibration hole, that is centered 15 ½ in. from the axial scan end surface. Maximize the signal amplitude at 80 percent of instrument display height.
 - d. Adjust the instrument delay control to place the trace deflection representing the angle calibration hole at 15.3 in. on the horizontal scale of the instrument and to display. (In this configuration, based on an incident angle of 11 degrees, distance measurement to reflector is accurate within approximately 1/8 in. for transducers that conform to the requirements of Section III-A-2-d.)
 - e. Reference level for scanning shall be determined by placing the transducer at position "C" of the TCS, with the angled beam directed toward the sensitivity notches. Establish and record the sensitivity reference level based on an 80 percent trace deflection amplitude resulting with the reflection from notch No.2.
 - f. Scanning level for testing shall be established at reference level with 14 dB added gain.
4. Radial straight beam transducer (A-3) for scan from center bore hole (SC-4).
- a. Establish horizontal linearity of the test instrument with a calibrated range of 10 in. presented on the instrument display.
 - b. Couple transducer A-3 at position "D" of the TCS to use direct reference landings for distance calibration. To achieve accurate horizontal linearity settings, the transducer must be centered at the index marks that correspond with 2 in., 5 in., and 6.5 in. reference landing, as indicated in Fig. UT-2 .
 - c. Couple the transducer at position "E" of the TCS to establish scanning reference level at the gain setting required to achieve 100 percent signal amplitude from the maximum outside trunnion radius.
 - d. Scanning level for testing shall be established at reference level with 12 dB added gain.

5. Radial angle beam shear wave transducer (A-4) for primary trunnion interrogation scan from the center bore hole (SC-5).
 - a. Establish horizontal linearity of the test instrument (set for shear mode) with a calibrated range of 10 in. presented on the instrument display.
 - b. Couple transducer A-4 at position "G" of the TCS to use the 5 in. and 9 in. radius for distance calibration.
 - c. Align the transducer with the index point of the 5 in. and 9 in. calibration radius to determine the sound entry point.
 - d. Reference level for skating shall be determined with the transducer coupled at position "F" of the TCS, and drawn axially along with bore hole surface to achieve the maximum trace deflection from the sensitivity notch at shoulder 2. Establish record the sensitivity reference level based on an 80 percent amplitude setting.
 - e. Scanning level for testing shall establish as reference level with 14 dB of added gain.
 6. Longitudinal transducer A-2 incident angle calibration.
 - a. Establish apparatus calibration according to Section III-B-3-a, b, and c.
 - b. Couple transducer A-2 at position "A" of the TCS.
 - c. With the ultrasonic beam directed toward the transducer angle calibration hole, maximize the trace deflection signal amplitude.
 - d. Align the sound entry point (center of transducer) with the scale inscribed at "A" on the side face of the TCS to determine the sound beam incident angle within the test piece.
 7. Shear wave transducer A-4 incident angle calibration.
 - a. Establish apparatus calibration according to Section III-B-5-a and b.
 - b. Couple the transducer at position "F" on the TCS.
 - c. With the ultrasonic beam directed toward the transducer calibration hole, maximize the trace deflection signal amplitude.
 - d. Align the sound entry point of the transducer with the scale inscribed at "F" on the side face of the TCS to determine the sound beam incident angle within the test piece.
- C. Implementation and application of ultrasonic scan plans for inspection of in service trunnions.
- i. Axial straight beam scan, using transducer A-1 for full length trunnion inspection (designated SC-1). This scan is intended to establish general continuity and approximate length of the trunnion. Some non-metallic inclusions, as well as major cracks or fractures may also be detected.

- a. Couple transducer A-1 with the trunnion end surface using a suitable couplant at the contact interface.
 - b. General inspection from the end surface shall utilize a uniformly distributed "star point" pattern as shown in Fig. UT-4-A.
 - c. Loss of back reflection signal amplitude height exceeding 50 percent of the instrument display shall be noted.
 - d. General proximity of indications detected within critical areas of the trunnion shall be identified for further investigation using more specific scans.
2. Axial straight beam scan, using transducer A-1 for near trunnion end inspection (designated SC-2). This scan plan provides a display range limited to 20 in., permitting broad spacing of potential indications through the critical area of the trunnion.
- a. Couple transducer A-1 with the end surface of the trunnion using a suitable couplant at the contact interface.
 - b. A scanning pattern shall be established with concentric circles as shown in Fig. UT-4-B. The innermost scan circle shall follow the mouth of the center bore with a distance spacing to the rim equal to the diameter of the transducer element. The outermost scan circle shall immediately follow the outside radius at the trunnion end. Two additional scan circles shall be established with approximately uniform concentric spacing between the outer and innermost circles.
 - c. Indications with trace deflection amplitude equal to 50 percent of reference level shall be noted. Indications 6 dB less severe that are detected from the outermost scan circle shall also be noted.
3. Axial longitudinal angle beam scan, using transducer A-2 for near end inspection of the outside radius (designated SC-3). Access to critical areas of the trunnion that exceed the practical inspection capability of straight beam transducers is accommodated with the low incident angle beam inspection. Most early cracking or discontinuities situated in the vicinity of the outside trunnion radius may be detected with this scan. Primary emphasis of the scan shall be directed towards former oilway groove locations and keyways.
- a. Couple transducer A-2 with the end surface of the trunnion using a suitable couplant at the contact interface.
 - b. The ultrasonic beam incident angle shall be maintained with orientation toward the outside radius of the trunnion.
 - c. With the leading edge positioned within $\frac{1}{2}$ in. of the outside radius, the transducer shall be drawn a distance of 3 in., towards the center bore hole. This scan, indicated in Fig. UT-4-C, shall be repeated sequentially to inspect the entire radius of the trunnion. The transducer shall be indexed half the transducer width in each successive scan.

- d. Identify indication location by azimuth, distance between the transducer index point and outside radius of the trunnion end, and cosine of the sound path distance (axial distance to reflector). Actual sound path distance shall be recorded as well.
 - e. Indications that require up to and inclusive of 10 dB additional gain to achieve a signal trace deflection equal to the amplitude generated at reference level from TCS sensitivity notch No. 1 (or 8 dB less than the reference level of notch No. 2) shall be recorded.
 - f. Indications with axial location exceeding the distance to shoulder No. 1 shall be recorded if trace deflection amplitude is 10 dB less severe than the reference level generated from sensitivity notch No. 2.
4. Radial straight beam scan, for use with transducer A-3 for determination of radial distance from the center bore surface, and inspection of former oilway groove and keyway areas (designated SC-4). This scan may also be useful for identification of relative location, for alternate scanning beam angle, and for characterization of indications.
- a. Couple transducer A-3 to the center bore surface of the trunnion using a suitable couplant at the contact interface.
 - b. Axial movement of the transducer towards the middle portion of the trunnion shall be employed to locate section changes, and to measure radial distance from the bore hole to the outside diameter surface.
 - c. Radial movement around the inside radius of the bore hole shall be used to locate keyways or former oilway grooves.
 - d. A combination of radial and axial transducer movement may be employed for inspection and characterization of specific indications.
 - e. Axial distance to the transducer center point shall be measured from the trunnion end at each change of section
 - f. Radial orientation shall be identified by azimuth to which the center of the ultrasonic beam is directed.
5. Center bore hole, angle beam shear wave scan using transducer A-4 for primary inspection of critical trunnion locations. (designated SC-4).
- a. Couple transducer A-4 to the center bore surface using a suitable couplant at the contact interface.
 - b. Axial movement of transducer A-4 shall initiate at the end of the standard diameter of the center bore (immediately past the "lip" of the counter bore) and continue toward the middle of the trunnion as indicated in Fig. UT-4-D. The travel distance of the scan shall extend between 2 ½ in. and 11 in. (inclusive) from the trunnion end.
 - c. Radial indexing of half the width of the active element of transducer A-4 shall accompany successive axial scanning movement.

- d. Identify indications by azimuth, axial distance from end to transducer index point and sound patch distance.
- e. Relative cross-sectional location of the indication shall be determined using mathematical calculations or sketches (with accurate angle measurements and relative distance).
- f. Indications with trace deflections equal to 10 dB less severe than the amplitude at reference level from sensitivity notch No. 2 shall be recorded.



IIW BLOCK

Fig. UT-1

IIW ULTRASONIC TEST STANDARD

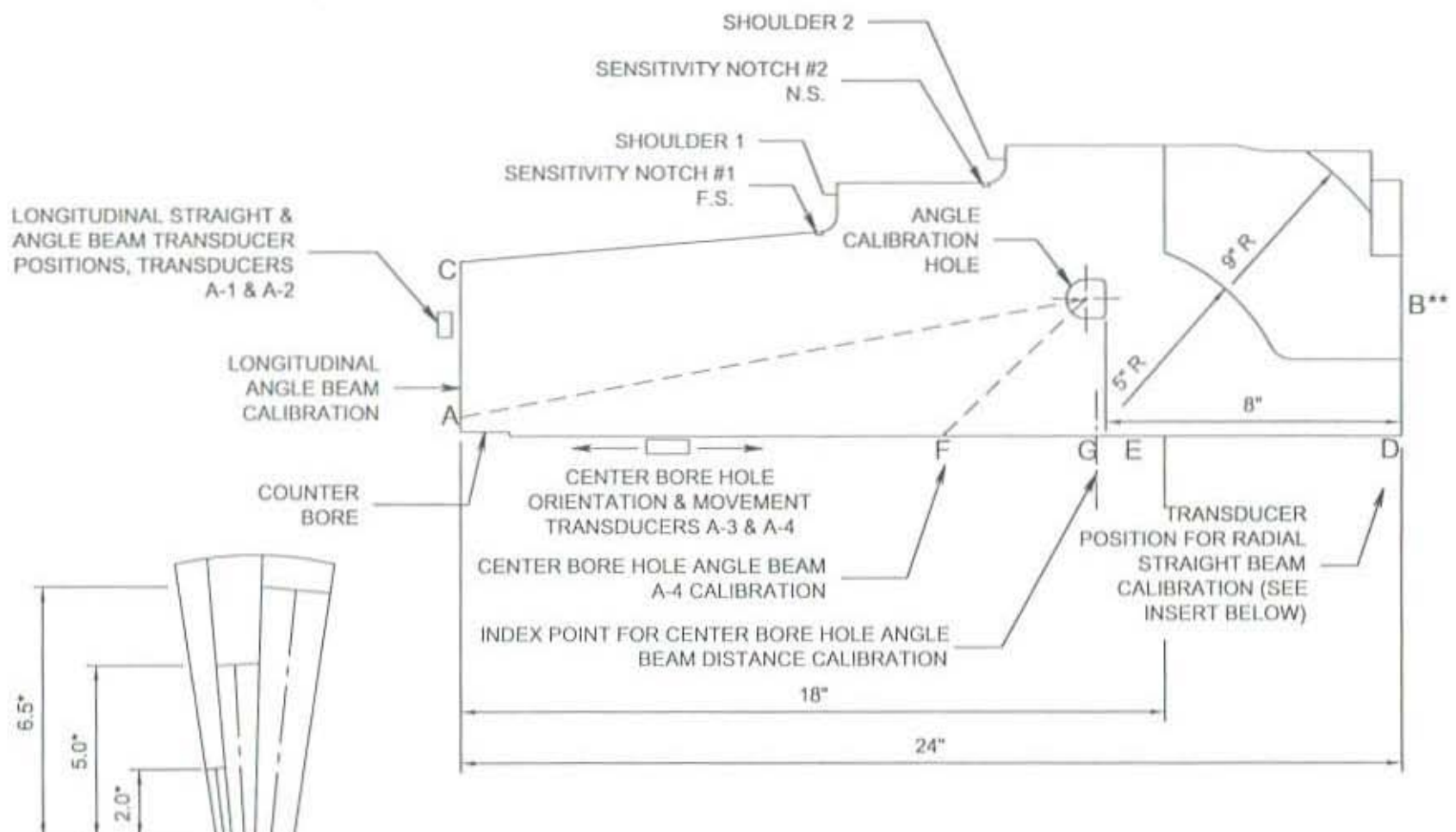


Fig. UT-2 Trunnion Calibration Standard (TCS)

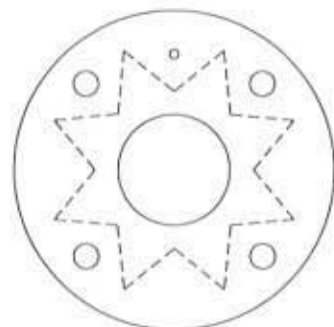
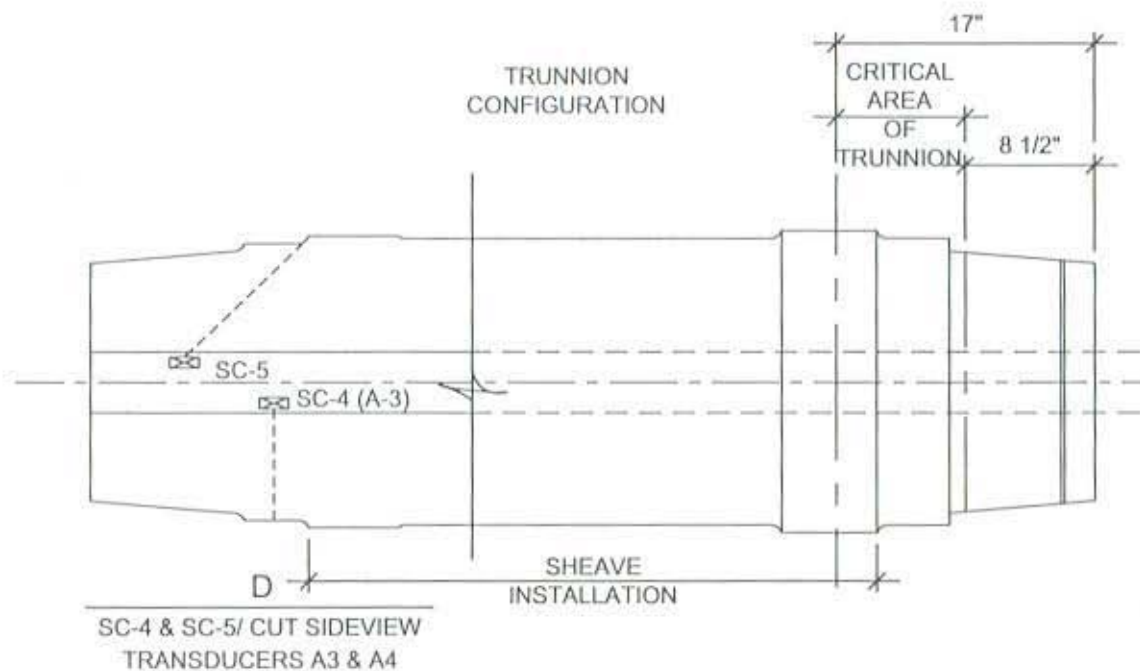
CENTER TRANSDUCER AT INSCRIBED MARKS

TRANSDUCER POSITION FOR RADIAL STRAIGHT BEAM CALIBRATION

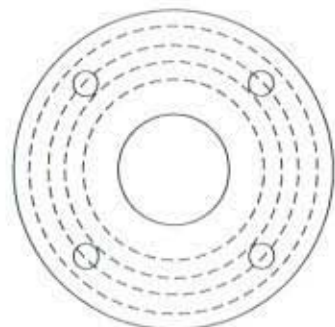
* ACTUAL SOUND PATH IS APPROXIMATELY 0.05 LESS THAN INDICATED. REFER TO PROCEDURES FOR RADIAL STRAIGHT BEAM CALIBRATION

** FAR SIDE OF STANDARD ONLY

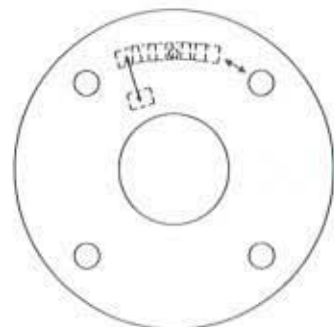
STANDARD FOR CALIBRATION OF ULTRASONIC APPARATUS PRIOR TO INSPECTION OF TRUNNIONS



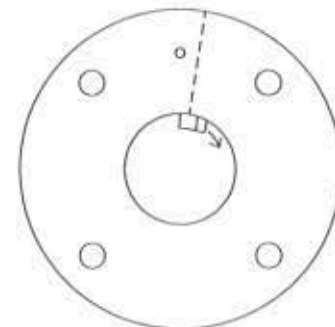
A
SC-1
TRANSDUCER A-1



B
SC-2
TRANSDUCER A-1



C
SC-3
TRANSDUCER A-2



E
SC-5
TRANSDUCER A-4

Fig. UT-4
ULTRASONIC SCAN PLANS